The Archaean of the Karelia Province in Finland
Edited by Pentti Hölttä
Geological Survey of Finland, Special Paper 54, 21–73, 2012

THE ARCHAEAN OF THE KARELIA PROVINCE IN FINLAND

by
Pentti Hölttä[1)], Esa Heilimo[2)], Hannu Huhma[1)], Asko Kontinen[2)], Satu Mertanen[1)], Perttu Mikkola[2)], Jorma Paavola[2)], Petri Peltonen[1,3)], Julia Semprich[5)], Alexander Slabunov[4)] and Peter Sorjonen-Ward[2)]

Hölttä, P., Heilimo, E., Huhma, H., Kontinen, A., Mertanen, S., Mikkola, P., Paavola, J., Peltonen, P., Semprich, J., Slabunov, A. & Sorjonen-Ward, P. 2012. The Archaean of the Karelia Province in Finland. *Geological Survey of Finland, Special Paper 54*, 21−73, 33 figures and 1 appendix.

The Archaean bedrock of the Karelia Province in Finland is mostly formed of granitoids whose ages vary from c. 3.50 to 2.66 Ga. Neoarchaean rocks dominate, since Paleoarchaean and Mesoarchaean granitoids (>2.9 Ga) are only locally present in the western and northern parts of the province. The granitoid rocks can be classified, based on their major and trace element compositions and age, into four main groups, which are the TTG (tonalite-trondhjemite-granodiorite), sanukitoid, QQ (quartz diorite-quartz monzodiorite) and GGM (granodiorite-granite-monzogranite) groups. Most ages obtained from TTGs are between 2.83–2.72 Ga, and they seem to define two age groups separated by a c. 20 Ma time gap. TTGs are 2.83–2.78 Ga in the older group and 2.76–2.72 Ga in the younger group. Sanukitoids have been dated at 2.74–2.72 Ga, QQs at c. 2.70 Ga and GGMs at 2.73–2.66 Ga. Based on REE, the TTGs fall into two major groups: low-HREE (heavy rare earth elements) and high-HREE TTGs, which obviously originated at differing crustal depths. Sanukitoids are interpreted in terms of melting of subcontinental metasomatized mantle. The GGM group probably represents partial melting of pre-existing TTG crust.

Migmatized amphibolites are found as layers and inclusions in TTGs. Their composition generally varies from basaltic to andesitic. Basaltic amphibolites (SiO_2 < 52 wt%) fall into two main groups on the basis of their trace element contents. Rocks of the first group have flat or LREE-depleted trace element patterns, resembling here the present mid-ocean ridge basalts, and have chondritic Nb/La ratios, low Zr/Y ratios and high Ni and Cr. Rocks of the second group are enriched in LILE and LREE. They have subchondritic Nb/La ratios and higher Zr/Y ratios than the first group of basaltic amphibolites. Compatible elements, especially Ni but also Cr, are lower in the LREE-enriched group than in the first group. The second group of LREE-enriched amphibolites could partly represent metamorphosed dykes with assimilated and/or diffused crustal signatures from their TTG country rocks.

The two largest Archaean greenstone belts are the Suomussalmi-Kuhmo-Tipasjärvi belt and the Ilomantsi belt. The latter is predominantly younger than the other greenstone belts in Finland. In the Ilomantsi greenstone belt, volcanic rocks and related dykes are 2.76–2.72 Ga, whereas in other belts they are mostly 2.84–2.80 Ga, and some are even older. The Kuhmo mafic and ultramafic volcanic rocks show an affinity to oceanic plateau basalts, and seem to derive from a slightly

depleted primitive mantle-type source. Ilomantsi komatiites have highly fractionated, LREE-enriched patterns that indicate extensive interaction with the associated felsic volcanics, and both the komatiites and the felsic volcanics bear arc signatures.

Metamorphism of the TTG complexes took place under upper amphibolite and granulite facies conditions at 2.70–2.60 Ga. The pressures of the regional metamorphism were mostly c. 6.5–7.5 kbar, and corresponding temperatures c. 650–740 °C. Medium pressure granulites, equilibrated at c. 9–11 kbar and 800–850 °C, are only found in the Iisalmi complex. The Siurua complex contains mafic granulites that were metamorphosed at c. 6 kbar and 750 °C. In greenstone belts, the metamorphic pressures and temperatures that are given by thermobarometry increase from inner to outer parts. P and T were c. 3–4 kbar and 550–590 °C in the inner parts of the Ilomantsi greenstone belt and c. 5 kbar and 630 °C in the outer parts. A similar increase in metamorphic temperatures was also observed in the Kuhmo belt. The Kuhmo and Oijärvi belts record extremely high pressures of up to 10–13 kbar, and in one locality near the eastern boundary of the Kuhmo belt even 16–17 kbar at 650–690 °C.

Neoarchaean accretion of exotic terranes at c. 2.83–2.75 Ga and subsequent collisional crustal stacking at around 2.73–2.68 Ga may have been the mechanism that generated the present structure of the Karelia Province, although it was again strongly reworked during the Svecofennian orogeny.

Keywords (GeoRef Thesaurus, AGI): Karelia Province, granites, amphibolites, greenstone belts, geochemistry, tectonics, Archean, Finland

[1)] *Geological Survey of Finland, P.O. Box 96, FI-02151 Espoo, Finland*
[2)] *Geological Survey of Finland, P.O. Box 1237, FI-70211 Kuopio, Finland*
[3)] *Present address: First Quantum Minerals Ltd, Kaikukuja 1, FI-99600 Sodankylä, Finland*
[4)] *Institute of Geology, Karelian Research Centre, RAS, Pushkinskaya St. 11, Petrozavodsk, 185910 Russia*
[5)] *Physics of Geological Processes, University of Oslo, Blindern, P.O. Box 1048, 0316 Oslo, Norway*

E-mail: pentti.holtta@gtk.fi

INTRODUCTION

There is no generally accepted geodynamic framework for the Archaean eon, as exists for the modern Earth via plate tectonics and the Wilson cycle (Benn et al. 2006). Nevertheless, it is commonly held that plate tectonics has been operating in some form at least since the Neoarchaean (e.g. deWit 1998, Condie & Benn 2006). However, there is considerable controversy concerning many of the fundamental aspects of Archaean plate tectonics, including serious doubts about the applicability of the concept at all (Hamilton 1998, 2011). Some views emphasize the likelihood of a much faster convection and ocean floor spreading rate in the Archaean than presently, while others suggest that plate velocities have been fairly similar throughout geological time (Blichert-Toft & Albarede 1994, Kröner & Layer 1994, Blake et al. 2004, van Hunen & van den Berg 2004, Strik et al. 2003, Korenaga 2006). Some recent simulations indicate that only after the development of the post-perovskite layer above the core-mantle boundary, after sufficient cooling of the early Earth, could the core have been able to release enough heat to the upper mantle to enable the rapid motion of plates. The earliest this event could probably have occurred was in the early Palaeoproterozoic (Tateno et al. 2009, Hirose 2010).

However, it is generally thought that the Archaean mantle was hotter than today, and the critical petrological evidence for this was komatiites and their much higher abundance in the Archaean than in the younger geological environments. Komatiites have been related to mantle plumes and reported to record very high mantle temperatures and melting pressures. On the other hand, it has also been argued that komatiites were, similarly to modern boninites, produced by hydrous melting at relatively shallow mantle depths in a subduction environment. This alternative interpretation predicts that the Archaean mantle was only slightly hotter than the present one (Grove & Parman 2004, Condie & Benn 2006).

Complete ophiolite sequences that would completely verify the existence of Phanerozoic-style oceanic crust are rare in Archaean areas. A Neoarchaean, 2.51 Ga ophiolite complex has been described from the North China craton (Kusky et al. 2001, 2004), and greenstone occurrences that share many – although not all - characteristics of modern ophiolites have also been found in other Archaean cratons, including the Belomorian province of the Fennoscandian shield (Kusky & Polat 1999, Corcoran et al. 2004, Puchtel 2004, Shchipansky et al. 2004). Archaean oceanic crust could have been thicker than Proterozoic and Phanerozoic oceanic crust, resembling that of modern oceanic plateaux. This would explain the rareness of complete modern MORB-type ophiolites, as in this case only the upper basaltic, pillow lava-dominated sections of the oceanic crust were likely to be accreted or obducted and thus preserved in the rock record (Kusky & Polat 1999). Şengör & Natal'in (2004) pointed out that in many Phanerozoic accretionary orogens, as in the western Altaids, evidence of closed oceans also only occurs in the form of separated fragments of variably complete ophiolitic sequences, without a single example of well-preserved major ophiolite nappe such as those in Oman or Newfoundland. Moreover, as the Altaids cover about as much of the Earth's land area as the Archaean crust, the rarity of indisputable Archaean ophiolite sequences already appears a less forceful argument against modern-style plate tectonism. Dilek & Polat (2008) and Dilek & Furnes (2011) also argued that the structure of the Archaean oceanic crust differed from that of the modern one; for example the Archaean sheeted dyke systems could be rare because spreading rates and magma supply were necessarily not in such a balance that is needed for their generation.

Tonalite-trondhjemite-granodiorite (TTG) gneisses are the major constituent of the Archaean crust, and more widespread in the Archaean than in younger regions (Condie & Benn 2006). The petrogenesis of HREE-depleted Archaean TTGs have been interpreted in terms of a process that begins with tectonic thickening and subduction of oceanic crust, followed by progressive metamorphism and partial melting of the basaltic rocks, producing TTG melts that for the most part were in equilibrium with anhydrous, eclogitic residues (Rapp et al. 2003). Foley et al. (2002) argued that even the earliest continental crust formed by melting of amphibolites in subduction zone environments rather than by the melting of eclogite or magnesium-rich amphibolites in lower parts of thick oceanic crust. Nair and Chacko (2008) proposed a model where oceanic plateaux served as the nuclei for Archaean cratons, and that TTGs originated in intraoceanic subduction systems where thinner oceanic lithosphere subducted beneath the thick oceanic plateaux.

On the basis of isotopic age distribution and εNd data, the most important Archaean crust-forming event was at c. 2.70 Ga, when obviously large volumes of continental crust were formed

worldwide. In some theories, this flare-up in crust formation was related to a large-scale mantle overturn event, which gave rise to a large number of plumes (Condie 1998, 2000, Condie & Benn 2006). The period 2.75–2.65 Ga was also a period when the pre-existing continental crust was intensively reworked in various Archaean provinces, as in the Kola and Karelia Provinces in the Fennoscandian and Superior Province in the Canadian Shield.

Archaean rocks cover roughly one-third of the Precambrian region in the Fennoscandian Shield. Most of these rocks are Neoarchaean (2.8–2.5 Ga). Mesoarchaean (3.2–2.8 Ga) juvenile or reworked formations are essential constituents of the bedrock only locally, and Palaeoarchaean rocks (3.6–3.2 Ga) are, overall, rare. The Neoarchaean 2.75–2.65 Ga event was very strong, including juvenile TTG magmatism, sedimentation, metamorphism and crustal melting producing granites. This article provides a review of previous studies and presents new data on the geochemistry, age determinations, metamorphism and palaeomagnetism of the Finnish part of the Archaean Karelia Province, and discusses the magmatic and tectonic processes that could explain its present constitution and structure, with an emphasis on the Neoarchaean evolution. All ages referred to are U-Pb zircon ages, unless otherwise stated.

GEOLOGICAL SETTING

The Archaean of Fennoscandia is traditionally divided into Norrbotten, Murmansk, Kola, Belomorian and Karelia Provinces (Fig. 1, Slabunov et al. 2006, Hölttä et al. 2008). Lobach-Zhuchenko et al. (2005) and Slabunov et al. (2006) subdivided the Karelia Province into three terranes: the Vodlozero, the Central Karelia and the Western Karelia (Fig. 1), which they observed with several singular lithological, structural and age characters. We have adopted this provincial division, but instead of the term terrane will use subprovince to reflect the uncertainty about the nature of the unit contacts. By definition, a tectonostratigraphic terrane should be a fault-bounded crustal block whose geological history differs from that of the surrounding areas (Jones et al. 1983, Jones 1990). The Karelia subprovinces clearly differ for their geological histories, but there is as yet little evidence that they are all bounded by major accretionary faults.

Important distinctive characteristics of the Karelia subprovinces include that, on the basis of existing age determinations, Mesoarchaean 3.2–2.8 Ga volcanic rocks and granitoids are common in the Vodlozero subprovince, and are also found in the Western Karelia subprovince, whereas granitoids and greenstones in the Central Karelia subprovince are Neoarchaean, ≤ 2.8 Ga, although they may locally contain recycled Mesoarchaean crustal material (Vaasjoki et al. 1993). The Belomorian province east of the Karelia Province largely consists of 2.93–2.72 Ga TTG gneisses, greenstones and paragneisses, but locally of occurrences of ophiolite-like rocks and eclogites that have not been discovered elsewhere in the Archaean parts of the Fennoscandian Shield (Shchipansky et al. 2004, Volodichev et al. 2004). Reflection seismic studies suggest that the Belomorian province comprises a stack of eastward-plunging subhorizontal nappes and thrusts, which is separated from the underlying Karelia Province by a major detachment zone (Mints et al. 2004).

Hölttä et al. (2012) divided the Finnish part of the Karelia Province into nine large complexes (Ilomantsi, Lentua, Kuopio, Iisalmi, Rautavaara, Manamansalo, Kalpio, Siurua and Ranua) that were possibly not all separately developed tectonostratigraphic terranes, but nevertheless have many distinguishable geological features such as differences in age and lithologies when compared with their neighbouring complexes.

Geochemistry of granitoids and migmatitic amphibolites

Figure 2 presents a lithological map of the Finnish part of the Karelia Province, showing that most of the area (c. 80%) consists of TTGs. The rest is mainly comprised of supracrustal rocks in greenstone belts and sedimentary gneisses, and migmatitic amphibolites in enclaves in the gneissic granitoids. On the basis of field observations, the gneissic granitoids include both true orthogneisses and TTG migmatites with amphibolite and paragneiss mesosomes.

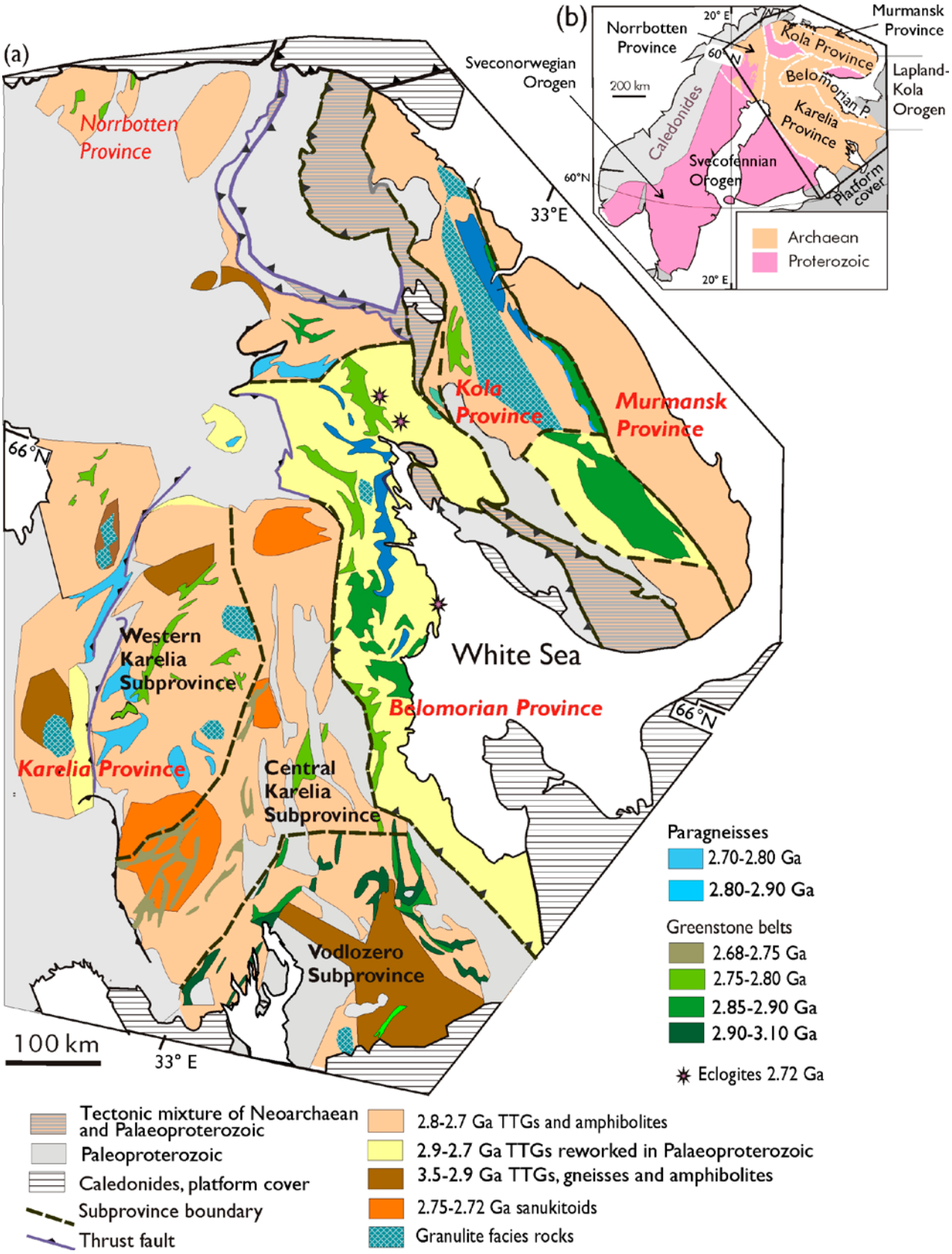

Fig. 1. A generalised geological map of the Archaean (a) of the Fennoscandian shield (b, inset), modified after Slabunov et al. (2006) and Hölttä et al. (2008).

Granitoids

Archaean granitoids in the Karelia Province can be divided into four main groups on the basis of their field and petrographic characters, major and trace element compositions and age. These are the TTG (tonalite-trondhjemite-granodiorite), sanukitoid, QQ (quartz diorite-quartz monzodiorite) and the GGM (granodiorite-granite-monzogranite) groups (Käpyaho et al. 2006, Mikkola et al. 2011a). For this work, 125 samples from granitoids representing various complexes were analysed for their major and trace elements (Appendix 1). Of these samples, 107 were TTGs and 29 from the QQ rocks. The dataset used in this work also includes Archaean rocks from the Rock Geochemical Database of Finland, where the analytical methods applied in this work are described (Rasilainen et al. 2007).

TTGs

TTGs represent the majority of the Archaean bedrock in Finland, and understanding of their origin is thus crucial. It is well recognized that Archaean TTGs share many geochemical features with adakites, i.e. silica-rich volcanic and plutonic rocks at volcanic arcs that are strongly depleted in Y and heavy rare earth elements, low in high-field-strength elements (HFSE) and high in their Sr/Y and La/Yb ratios (Defant & Drummond 1990). The chemical criteria for adakites are listed in the original paper by Defant and Drummond (1990), and later, for example, in Richards and Kerrich (2007), who use the following critical composition to define adakite: $SiO_2 \geq 56$ wt%, $Al_2O_3 \geq 15$ wt%, MgO < 3 wt%, Mg number ~ 50, $Na_2O \geq$ wt 3.5 %, $K_2O \leq 3$ wt%, $K_2O/Na_2O \sim 0.42$, Rb ≤ 65 ppm, Sr ≥ 400 ppm, Y ≤ 18 ppm, Yb ≤ 1.9 ppm, Ni ≥ 20 ppm, Cr ≥ 30 ppm, Sr/Y ≥ 20 and $La_N/Yb_N \geq 20$. Martin and Moyen (2003) divided the adakites into the low silica (<60 wt% SiO_2) and high silica (HSA, >60 wt% SiO_2) groups, relating the HSA group to slab melting with some interaction with mantle-wedge peridotite and the LSA group to melting of wedge peridotites beforehand metasomatised by slab melts.

Most TTGs in the Karelia Province fulfil the adakite criteria, apart from the Cr and Ni contents, which are normally below the detection limits of the XRF analysis used, 30 and 20 ppm, respectively. Mg contents are also normally low, in most of the TTGs in the range of 0.35–0.45, which means that they have gained minor components from mantle peridotites (Halla 2005, Lobach-Zhuchenko et al. 2005, 2008). Halla et al. (2009) divided the TTGs into two major groups, low-HREE (heavy rare earth elements) and high-HREE TTGs, which obviously originated at different lithospheric depths. Here we follow the proposal of Halla et al. (2009), but instead of the HREE content – which depends, besides melting pressure, on the source composition and post-melting fractionation – we use the $(La/Yb)_N$ ratio, as low-HREE rocks generally have high $(La/Yb)_N$ ratios. We further divide the low-HREE group into Eu-positive and Eu-negative subgroups. Our dataset demonstrates that the two TTG groups are not separated in compositional space but rather represent end members between which there is full compositional continuity.

Moyen (2011) studied a large set of analyses from rocks generally regarded as TTGs, ultimately dividing these rocks into four groups: the potassic group and the high-, medium- and low-pressure groups of 'proper' juvenile TTGs. The high-pressure group, equivalent to the low HREE group, has TTGs with high Al_2O_3, Na_2O, Sr and low Y, Yb, Nb and Ta. The TTGs of the low-pressure group, equivalent to the high-HREE group, show opposite values in these respects. The potassic group rocks that show enrichment in K and LIL elements are thought by Moyen (2011) to have formed by melting of pre-existing crustal rocks. If the criteria for true TTGs include $K_2O/Na_2O <$ 0.5 (Martin et al. 2005), c. 20% of our samples collected in the field as TTG suite rocks would actuially belong to the potassic or transitional TTGs, as these types of rocks were referred to by Champion and Smithies (2007). On the other hand, this is a definitional problem, because in granodiorites the K_2O/Na_2O ratio is typically 0.5–1, and rocks whose K_2O/Na_2O is < 0.5 are tonalites and trondhjemites, i.e. TTs rather than TTGs.

The rocks in the low-HREE group are trondhjemitic and tonalitic when classified using normative compositions and the QAPF diagram in Streckeisen (1973) or the Ab-An-Or diagram in O'Connor (1965, Fig. 3). In the Eu-negative subgroup, SiO_2 is generally 62–74 wt%, mg# 30–55 and Al_2O_3 15–17 wt%. Most of the samples have fractionated REE patterns with low HREE and high Sr/Y (median 81). They also have high La_N/Yb_N ratios of 20–120 with a median of 49, showing negative Eu anomalies (Fig. 5) and low abundances of compatible elements.

SiO_2 in the Eu-positive, low-HREE TTGs typically varies from 68–76 wt%, and they often have low abundances of FeO and MgO, which is reflected in their near-white to light grey colour in outcrops and samples. Mg# is generally 28–55 and Al_2O_3 14.5–17.5 wt%. These TTGs are associated with negative magnetic anomalies on airborne

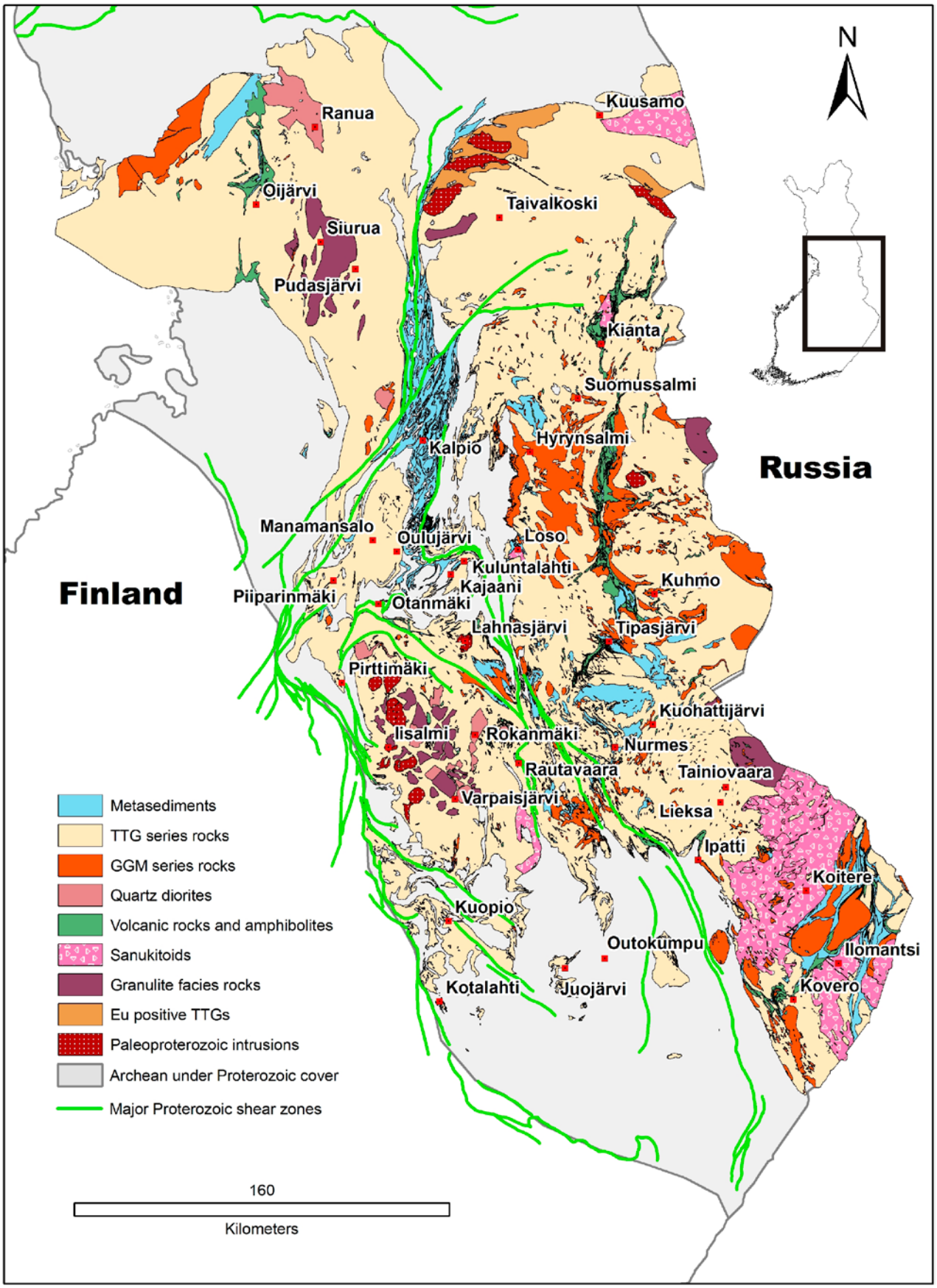

Fig. 2. A generalised geological map of the Finnish part of the Karelia Province. The inset shows the location of the map area in Finland. Basemap © National Land Survey of Finland, licence no 13/MML/12.

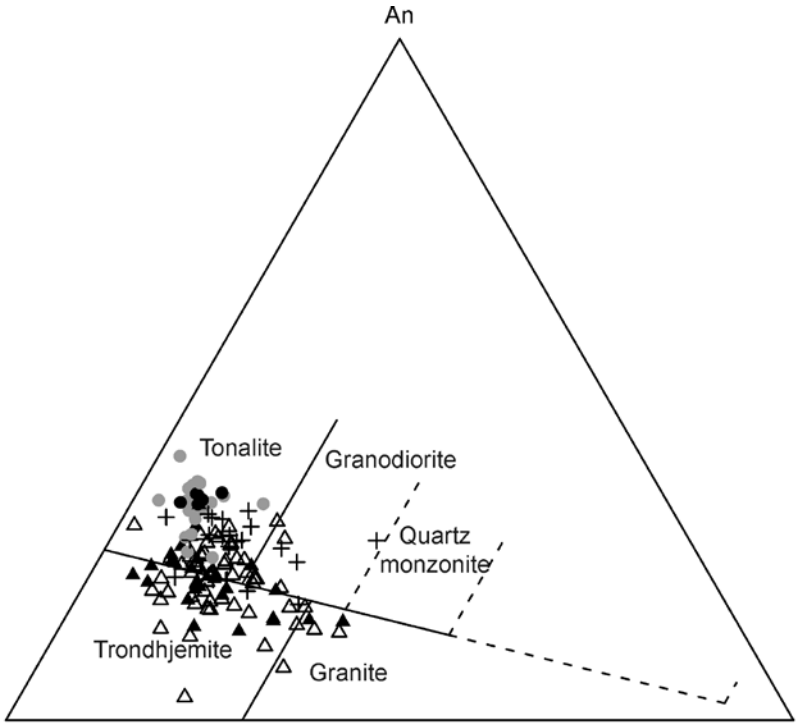

Fig. 3. A normative Ab-An-Or diagram (O'Connor 1965) for TTGs and QQs. Open triangles = low-HREE TTGs, black triangles = low-HREE, Eu-positive TTGs, crosses = high-HREE TTGs, grey dots = QQs, black dots = orthopyroxene-bearing QQs (enderbites).

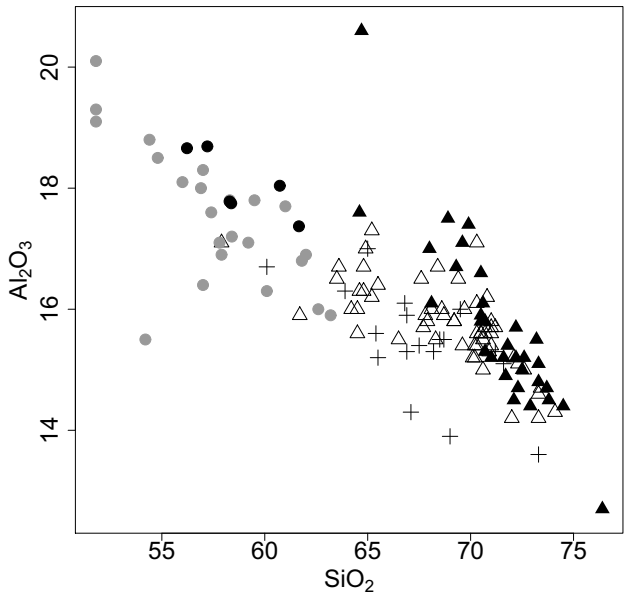

Fig. 4. Al_2O_3 vs. SiO_2 in TTGs and QQs. Symbols are as in Fig. 3.

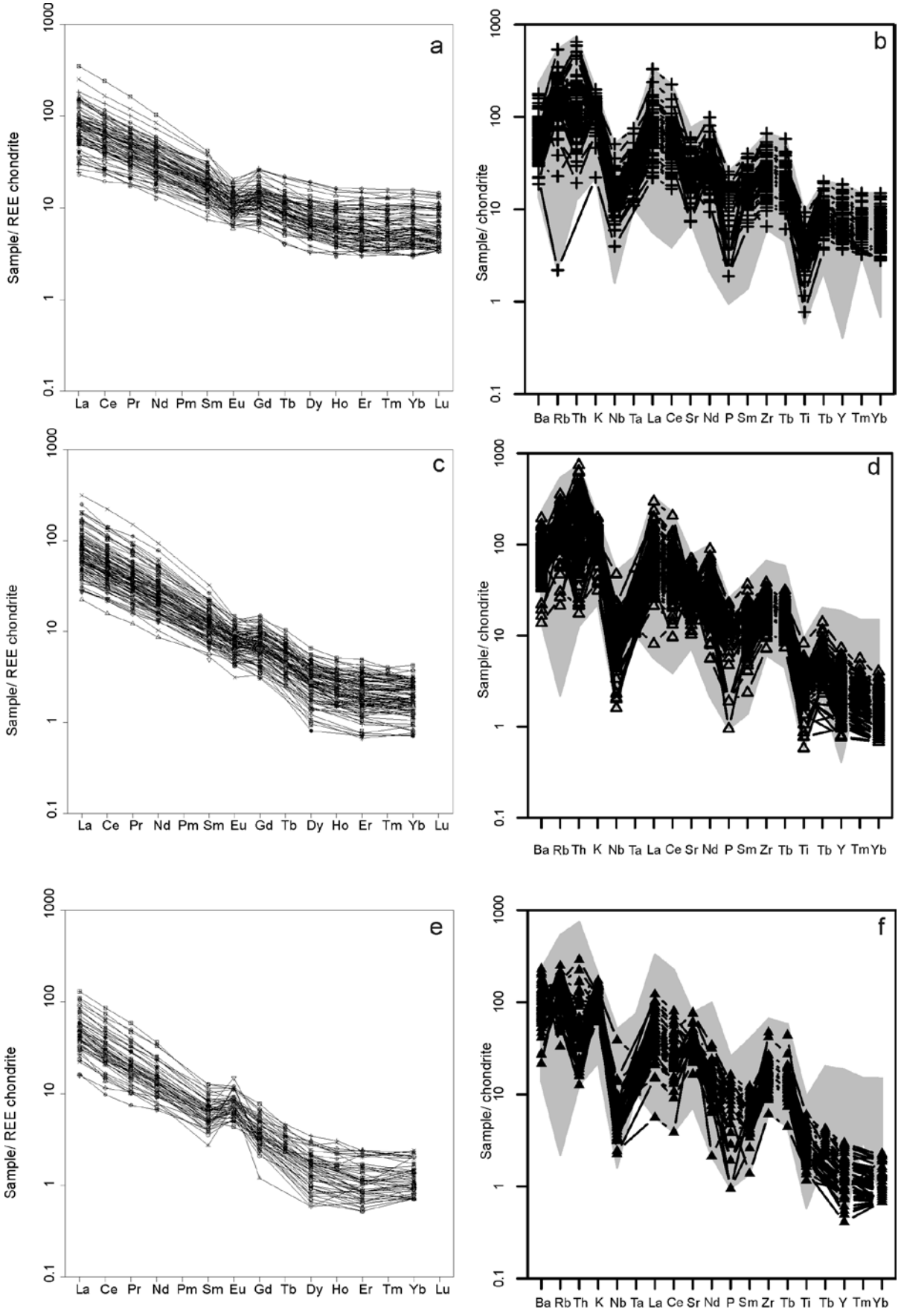

Fig. 5. Trace element patterns of TTGs: a, b = high HREE group, c, d = low HREE group, e, f = Eu-positive group. Diagrams represent 255 analyses where the K_2O/Na_2O ratio is < 0.5, taken from the Rock Geochemical Database of Finland (Rasilainen et al. 2007). Normalising factors for a, c and e are from Boynton (1984) and for b, d and f from Thompson (1982). The shaded area is for all data.

magnetic maps, and especially in the northern part of the Karelia Province in Finland they cover large areas (Fig. 2). Most samples show, apart from positive Eu anomalies, strongly fractionated REE patterns with HREE mostly below the detection limits, low Y, Sc and Nb, high Sr/Y, La_N/Yb_N and Zr/Sm ratios and low abundances of compatible elements (Figs. 5–7). In outcrops, part of these rocks show diatexitic migmatite structures and seem to represent almost complete fusion of amphibolites, but there are also many occurrences of this group that appear to be homogeneous orthogneisses.

The high-HREE group is normatively granodioritic and tonalitic. SiO_2 is c. 60–72 wt%, mg# generally 30–55 and Al_2O_3 15–17 wt%. Al_2O_3/SiO_2 is generally lower in samples of this than the other TTG groups (Fig. 4). Rocks in this group have low Sr/Y ratios (median 22) and higher abundances of compatible elements and HREE than the other TTGs. The La_N/Yb_N is < 20 with a median of 10. On average, the high-HREE group has higher Nb contents (c. 5–15 ppm) than the low HREE group (c. 1–8 ppm).

Sanukitoids

Sanukitoid granitoids (most commonly grano-diorites) with low silica, high K, Ba, Sr and elevated Mg, Cr and Ni contents are relatively common in the Western and Central Karelia subprovinces. As a group they postdate the TTGs, being generally 2.74–2.72 Ga (Fig. 21). These sanukitoids resem-

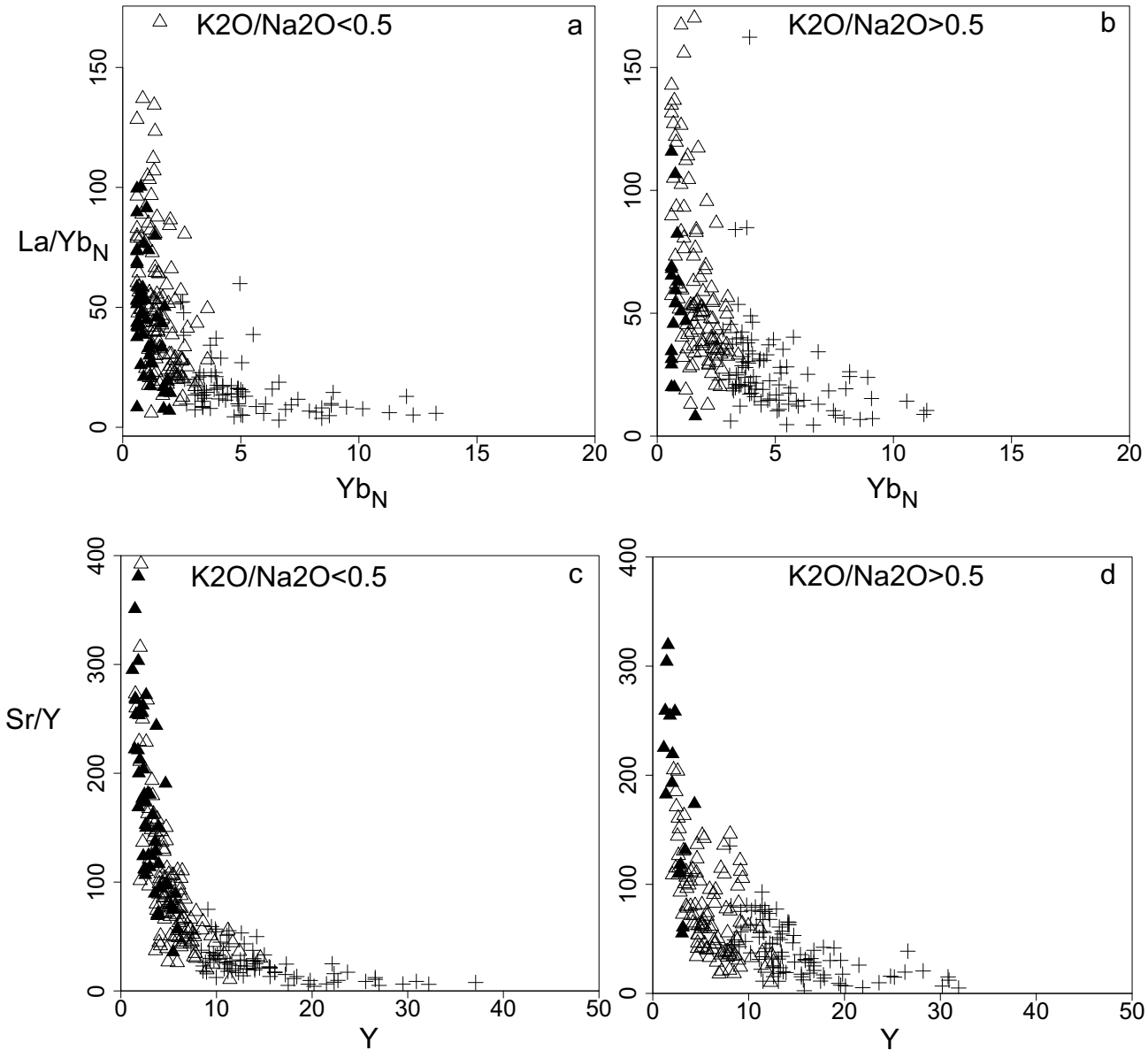

Fig. 6. Chondrite-normalized La/Yb vs Yb ratios and Sr/Y vs Y ratios for "true" (a, c) and potassic (b, d) TTGs. Normalising factors are from Thompson (1982). Symbols as in Fig. 3.

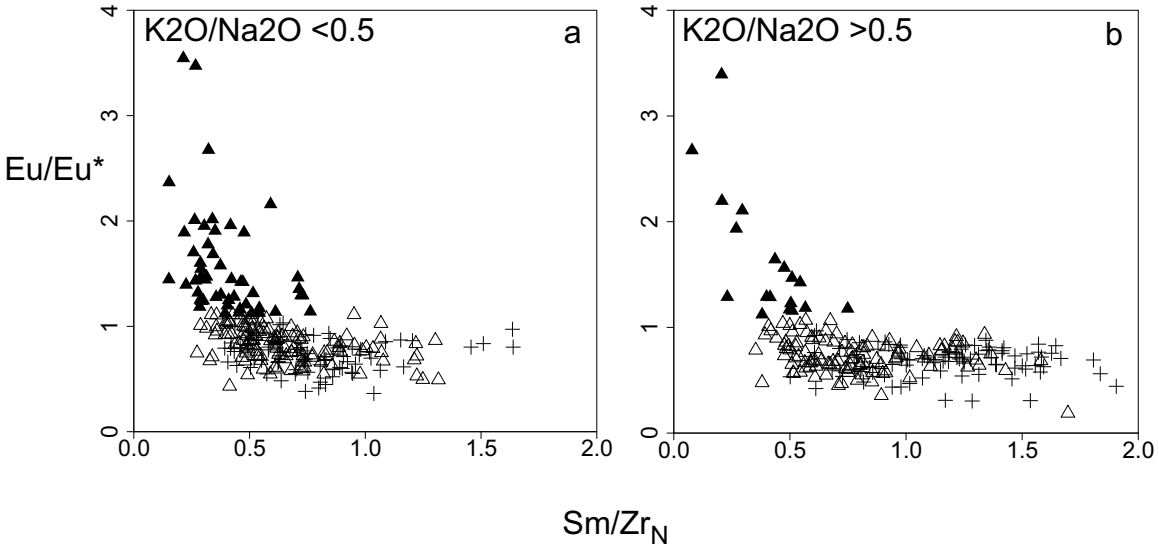

Fig. 7. Eu/Eu* vs. chondrite-normalised Zr/Sm for "true" (a) and potassic (b) TTGs. Normalising factors are from Thompson (1982). Symbols as in Fig. 3.

ble in several aspects Mesozoic mantle-derived high Ba-Sr granitoids in Scotland (Fowler et al. 2008, Halla et al. 2009). They have been related to melting of subcontinental metasomatized mantle, possibly induced by late- or postorogenic slab breakoff (Lobach-Zhuchenko et al. 2005, 2008, Halla 2005, Halla et al. 2009, Heilimo et al. 2010, 2012). However, given that most of these sanukitoids emplaced shortly before the main phases of metamorphism and deformation (2.71–2.64 Ga), they should rather be classified as late orogenic. The geochemical data for Karelian sanukitoids are found in Heilimo et al. (2010), U-Pb zircon ages in Heilimo et al. (2011) and Hf, Nd, Pb and O isotope geochemistry in Heilimo et al. (2013).

QQ

Another important group of non-TTG granitoids comprises rocks whose normative composition is mostly quartz dioritic and quartz monzonitic, but locally also dioritic and monzodioritic. Rocks belonging to this QQ group are especially found in the Western Karelia subprovince. Most QQ intrusions are located west of the sanukitoids described above, but whether there is a genetic link between the sanukitoid and QQ groups is not yet clear. The QQs include the enderbites in the Iisalmi complex (Hölttä 1997), the Ranua diorite in the Ranua complex (Mutanen & Huhma 2003) and some smaller plutons in Ranua and in the northern part of the Lentua complex (Mikkola 2008, Mikkola et al. 2011a). The QQs have zircon U-Pb ages close to 2.70 Ga apart from the 2.68 Ga Rokanmäki intrusion (Paavola 1999) in the Rautavaara complex . ε_{Nd} values at 2.7 Ga are positive, for example +0.2 and +1 in the two analyzed enderbites of the Iisalmi complex (Hölttä et al. 2000) and +0.8 in the Ranua diorite (Mutanen & Huhma 2003). Many compositional features in these rocks also fulfil the definition of adakites, as SiO_2 is in most analysed samples 52–62 wt%, Al_2O_3 a high 15.4–20.1 wt%, MgO 2.5–4.0 wt%, mg# 44–54, Na_2O 3.3–5.4 wt%, K_2O 0.8–1.8 wt%, Rb 13–52 ppm, Sr 630–1170 ppm, Sr/Y 21–80, Ba 200–800 ppm, Y < 18 ppm and Yb < 1.9 ppm. Furthermore, Cr in most samples is > 30 ppm and Ni >20 ppm, except for values of 10–28 ppm and 6–13 ppm, respectively, in the Ranua diorite. However, the QQs have only moderately fractionated REE patterns with La_N/Yb_N ratios of 6–15, and the enderbites in the Iisalmi area, as well as the Naimakangas quartz diorites (located in the Iisalmi complex north of the enderbites) and some diorites in Ranua, have a typically flat HREE (Fig. 8). This type of REE pattern is a distinctive feature of the enderbites and was not observed in any other Archaean igneous rocks, apart from 2.74 Ga alkaline rocks in Suomussalmi, which have a similar REE distribution but generally higher REE abundances (Mikkola et al. 2011b). The enderbites have lower Rb, U and Th contents than the other quartz diorites, probably because of the loss in these elements during the granulite facies metamorphism that they underwent at 2.7–2.6 Ga (Mänttäri & Hölttä 2002). The Ranua diorite has syenogabbro and alkali gabbro inclusions that have higher P_2O_5 and REE contents than the enclosing diorites (Fig. 9). Although mafic, the gabbroic inclusions do not contain more Cr and Ni than the host diorite.

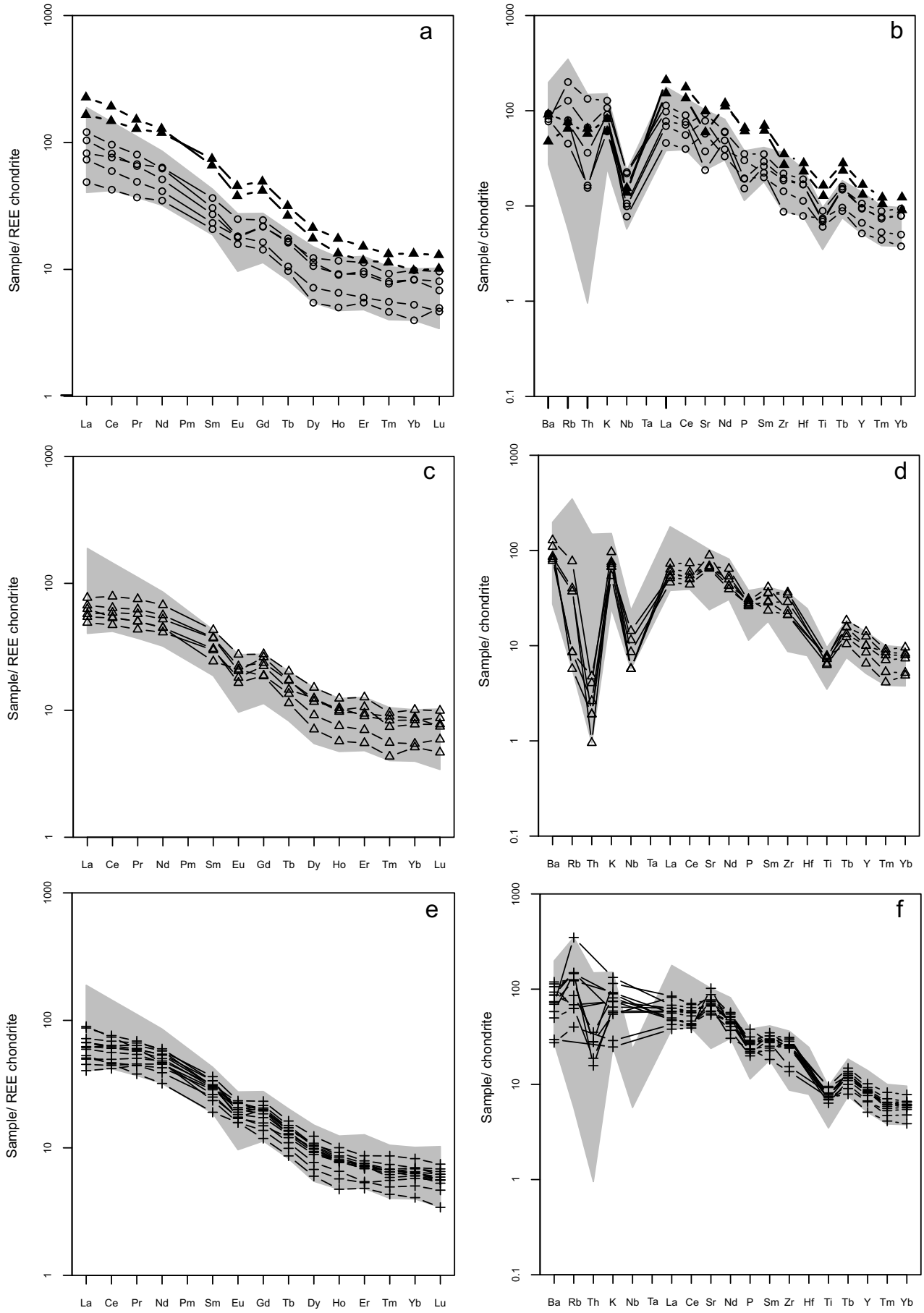

Fig. 8. Trace element patterns of QQs. a, b = Ranua, black triangles denote alkali gabbroic inclusions in diorite-quartz diorite; c, d = enderbites of the Iisalmi complex; e,f = Naimakangas. The shaded area is for all data. Normalising factors are as in Fig. 5

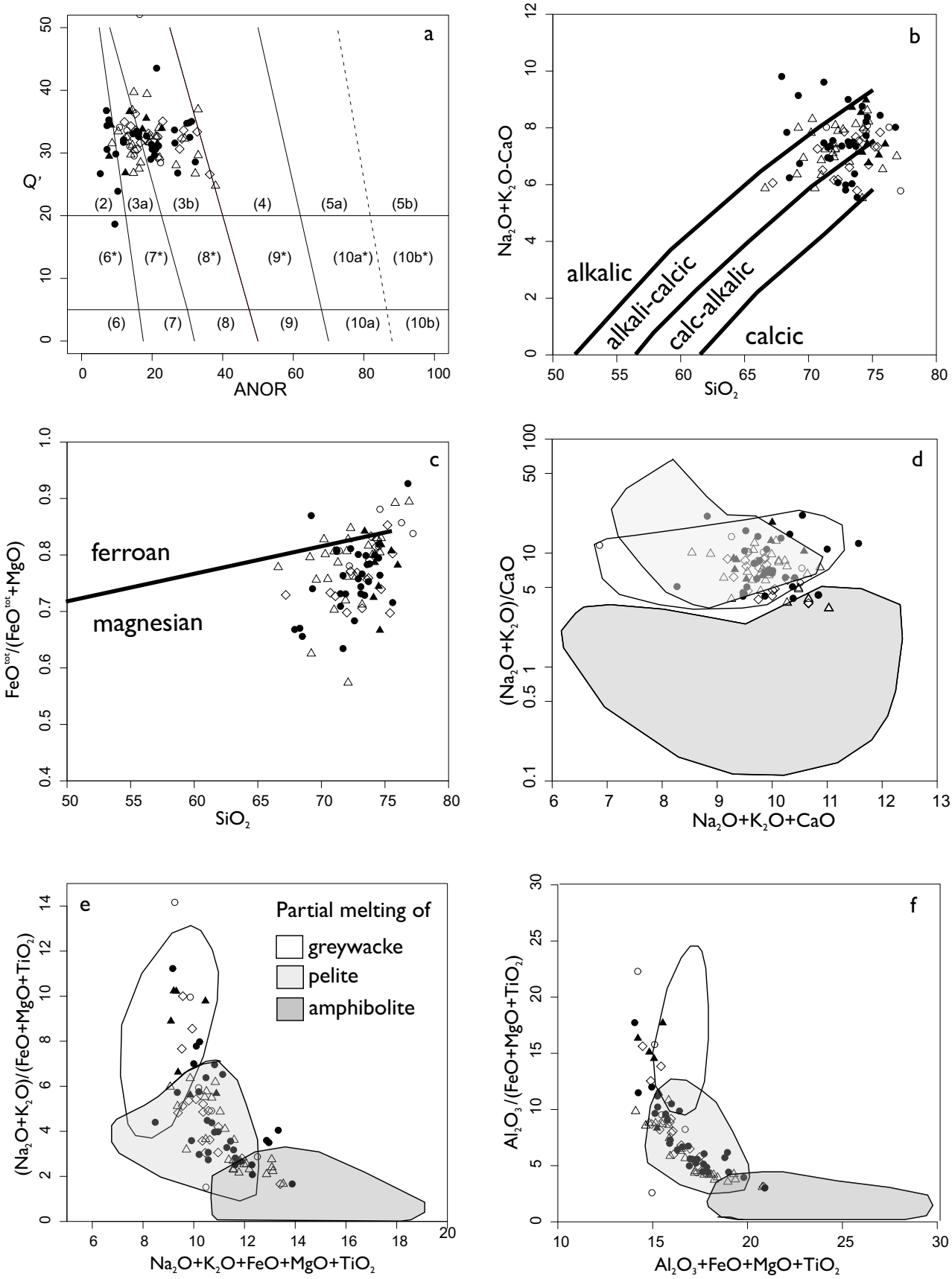

Fig. 9. Compositions of the granodiorite-granite-monzogranite series rocks. a Q'-ANOR diagram of Streckeisen & Le Maitre (1979), fields: 2 = alkali feldspar granite, 3 = granite, 4 = granodiorite, 5 = tonalite, 6* = quartz alkali feldspar syenite, 7* = quartz syenite, 8* = quartz monzonite, 9* = quartz monzodiorite/quartz monzogabbro, 10* = quartz diorite/quartz gabbro, 6 = alkali feldspar syenite, 7 = syenite, 8 = monzonite, 9 = monzodiorite/monzogabbro, 10 = diorite/gabbro. b,c = classifications after Frost (2001), d–f : diagrams after Patiño Douce (1999). Symbols: open circles = high HREE GGMs, open triangles = medium HREE GGMs, black circles = low HREE GGMs, diamonds = low HREE GGMs without Eu anomaly, black triangles = low HREE GGMs with positive Eu/Eu*.

GGM

Granodiorite-granite-monzogranite (GGM) suite rocks dated to 2.73–2.66 Ga are the youngest Neoarchaean rocks occurring in large volumes in the Western Karelia subprovince (Käpyaho et al. 2006). They are relatively weakly deformed, reddish and medium- to coarse-grained rocks. The diagrams in Figures 9–10 illustrate some of the prime geochemical characteristics of the GGM granites. Analyses for the plots are taken from the Rock Geochemical Database of Finland (Rasilainen et al. 2007), and they are also presented in Appendix 1. Most of these data are for granites, which are peraluminous and metaluminous, and according to the classification by Frost et al. (2001) mostly magnesian, calc-alkalic and alkali-calcic (Fig. 9). In the classification schema by Patiño Douce (1999) based on the major elements, these granites have compositions that correspond to the experimental dehydration melting products of felsic pelites and greywackes, and some may have reacted with basaltic rocks (Figs. 9d–f, 10). Many of the granites have highly fractionated, HREE-depleted patterns with negative or no Eu anomalies, but some are less fractionated with relatively high HREE. In Figure 11, the GGMs are classified on the basis of their REE distributions into five groups: high-HREE GGMs with a low Gd/Yb_N ratio, medium-HREE GGMs, low-HREE GGMs, low-HREE GGMs without an Eu anomaly and low-HREE GGMs with a positive Eu/Eu*. At least part of the granites could represent the melting products of sedimentary gneisses. On the other hand, according to experimental studies, dehydration melting of sodic TTG gneisses can also produce granitic to

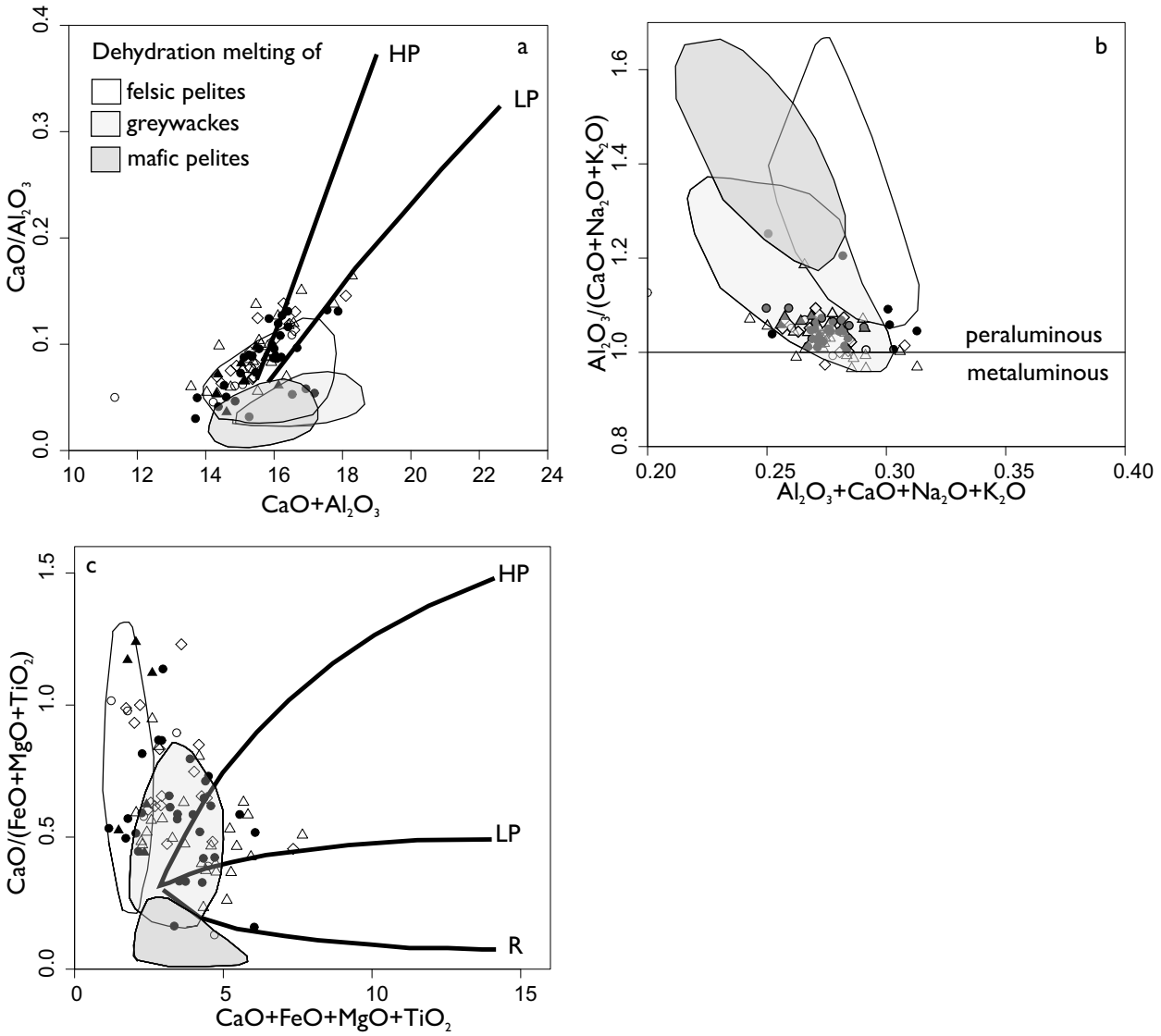

Fig. 10. Compositions of GGM rocks plotted on the diagrams after Patiño Douce (1999). The curves model the melt compositions that result when high-Al olivine tholeiite is hybridized with metapelite: HP = in high pressure; LP = in low pressure; R = in melt-restite mixing without the addition of basaltic components. Symbols as in Fig. 9.

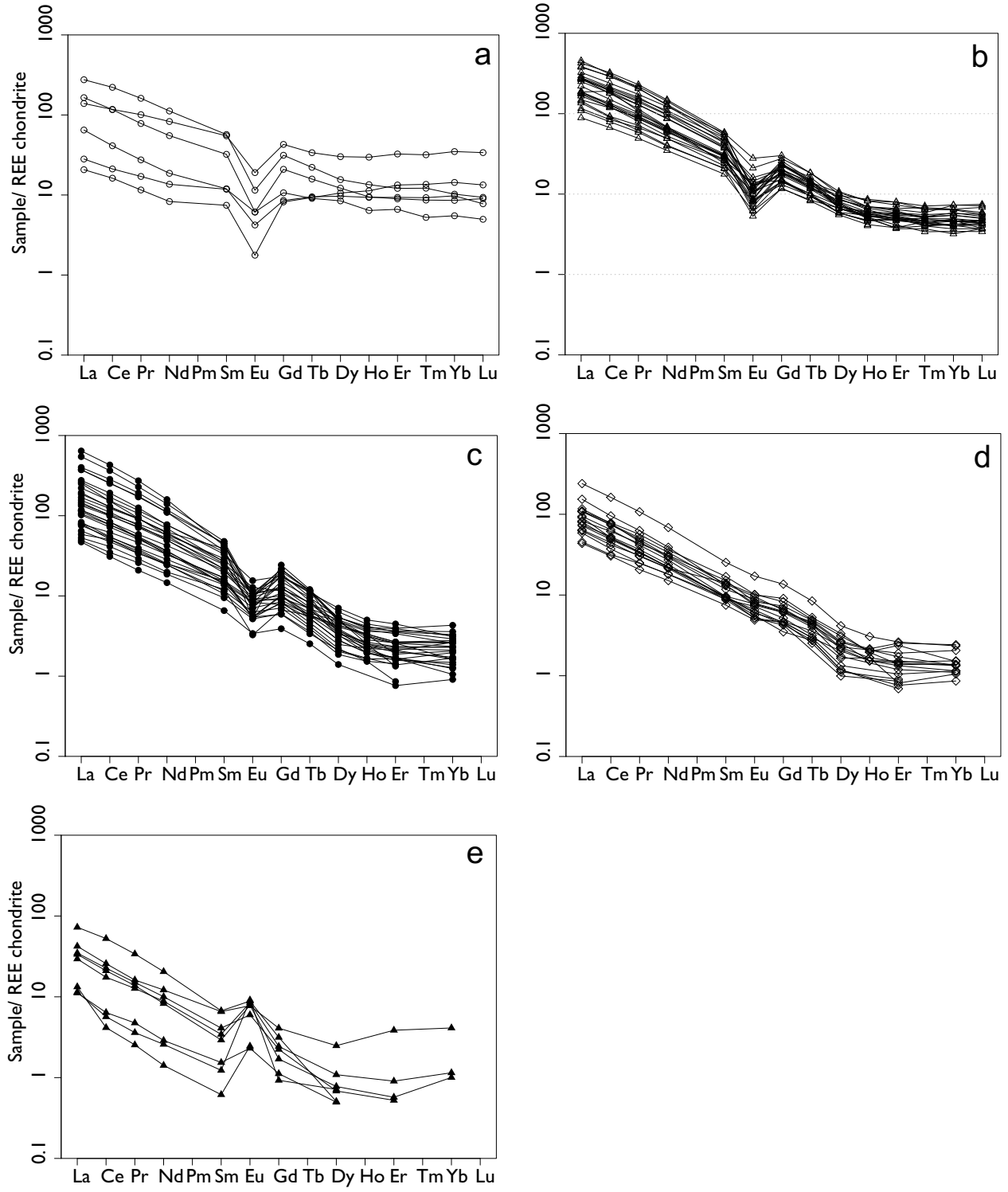

Fig. 11. Rare earth element patterns of the various GGM rocks. Symbols as in Fig. 9. Normalising factors are after Boynton (1984).

granodioritic melts (Patiño Douce 2004, Watkins et al. 2007). Skjerlie et al. (1993) have shown experimentally that when interlayered, the melt productivity of tonalite and pelite increases via the interchange of components that lower the required melting temperatures. Anatectic granites therefore tend to contain material from two or more different source rocks, which is reflected in their isotopic and chemical compositions (Skjerlie et al. 1993). This could also be the case with the Archaean GGMs, which could represent the melting products of TTGs and paragneisses, and mixing of the derived melts with contemporaneous mafic magmas. The range in ε_{Nd} (2700 Ma) values of the CGMs is c. -1.5 to +1.0, indicating that some of them might represent the melting of juvenile 2.72–2.78 TTGs, whereas others could originate from older material. However, in the Suomussalmi area, the average $\delta^{18}O$ values of zircon from GGMs are normally only slightly higher (6.42 ± 0.10) than that of the TTGs, 6.10 ± 0.19. This means that at least in Suomussalmi the GGMs do not necessarily have a significant sedimentary input in their source but rather represent melting products of TTGs (Mikkola et al. 2012). However, in the Suomussalmi area the abundance of exposed sedimentary gneisses is also low, while in other areas they may have had a more significant contribution to GGM genesis.

Amphibolites in gneissic complexes

Amphibolites are a ubiquitous component of nearly all of the studied migmatitic TTG complexes, in which they can typically be found as layers and inclusions whose widths vary from a few tens of centimetres to tens of metres. Normally, the gneiss-associated amphibolites are all migmatized, the volume of felsic neosome ranging in the exposures from < 10% up to c. 90% (Fig. 12). Extensively melted and deformed amphibolites closely resemble strongly deformed, plutonic TTGs with amphibolite rafts, making their distinction difficult. In metatexitic amphibolites, palaeosomes have mostly amphibolite facies mineral assemblages, typically hornblende-plagioclase-quartz, often with retrograde epidote. In granulite facies areas, amphibolites often have coexisting orthopyroxene and clinopyroxene. Garnet-bearing two-pyroxene mafic and intermediate granulites, which are common in the Iisalmi complex, represent high-temperature-medium pressure equivalents of the common hornblende amphibolites.

The ages of the amphibolites are problematic to resolve, because they often appear to contain predominantly metamorphic zircon grains (e.g. Mutanen & Huhma 2003). Intermediate granulites and amphibolites in the Iisalmi complex have been dated for their protoliths at c. 3.2 Ga (Paavola 1986, Mänttäri & Hölttä 2002, Lauri et al. 2011), but this complex is older overall than most other areas in the western part of the Karelia Province.

In this work, 73 amphibolite samples were collected from all Archaean gneissic complexes and were analysed for their major and trace element compositions. The data are presented in Appendix 1. On the basis of major element composition, and using the TAS classification, the amphibolites are mostly basalts and andesitic basalts. Some amphibolites are andesitic and some have a slightly alkaline character. In the Jensen cation plot, most compositions are in the field of high-Mg tholeiites, and some even in the komatiitic basalt field, the latter probably because of cumulus olivine. The Al_2O_3 contents vary mostly from c. 13–16 wt%. In the komatiitic basalts, the Al_2O_3 content is c. 10–12 wt%. MgO comprises c. 4–10 wt% in basaltic rocks, c. 11–14 wt% in komatiitic basalts and c. 3–6 wt% in andesites.

Basaltic amphibolites (SiO_2 < 52 wt%) fall into two main groups on the basis of their trace element contents. Samples of the first group have flat or LREE-depleted trace element patterns, resembling those of the present mid-ocean ridge basalts. Further characteristics of these samples are high $(Nb/La)_N$ ratios, low Zr/Y ratios and high Ni and Cr contents (Hölttä 1997, Nehring et al. 2009). Samples of the second group are enriched in LILE and LREE (Fig. 13) and have lower Nb/La_N ratios and higher Zr/Y ratios than those in the first group. Compatible elements, especially Ni but also Cr, are lower in the LREE-enriched than in the group of LREE-depleted samples (Fig. 14). Andesitic amphibolites (SiO2 c. 52–60 wt%) have similar flat to LREE-enriched trace element patterns to the basalts (Fig. 15). However, unlike the basalts, the $(La/Yb)_N$ ratio normally increases and the abundance of compatible elements decreases as a function of increasing SiO_2. Cr and Ni contents are higher in the komatiitic basalts than in basaltic and andesitic amphibolites (Fig. 14). Some of the komatiitic basalts are also enriched in LREE (Fig. 13).

Condie (2005) used the high field strength element (HFSE) ratios of Archaean basalts to demonstrate their possible mantle source domains, assuming that their magmatectonic framework was broadly similar to that of young oceanic basalts. He noted that on the basis of the Nb/Th, Zr/Nb, Nb/Y and Zr/Y ratios, most non-arc-type Archae-

an basalts from greenstone belts resemble oceanic plateau basalts, which are thought to originate from plumes variably comprising deep primitive and shallow depleted mantle. Figure 16 shows a plot of Nb/Y vs. Zr/Y for the basaltic amphibolites in the Finnish part of the Karelia Province. Given the depletion of granulite facies rocks in U and Th, thorium-based ratios are probably useless for the high-grade migmatitic amphibolites. As Zr/Nb ratios in all samples of the amphibolites are c. 10–30, they probably do not contain recycled oceanic lithospheric material. Most of the analysed amphibolites have LREE-depleted or flat REE patterns, relatively low Zr/Y ratios of

Fig. 12. Field photographs of migmatitic amphibolites of the Ranua complex. Map coordinates of the photograph sites (Finnish national grid, in KKJ zone 3/YKJ): a: 7274813, 3413614; b: 7271283, 3419703; c, d: 7265242, 3424052; e: 7280653, 3412406; f: 7286789, 3422595.

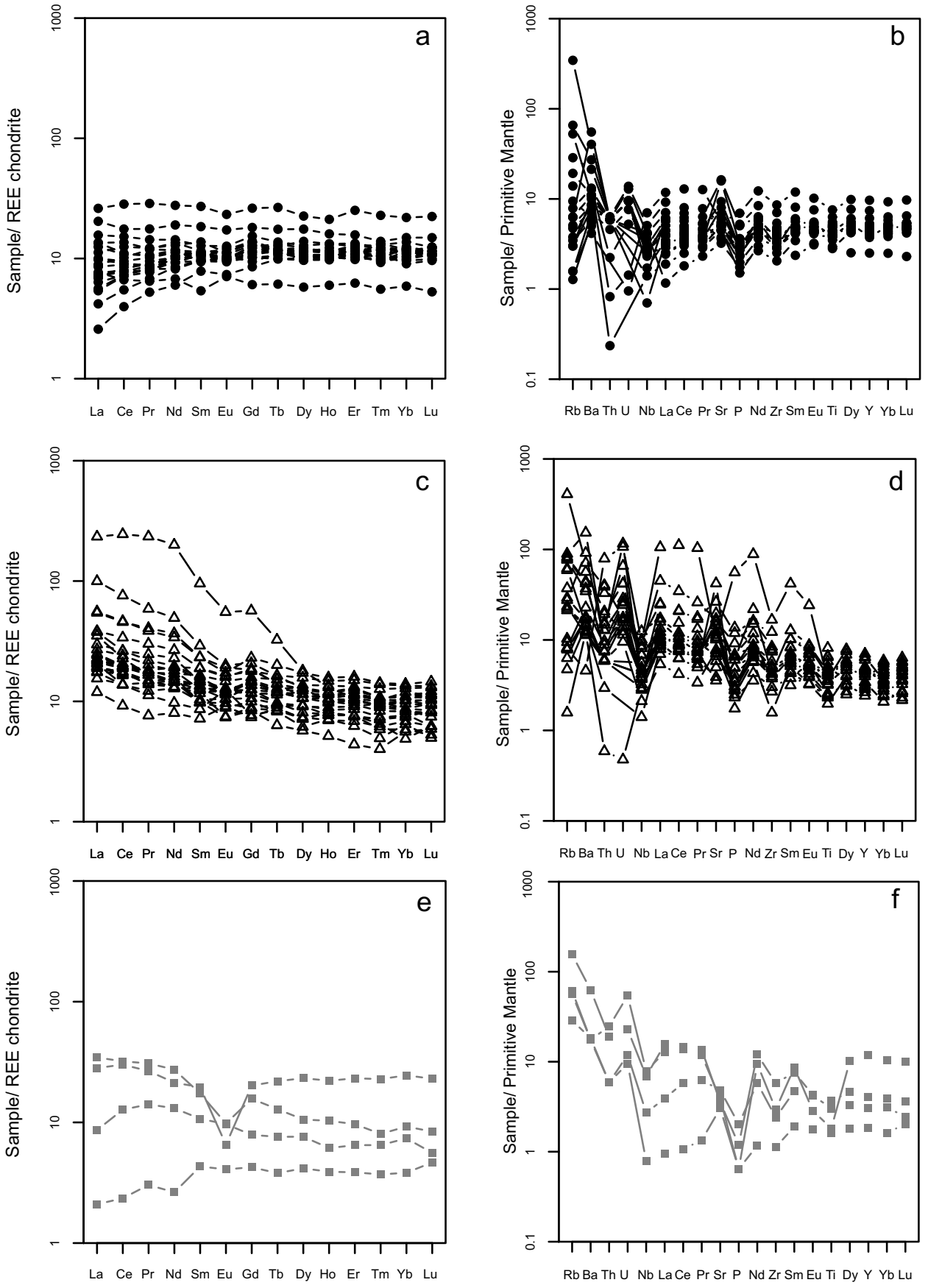

Fig. 13. Trace element patterns of basaltic amphibolites. a, b = LREE-depleted group; c, d = LREE-enriched group; e, f = komatiitic basalts. Normalising factors for a, c and e are from Boynton (1984) and for b, d and f from Sun & McDonough (1989).

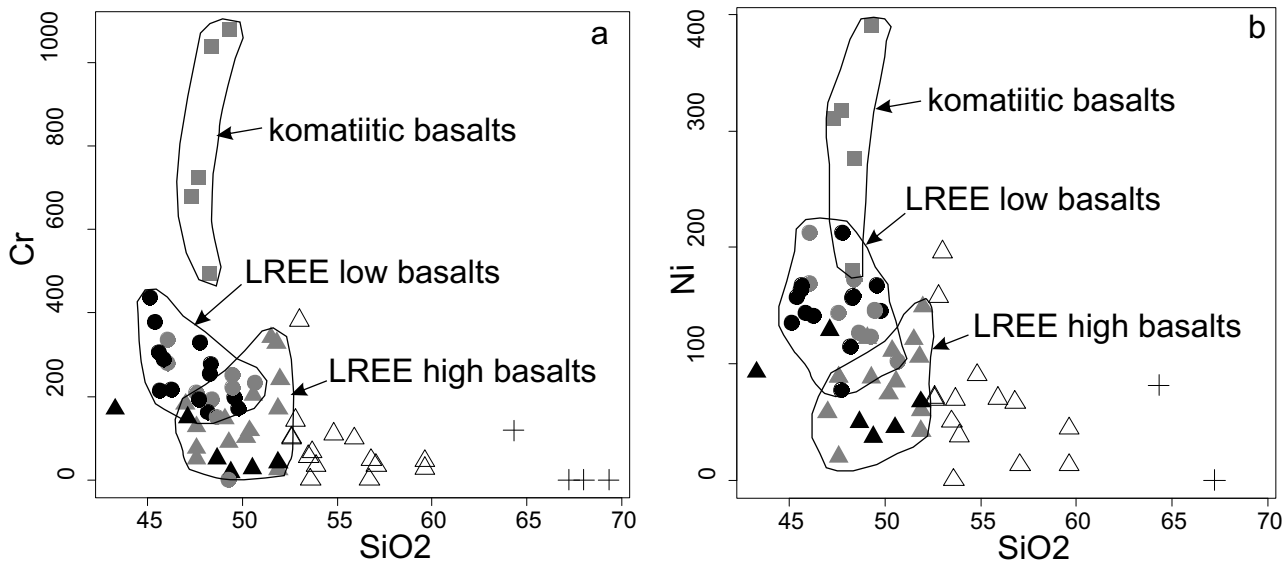

Fig. 14. Cr and Ni vs. SiO2 in LREE-depleted basaltic amphibolites (filled circles), LREE-enriched basaltic amphibolites (filled triangles), andesitic amphibolites (open triangles) and dacitic and rhyolitic amphibolites (crosses). Black symbols denote granulite facies rocks in the Iisalmi and Rautavaara complexes.

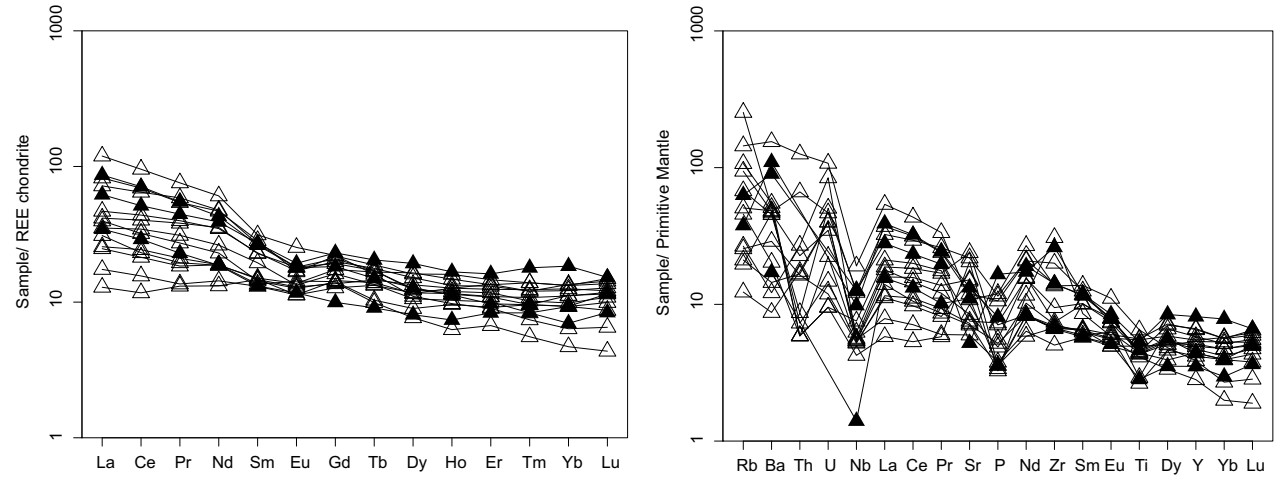

Fig. 15. Trace element patterns of andesitic amphibolites. Black triangles denote granulite facies rocks in the Iisalmi and Rautavaara complexes. Normalising factors as in Fig. 13.

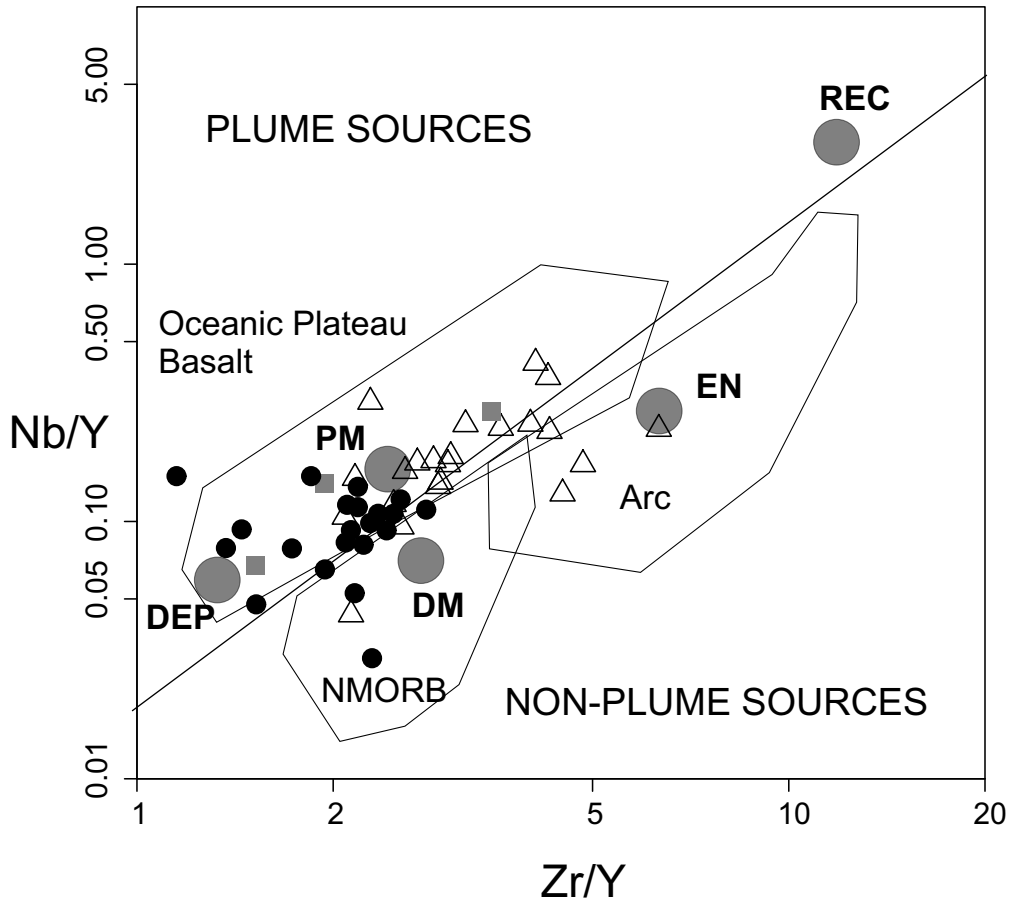

Fig. 16. Nb/Y vs. Zr/Y of basaltic amphibolites. Black circles = LREE depleted basalts, triangles = LREE enriched basalts, grey squares = komatiitic basalts. Abbreviations: PM, primitive mantle; DM, shallow depleted mantle; ARC, arc-related basalts; NMORB, normal ocean ridge basalt; DEP, deep depleted mantle; EN, enriched component; REC, recycled component.

c. 1–2, and tendency to plot between the primitive and deep depleted mantle compositions in the diagram in Figure 16. A smaller number of the amphibolites are LREE enriched, have Zr/Y ratios of c. 3–5 and define on the Nb/Y vs. Zr/Y diagram a trend towards enriched sources that could be the lithospheric mantle or the continental crust. In the field, some of the amphibolites show dyke-like relationships with the host TTGs (Fig. 12f), suggesting that amphibolites in the second group could represent metamorphosed and deformed dykes that have chemically reacted with the TTG crust. This is supported by the higher LILE contents in these amphibolites compared with the first group of amphibolites, which could be restites of the plateau basalts after melting that produced the TTGs.

In terms of primitive mantle-normalized contents, granulite facies rocks are depleted, and amphibolite facies rocks are enriched in U and Th, and there is less enrichment of Ba and especially Rb in granulite than in amphibolite facies rocks (Nehring et al. 2009). This probably reflects a higher degree of melting in granulite facies rocks compared with amphibolites (Nehring et al. 2009).

Greenstone belts

The Karelia Province includes at least sixteen, generally NNW-trending greenstone belts (Slabunov et al. 2006). Case studies have proposed distinct formative settings for the individual belts, i.e. an oceanic plateau setting for the Kostomuksha belt (Puchtel et al. 1998), an island arc setting for the Sumozero-Kenozero belt (Puchtel et al. 1999) and a continental rift setting for the Suomussalmi-Kuhmo-Tipasjärvi and Matkalahta belts (Luukkonen 1992, Papunen et al. 2009, Kozhevnikov et al. 2006). The Finnish part of the Karelia Province contains three major green-

stone belts, the Suomussalmi-Kuhmo-Tipasjärvi belt, the Ilomantsi belt and the Oijärvi belt (Fig. 2). We have new high-precision geochemical data for komatiitic and associated basaltic rocks from the two first named and largest of the belts (Appendix 1). Komatiites are potentially particularly useful in constraining the geotectonic setting of magmatism, because they represent primitive magmas formed during large degree (>30%) melting of the mantle. Consequently, komatiites tend to have low concentrations of incompatible elements, and it is only interaction of the komatiites with lithospheric materials during magma ascent and emplacement (and post-emplacement alteration) that may result in marked decoupling of compatible and incompatible elements.

Kuhmo greenstone belt

The Kuhmo greenstone belt forms the central part of the c. 220-km-long Suomussalmi-Kuhmo-Tipasjärvi greenstone belt (Fig. 2). The supracrustal succession in the Kuhmo belt starts with rhyolitic-dacitic lavas and pyroclastics, whose depositional basement and original thickness is unknown. Felsic volcanic rocks occur in two age groups, 2.84–2.82 Ga and c. 2.80 Ga (Huhma et al. 2012a). The felsic volcanics are overlain by an up to one-kilometre-thick sequence of tholeiitic pillow lavas and hyaloclastites, with sporadic layers of Algoma-type BIF and hydrothermal Mg-Fe precipitates in the middle part of the sequence. The tholeiitic strata are overlain by a sequence of komatiites (total thickness ~ 500 m), komatiitic basalts (~ 300 m), interlayered high-Cr basalts (~ 250 m) and komatiites, high-Cr basalts (~ 250 m) and finally pyroclastic intermediate-mafic volcanics (Papunen et al. 1999, 2009).

The Kuhmo greenstone belt is bounded by TTGs, sanukitoids and GGM-suite plutons. Several previous studies have suggested that the Kuhmo greenstone succession was deposited on older continental crust represented by the TTGs (Martin et al. 1984, Luukkonen 1992, Papunen et al. 1999, 2009). However, no unconformity or superposition relationship between the TTGs and the greenstone belt supracrustals has ever been demonstrated. Nor is the concept of an old sialic

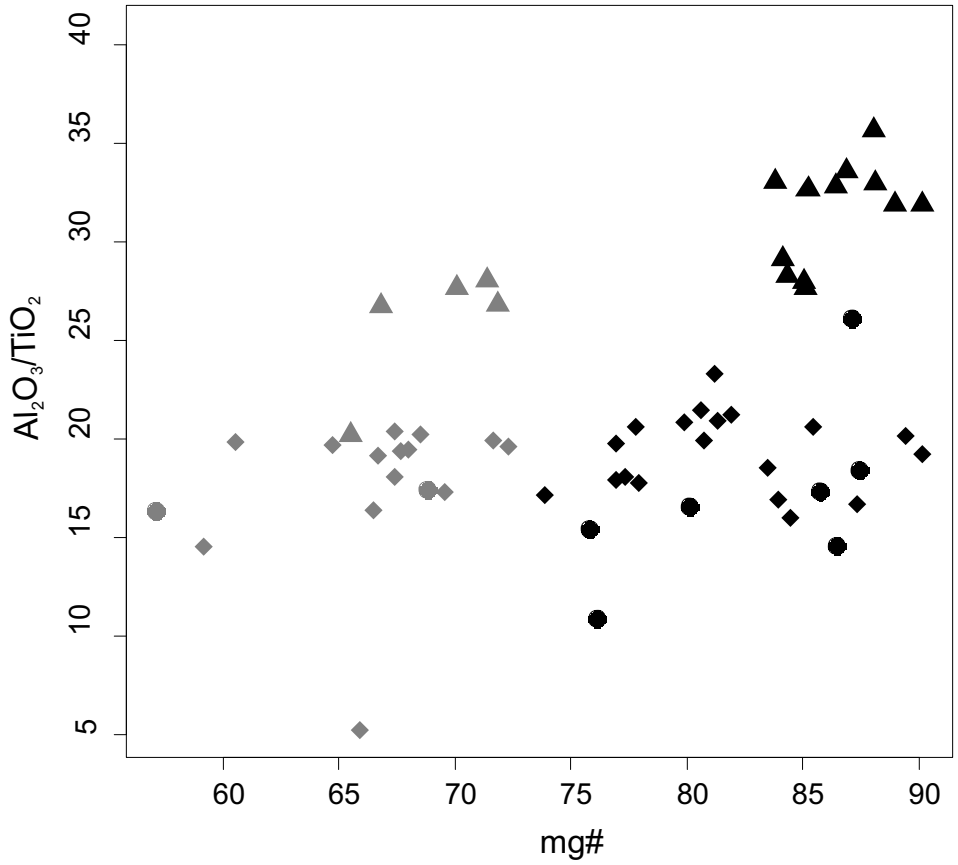

Fig. 17. Al_2O3/TiO_2 vs. mg# of komatiites (black symbols) and komatiitic basalts (grey symbols) in Kuhmo (diamonds), Ilomantsi (filled circles) and Kovero (filled triangles).

basement supported by the more recent isotope geochemical and age data (e.g. Käpyaho et al. 2006, Huhma et al. 2012a). With the exception of one sample from the mesosome of a migmatite from Lylyvaara, c. 30 km east of the Kuhmo greenstone belt (2942 ± 6 Ma; Käpyaho et al. 2007), all samples from the surrounding TTGs yield crystallisation ages younger than the volcanic rocks of the greenstone belt. Furthermore, Käpyaho et al. (2006) concluded, based on an extensive Sm-Nd isotope study, that the plutonic rocks in the Kuhmo area represent relatively juvenile material without a major input from significantly older crust. Neither do the εNd from +1.2 to +2.4 of intermediate and felsic volcanic rocks in Kuhmo (Huhma et al. 2012b) indicate that they would contain significant amounts of older crustal material, as one could expect if they originated in a narrow continental rift as suggested by Papunen et al. (2009). However, Mesoarchaean, 2.94 Ga felsic volcanic rocks with negative εNd values exist in the Suomussalmi belt north of the Kuhmo belt (Huhma et al. 2012a, b). This difference suggests that the Suomussalmi and Kuhmo belts may represent separate volcanic belts that were juxtaposed just during the Neoarchaean terminal accretional/collisional events.

Ilomantsi greenstone belt

The supracrustal sequence in the Ilomantsi greenstone belt is dominated by sedimentary rocks intercalated with less abundant komatiites, tholeiites, low-Ti tholeiites, andesites, dacites and banded iron formations. The lowermost unit starts with mafic pillow lavas, but predominantly consists of felsic pyroclastic and epiclastic sedimentary rocks. The depositional environment was dominated by two distinct but overlapping felsic volcanic complexes, probably locally subaerial, but that nevertheless developed within mostly relatively deep, turbidite-dominated basins (Sorjonen-Ward 1993). Thin tholeiitic intercalations and komatiitic sheet flows occur in the upper part of the succession, typically associated with banded iron formations. The komatiites are generally massive recrystallized in structure, and only locally preserve such relict features as cumulus textures or flow top breccias (O´Brien et al. 1993). No primary silicate minerals are preserved in the komatiites, as they have been pervasively altered and recrystallised to tremolite-chlorite-serpentine rocks or chlorite-talc-rich schists. Locally, the komatiites are demonstrably intercalated with felsic volcanic rocks.

Vaasjoki et al. (1993) reported a TIMS U-Pb age of 2754 ± 6 Ma on zircon from a plagioclase-phyric andesite that represents the stratigraphically lowermost units of the Ilomantsi greenstone belt. The majority of detrital zircon grains in the nearby metasediments are of the same age (Huhma et al. 2012a). Previous studies on the Ilomantsi belt have documented a close relationship between volcanism, sedimentation, deformation and pluton emplacement (Sorjonen-Ward 1993) implying rapid c. 2.75 Ga crustal growth in the region. All exposed contacts between supracrustal rocks and granitoids have been interpreted to be intrusive (Sorjonen-Ward & Luukkonen 2005), and the granitoids cannot therefore represent the basement to the Ilomantsi greenstone belt, nor a dominant source of the material in the supracrustal sequences.

Chemical composition of komatiites in Kuhmo and Ilomantsi

Komatiitic rocks from Kuhmo and Ilomantsi show generally similar major element compositions (Appendix 1), but differ significantly in terms of their trace element concentrations. Both suites have the characteristics of the aluminium-undepleted, Munro-type komatiites, having average Al_2O_3/TiO_2 ratios of c. 18.9 (Kuhmo) and 17.4 (Ilomantsi), but there is considerable scatter, particularly in the Ilomantsi data. Komatiites and komatiitic basalts of the Kovero greenstone belt, which flanks the Ilomantsi belt in the SW, have high Al_2O_3/TiO_2 ratios, reflecting their low TiO_2 content at a given Al_2O_3 and MgO level (Figs. 17–18). In both the Ilomantsi and Kuhmo lavas, Ni, Co and Cr increase as a function of MgO and Mg# in a way that is indicative of low-pressure fractionation of olivine and chromite being the main factor controlling compositional variation. This is consistent with the relatively differentiated nature of the lavas, as chromite is usually undersaturated in komatiites with > c. 25% MgO (Barnes & Roeder 2001). Kovero komatiites seem to differ from the Ilomantsi and Kuhmo komatiites, having overall higher Cr/MgO ratios (Fig. 18).

Komatiites from the Kuhmo and Ilomantsi belts show distinct variation in their incompatible trace element concentrations. The Kuhmo komatiites and komatiitic basalts have generally flat primitive mantle normalised patterns showing only moderate depletion in LREE (Fig. 19), as is common for Al-undepleted komatiites. In contrast, Ilomantsi komatiites have highly fractionated patterns with high LREE/HREE ratios and distinct negative Nb-Ta and Ti-anomalies. The close similarity in trace element patterns

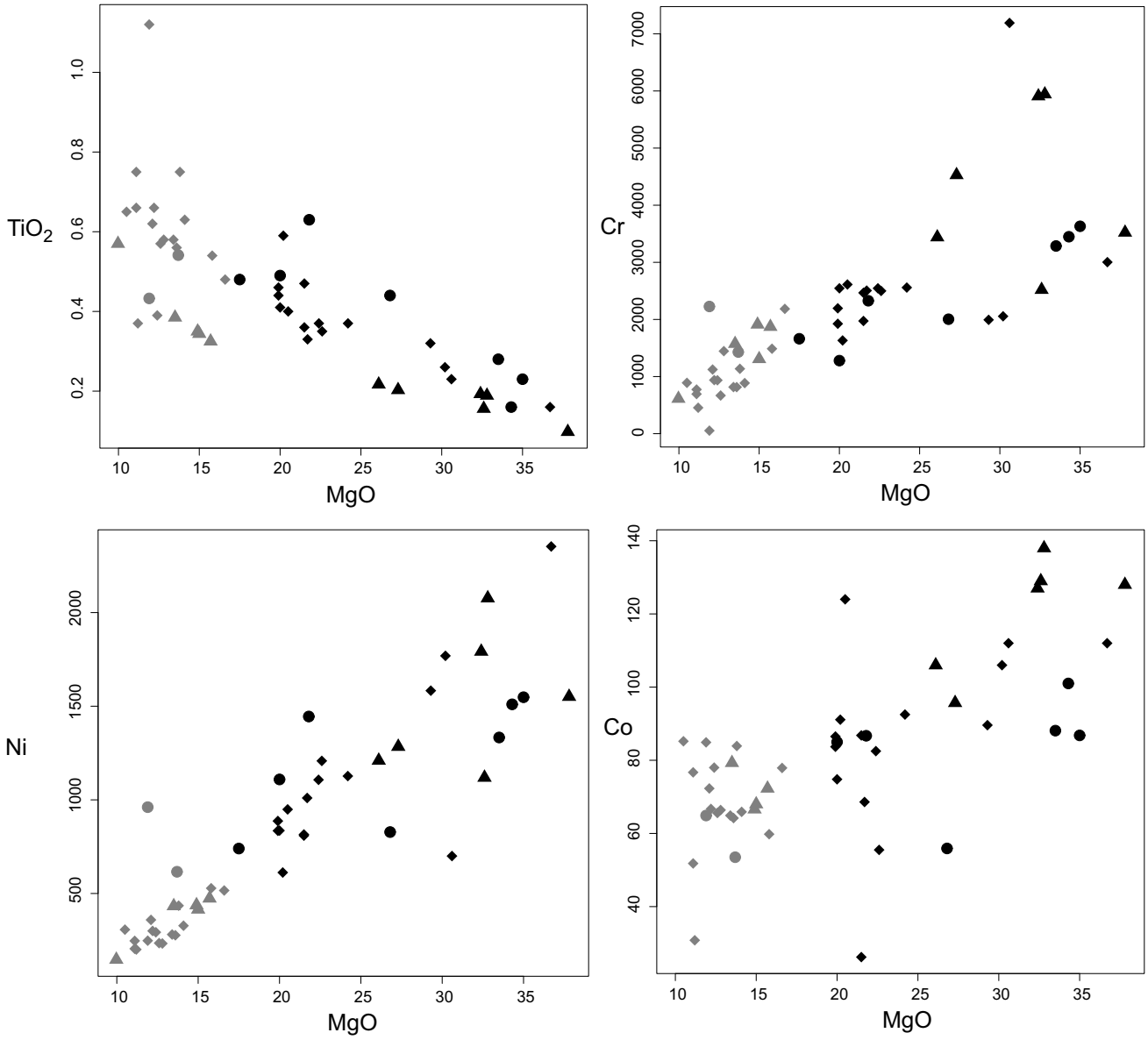

Fig. 18. TiO_2 (wt%), Cr, Ni and Co (ppm) vs. MgO of komatiites and komatiitic basalts in Kuhmo, Ilomantsi and Kovero. Symbols as in Fig. 17.

between the komatiites and associated rhyolites and dacites (O'Brien et al. 1993) is a clear indication of extensive interaction of the komatiites with the felsic volcanics. Interestingly, the komatiitic basalts from Ilomantsi show less fractionated incompatible trace element patterns than the komatiites, which is inconsistent with derivation of the basalts from the komatiites by crystal fractionation. A likely explanation is that the komatiitic basalts evolved from the komatiitic magma already prior to the eruption, within transient storage chamber(s) at depth. During subsequent eruptions the komatiites assimilated more felsic volcanics than the komatiitic basalts, possibly due to their higher eruption temperatures.

Owing to post-eruption alteration, obviously in multiple episodes, the Kuhmo and Ilomantsi komatiites are disturbed to various degrees in their isotope systems. For example, in a Sm-Nd isotope study by Gruau et al. (1992), it has been shown that the Kuhmo komatiites produce a Sm-Nd isochron yielding an age of c. 1.9 Ga, indicative of resetting of the Sm-Nd isotope system of these Archaean rocks during Proterozoic metamorphism. We have also conducted Sm-Nd studies for both Kuhmo and Ilomantsi komatiites, for most part on samples that we believe represented the least altered materials (Huhma et al. 2012b). The results are nevertheless broadly similar to those of Gruau et al. (1992). Therefore, Sm-Nd

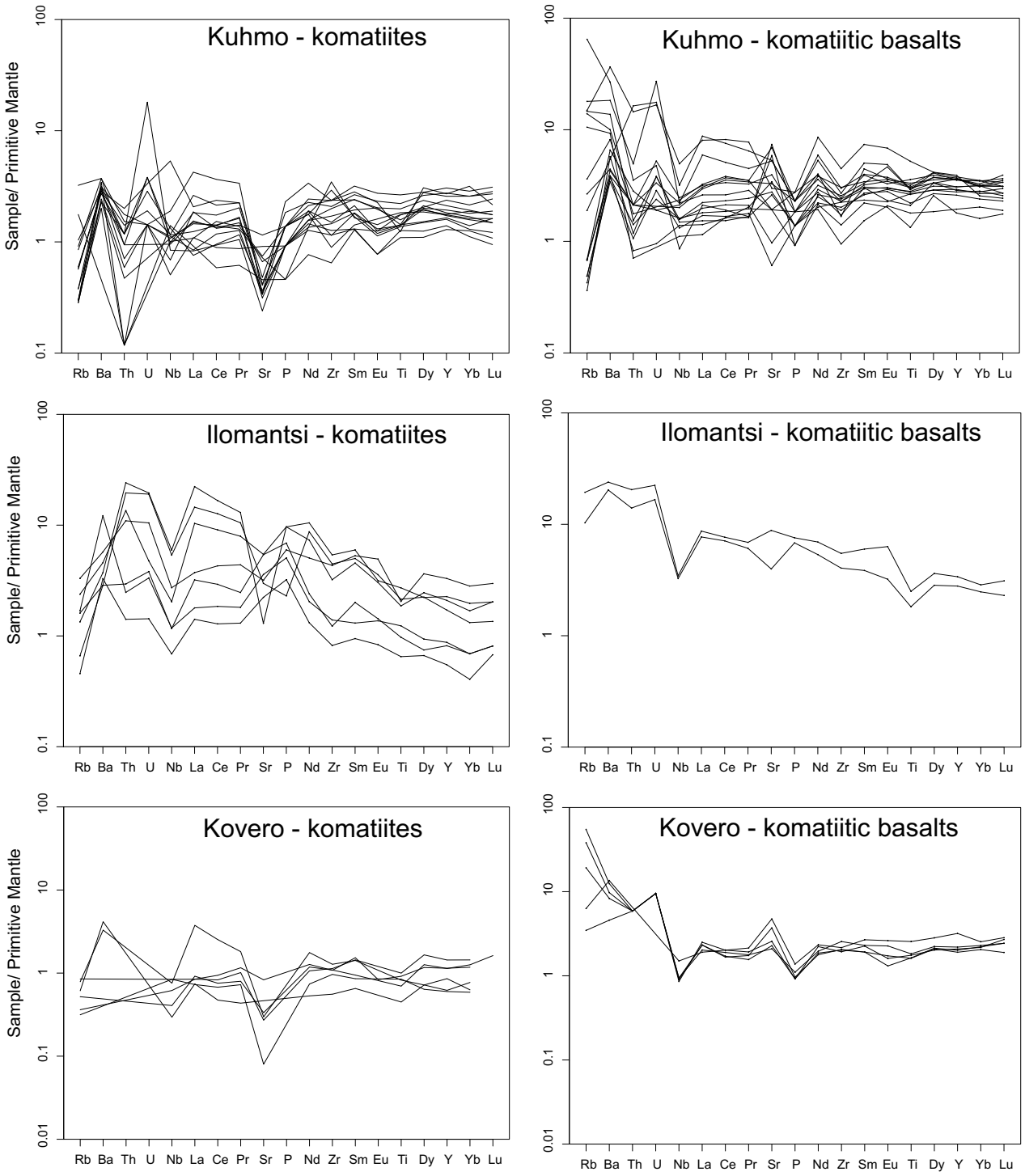

Fig. 19. Primitive mantle-normalized trace element patterns of komatiites and komatiitic basalts in Kuhmo, Ilomantsi and Kovero. Normalising factors are from Sun and McDonough (1989).

isotope analyses for these rocks are unlikely to provide any precise information on their mantle source domains.

Condie (2005) has shown that using ratios of highly immobile elements such as Nb/Th, Zr/Nb, Zr/Y and Nb/Y it is possible to characterise at least some isotopically distinct mantle domains, as they are inferred for young oceanic basalts.. In terms of Nb/Y and Zr/Y ratios, Kuhmo komatiites plot close to the demarcation line between plume and non-plume source compositions (Fig. 20c). Most samples cluster between primitive mantle (PM) and shallow depleted mantle (DM) compositions, and there are many plottings towards the deep depleted plume component (DEP). In the Zr/Nb vs. Nb/Th plot (Fig. 20d), the Kuhmo komatiites also plot close to the oceanic plateau basalts, but at somewhat higher Zr/Y values, probably indicating minor pre-eruption fractionation of chromite (cf. sita). Overall, the Kuhmo komatiites show an affinity to oceanic plateau basalts derived from a slightly depleted primitive mantle (PM)-type source, with a minor deep plume signature. Importantly, these komatiites clearly have not been derived from a depleted MORB-type source, and there is also little indication of enriched and recycled mantle components in their source, or input from continental crust during their ascent and eruption.

Radiometric age determinations

U-Pb

During the past decades, a large number of thermal ionisation mass spectrometry (TIMS) U-Pb age determinations on zircon from Archaean rocks have been carried out at the Isotope Laboratory of the Geological Survey of Finland (GTK). Recently, the secondary ion mass spectrometer (SIMS) of the Nordsim laboratory and

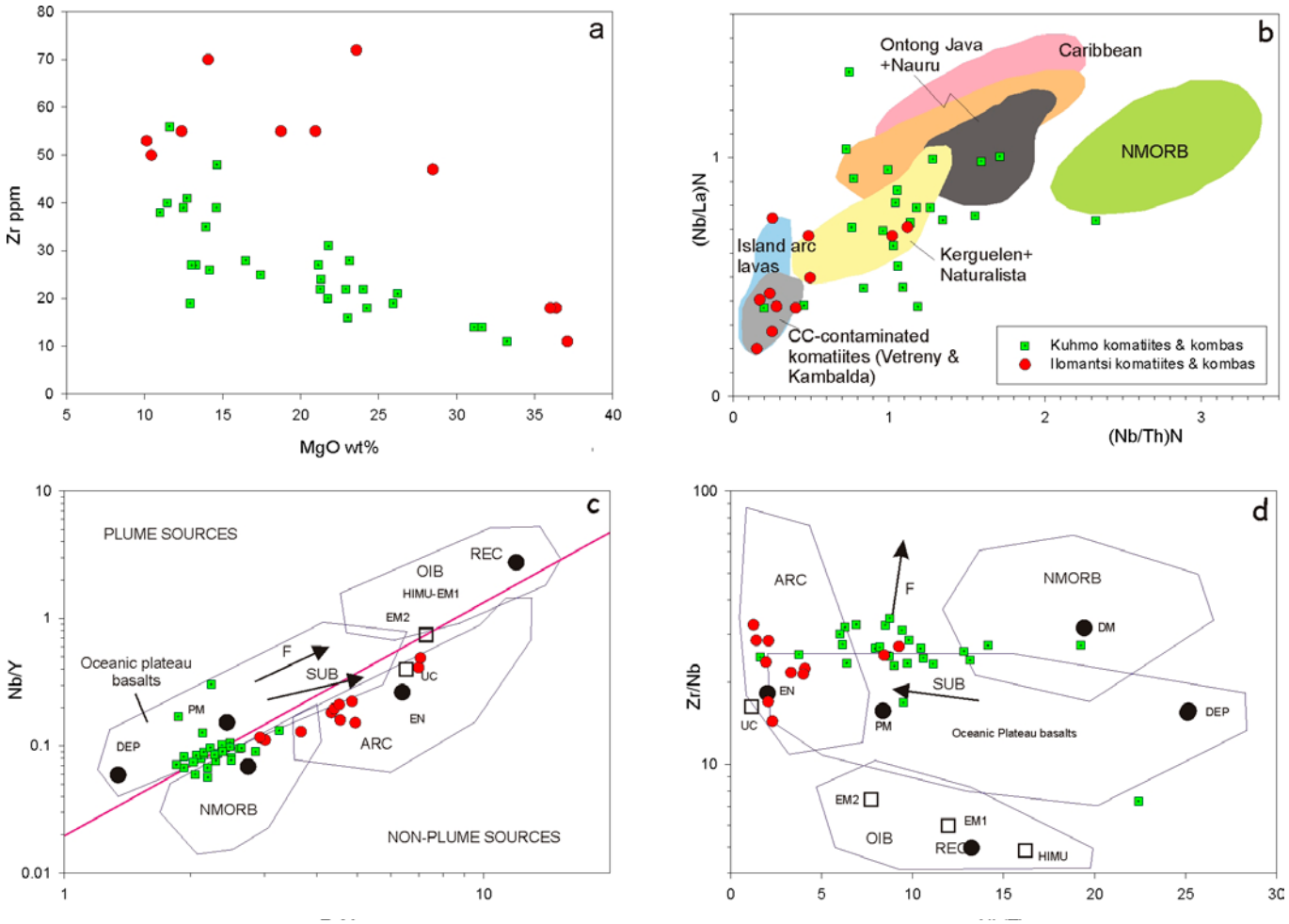

Fig. 20. Zr-Nb-Y-Th-La ratios in the komatiites and komatiitic basalts of Kuhmo and Ilomantsi. Abbreviations (Condie 2005): UC, upper continental crust; PM, primitive mantle; DM, shallow depleted mantle; HIMU, high mu (U/Pb) source; EM1 and EM2, enriched mantle sources; ARC, arc-related basalts; NMORB, normal ocean ridge basalt; OIB, oceanic island basalt; DEP, deep depleted mantle; EN, enriched component; REC, recycled component. Arrows indicate the effects of batch melting (F) and subduction (SUB).

multiple-collector inductively coupled plasma mass spectrometer (LA-MC-ICPMS) of GTK have also been used in the age determination of Archaean rocks. Figures 21–22 present most of the zircon age data available from plutonic and volcanic rocks in the Finnish part of the Karelia Province. It is evident from the diagrams that TTGs age mostly between 2.83–2.72 Ga, and within this range cluster in two groups separated by a c. 20 Ma time gap; in the older group, TTGs are 2.83–2.78 Ga, and in the younger group 2.76–2.72 Ga. The >2.78 Ga TTGs occur almost exclusively outside the Ilomantsi complex (Fig. 21). In the Ilomantsi greenstone belt, volcanic rocks and related dykes are 2.76–2.72 Ga. From the Ilomantsi complex there have thus far been only two observations of Mesoarchaean rocks (Huhma et al. 2012a), which is consistent with observations from the Central Karelia subprovince in Russia (Lobach-Zhuchenko et al. 2005, Bibikova et al. 2005, Slabunov et al. 2006), suggesting that most of the Central Karelia crust is relatively young, c. 2.76–2.72 Ga. However, some porphyritic dykes that intruded into mafic volcanic rocks have older, c. 3.0 Ga zircon populations (Vaasjoki et al. 1993). Two datings for felsic volcanic rocks from the Kovero greenstone belt SW of Ilomantsi give ages of c. 2.88 Ga (Huhma et al. 2012a). These results indicate that the Ilomantsi greenstone belt is not a completely juvenile Neoarchaean formation, but includes at least some reworked Mesoarchaean material. Volcanic rocks in the other greenstone belts are dated mostly at 2.84–2.80 Ga (Huhma et al. 2012a). Mesoarchaean c. 2.95 Ga ages are yielded by some volcanic rocks and TTGs in the northern part of the Lentua complex and by some TTGs in the Siurua complex. In the Western Karelia subprovince, rocks whose zircon ages are > 3.0 Ga seem to exist only in the Iisalmi and Siurua complexes (Hölttä et al. 2000, Mutanen & Huhma 2003, Lauri et al. 2011). The GGM suite rocks, mostly of c. 2.73–2.66 Ga, occur all over the studied area. The youngest Neoarchaean zircon ages are from granulites in the Rautavaara and Siurua complexes and leucosomes of migmatites giving ages of c. 2.65–2.63 Ga and c. 2.71–2.65 Ga, respectively. These ages have been interpreted to date the high-grade metamorphism of lower and mid-crust (Mutanen & Huhma 2003, Mänttäri & Hölttä 2002, Käpyaho et al. 2007, Lauri et al. 2011).

Sm-Nd

The TIMS/SIMS/LAMS U-Pb zircon age determination localities do not yet evenly cover

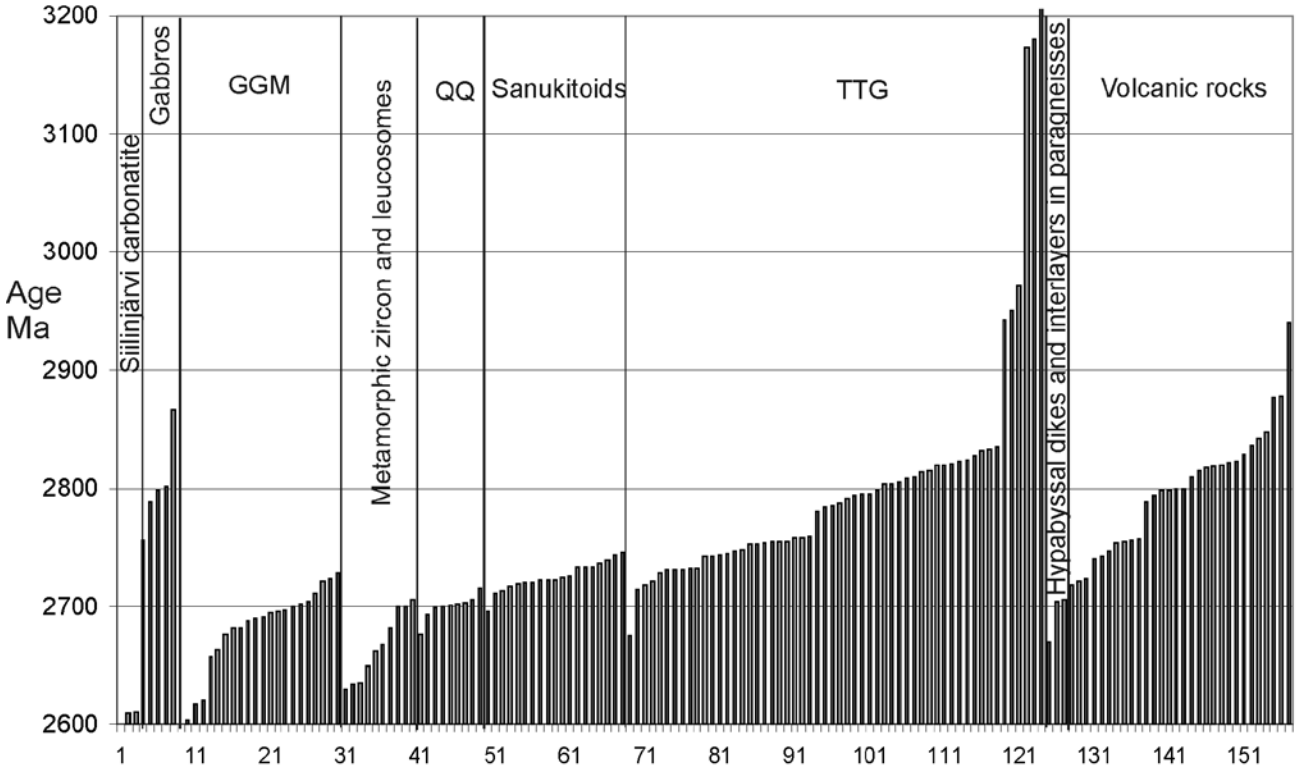

Fig. 21. Histogram showing the distribution of the U-Pb ages on zircon of various Archaean lithologies in the Finnish part of the Karelia Province.

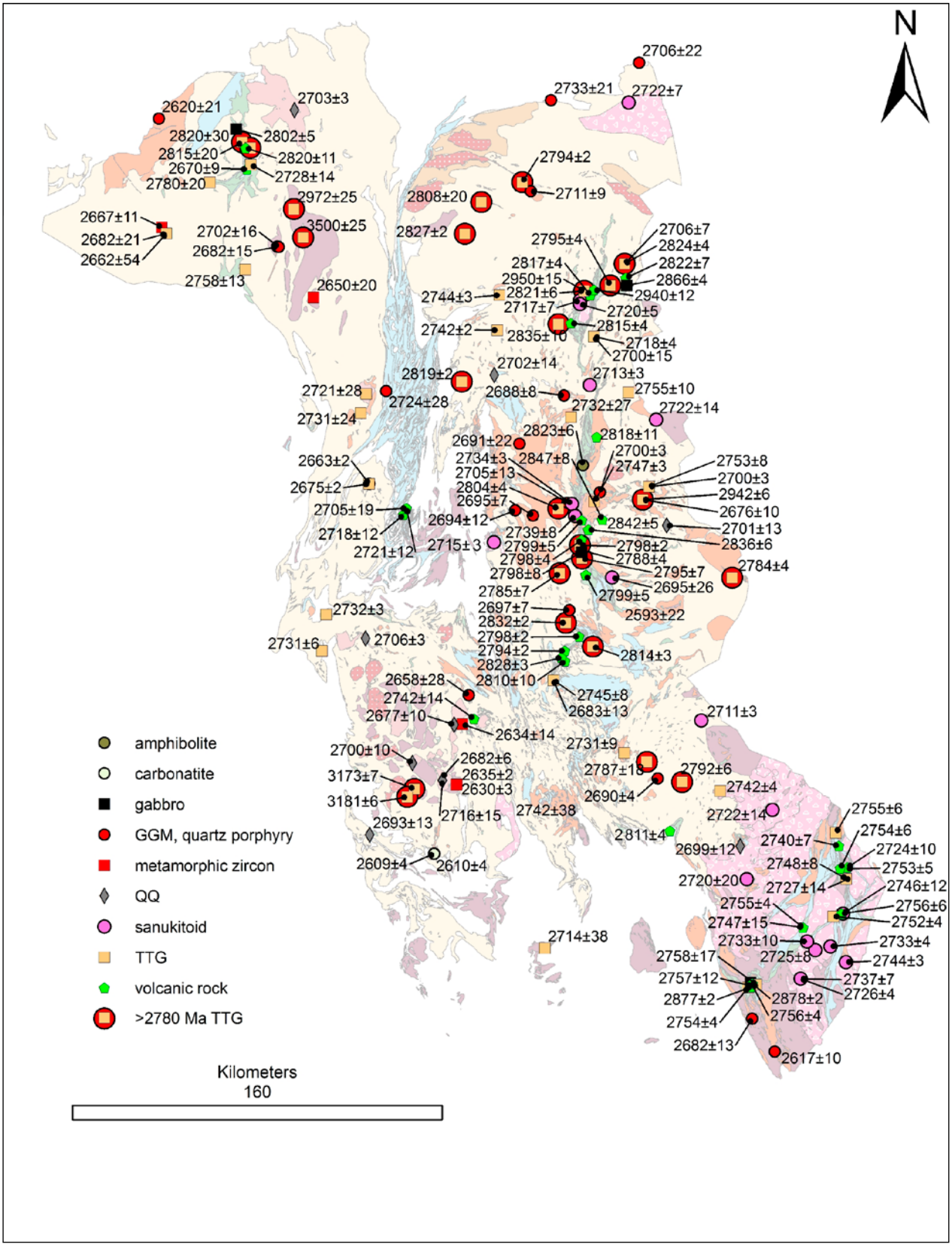

Fig. 22. Sites for the U-Pb age determination samples (Ma). The base map is from Fig. 2.

the Archaean area of Finland (Fig. 22), and some relatively large areas remain untouched. Hence, some surprises may arise with future gap filling, remembering, for example, the small area of the 3.5 Ga Siurua gneisses. Sm-Nd analyses have been carried out from most of the samples used for the U-Pb analyses on zircon. For this work, many additional TTG samples were analysed to improve the regional cover of the Sm-Nd data. These samples were partly from our own sample sets and partly from the Rock Geochemical Database of Finland (Rasilainen et al. 2007). Whole rock chemistry was used to select samples with the least obvious metamorphic alteration. The analytical data are presented by Huhma et al. (2012b). Figure 23 shows the distribution of the T_{DM} model ages on a geological map of the study area.

The various geochemical groups of TTGs observed in this work do not correlate with Sm-Nd model ages or ε_{Nd} values in any simple way. The diagrams in Figure 24 show the REE patterns and the Sm-Nd (T_{DM}) model ages of a large number of the analysed TTGs. Even in the youngest age group, where the model ages are < 2.8 Ga and ε_{Nd} +0.9 - +2.4, and which thus by and large represents juvenile Neoarchaean materials, all geochemical types are represented, and the same pattern also holds true in the oldest model age group. The granodioritic 3.5 Ga Siurua gneiss has a high REE content, strongly fractionated REE pattern (sample A1602 in Fig. 24d) and negative ε_{Nd}(2.7 Ga) of –10.8, in contrast to the 2.96 Ga Isokumpu granulite facies orthogneiss, which belongs to the HREE-depleted and Eu-positive group (sample A1603 in Fig. 24d and Mutanen & Huhma 2003). With a few exceptions, model ages that are around or older than 3.0 Ga are from the Siurua complex and from the northern parts of the Lentua complex, indicating that rocks in these areas include a greater Mesoarchaean component than elsewhere in the Finnish Archaean.

SIMS ages on detrital zircon in paragneisses

Kontinen et al. (2007) concluded in their study on the Nurmes paragneisses that the deposition of the protolith wackes took place at c. 2.70 Ga, which is in the range observed in U-Pb ages of the youngest dated detrital zircon grains. Nearly 50% of the grains were dated at 2.75–2.70 Ga. The whole rock compositions of the Nurmes paragneisses suggest that the source terrains mainly comprised TTGs and sanukitoid-type plutonic and mafic volcanic rocks. Huhma et al. (2000) analysed zircon from metasediments in the Kalpio complex (Hölttä et al. 2012) and found that most zircon grains are c. 2.73 Ga and the others from 2.8 to > 3.0 Ga. Huhma et al. (2012a) analysed detrital zircon in metasediments from five other localities in the Karelia Province, and the results were similar to those from the previous studies. Most of these samples predominantly contain c. 2.73–2.75 Ga zircon grains, which suggests that the Neoarchaean intrusions of this age produced most of the sedimentary detritus. Mesoarchaean 3.2-2.8 Ga zircon grains were rare in all paragneiss and also other metasedimentary samples.

According to Bibikova et al. (2005), zircon from sanukitoids has higher Th/U ratios (>0.5) than zircon in TTGs (<0.5). Given that most 2.75–2.72 Ga zircon grains from paragneisses have Th/U ratios > 0.5 (Fig. 25), sanukitoids indeed may have been one of their main sources, although it has to be noted that high Th/U in zircon is not restricted to sanukitoids, but is also found in samples of the other main rock groups.

Lower crustal xenoliths

Mantle and lower crustal xenoliths recovered from c. 500- to 600-Ma-old kimberlites near the southern boundary of the Lentua complex provide pertinent information on the petrology and physical properties of the lower crust of the Archaean Karelia Province (Hölttä et al. 2000, Peltonen et al. 2006). The lower crustal xenoliths are almost exclusively from mafic granulites. Mineral thermobarometry, together with isotopic, petrological and seismic velocity constraints, imply that the lower crustal xenoliths are derived from the weakly reflective, high-V_p layer at the base of the crust (40–58 km depth; Hölttä et al. 2000, Peltonen et al. 2006). Single grain zircon U–Pb dates and Nd model ages (T_{DM}) from the xenoliths imply that the bottom high velocity layer is a hybrid layer consisting of both Archaean and Proterozoic mafic granulites. Many of the studied xenoliths record only Proterozoic zircon ages (2.5–1.7 Ga) and Nd model ages (2.3–1.9 Ga), implying that the lower crust contains a significant juvenile Palaeoproterozoic component (Hölttä et al. 2000, Peltonen et al. 2006). Only a small fraction of zircon grains separated from the xenoliths give Archaean ages typically in the range of 2.7–2.6 Ga. Mesoarchaean zircon grains are almost absent. The oldest zircon ages, up to c. 3.5 Ga, and Nd T_{DM} model ages of c. 3.7 Ga of the xenoliths

are similar to those from the oldest gneisses in the Siurua complex. Based on these data, the lowermost crust probably originated as Archaean mafic gneisses, but was repeatedly intruded by Proterozoic mafic magmas 2.5–1.80 Ga ago.

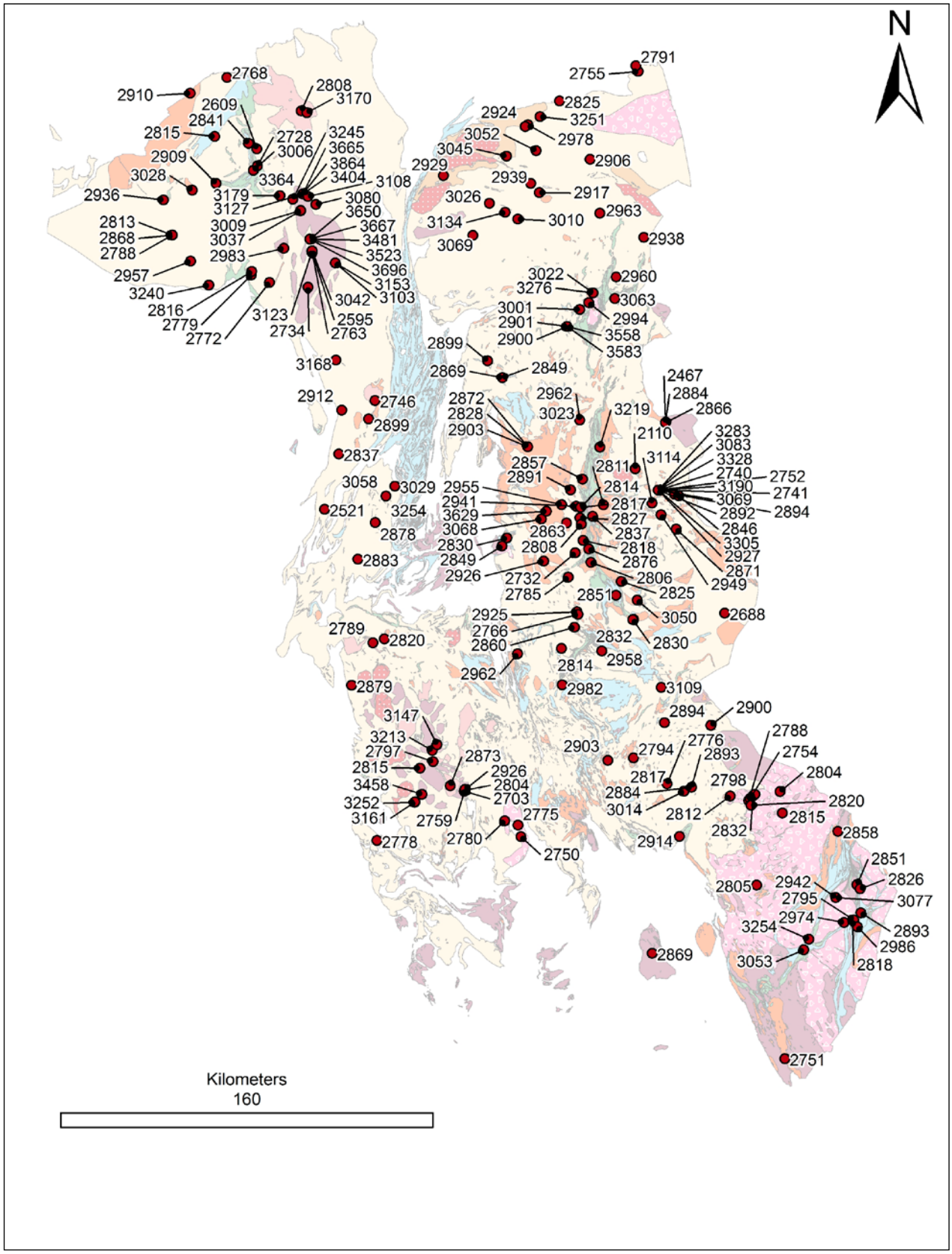

Fig. 23. Distribution of the T_{DM} model ages (Ma). The geological base map is from Fig. 2.

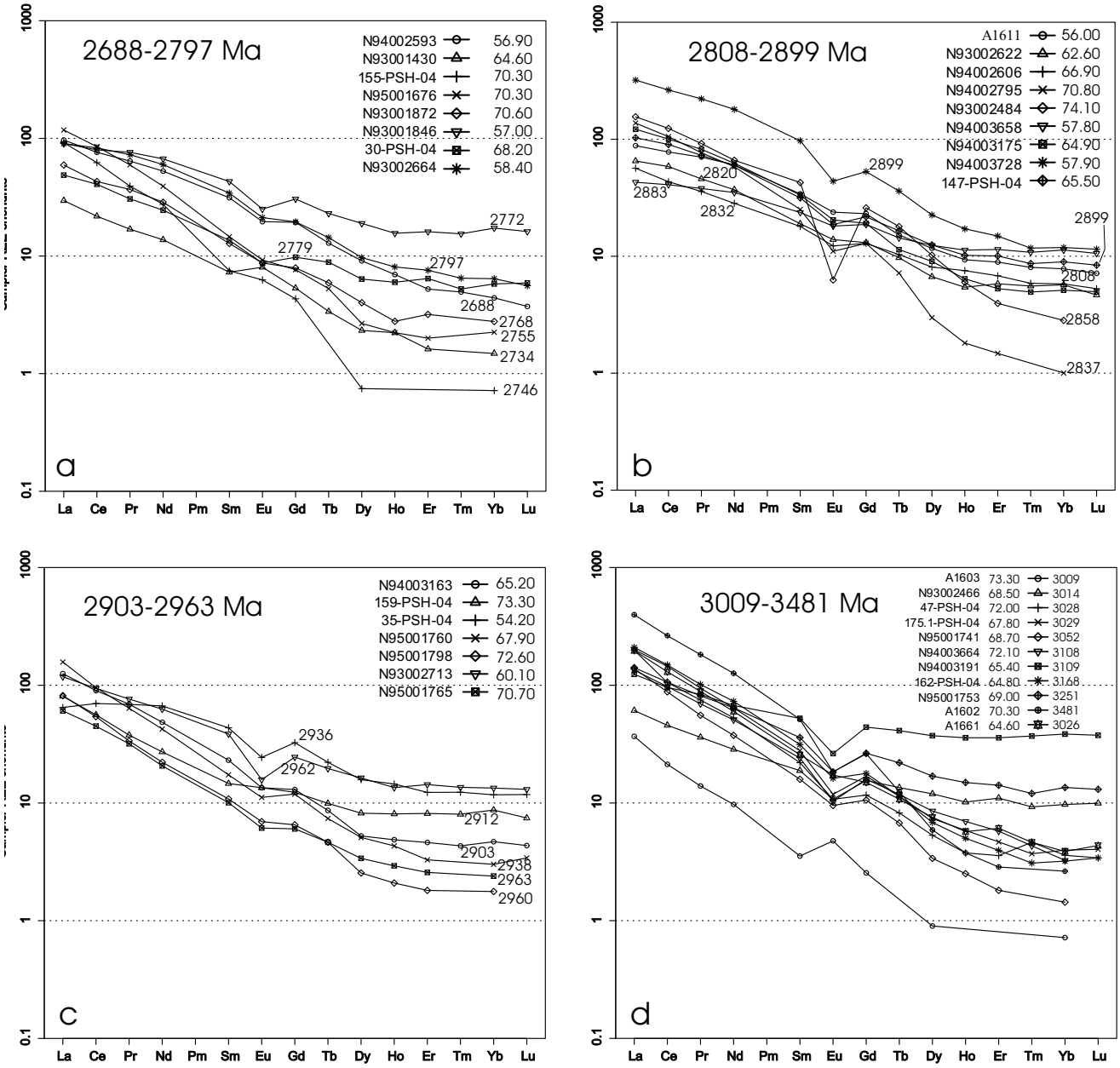

Fig. 24. REE patterns of the samples used for Sm-Nd analyses. The numbers next to the curves are for the model ages and the insets in the upper right corner of the boxes show the SiO_2 content of the sample.

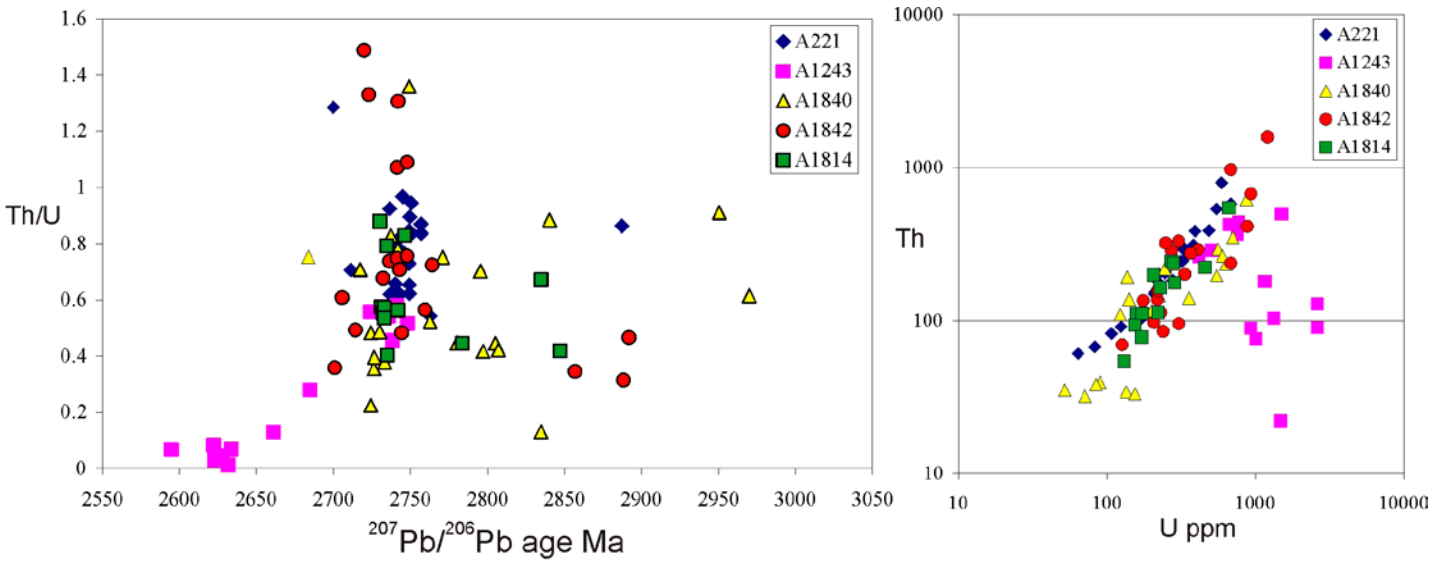

Fig. 25. Th/U ratios in zircons of the paragneisses, based on analyses by Huhma et al. (2012a). The sample A1243 is from a metasediment which was metamorphosed in granulite facies.

Metamorphism

Amphibolites and paragneisses in TTG complexes

Ubiquitous evidence of melting and migmatisation of felsic but also mafic rocks within the Western Karelia Province implies it was mostly metamorphosed in upper amphibolite and granulite facies conditions. Partial melting was often extensive, leading to the intense migmatisation that characterizes so many localities. Lower grade rocks are found in the inner parts of the Kuhmo-Suomussalmi and Ilomantsi greenstone belts that often show mid- or low amphibolite facies mineral assemblages, well preserved primary structures and only a little or no migmatisation. Because of the dominance of the mineralogically monotonous gneissic TTG rocks, suitable mineral assemblages - especially garnet-bearing paragenesis - for the study of pressure-temperature evolution are not common.

For this work, samples were taken from garnet-bearing amphibolites and paragneisses that sometimes have a garnet-hornblende-plagioclase-quartz or garnet-biotite-plagioclase-quartz mineral assemblage. Figures 26 and 27 show the localities for which pressures and temperatures have been obtained, using Thermocalc (Powell et al. 1998) and TWQ (Berman 1988, 1991) average PT calculations and grt-bt-pl-qtz thermobarometry (Wu et al. 2004). Low P/T granulite facies rocks occur sporadically in all complexes, but medium-pressure granulites, metamorphosed at c. 9–11 kbar and 800–850 °C, are only found in the Iisalmi complex (Hölttä & Paavola 2000). The Siurua complex comprises mafic granulites with hbl-cpx-opx-pl-qtz±grt assemblages, for which maximum metamorphic pressures and temperatures of c. 6 kbar and 750 °C have been calculated (Lalli 2002). Compared with the mafic pyroxene granulites of the Iisalmi area, garnet is rare in the Siurua mafic granulites, which is also an indication of lower pressures. The granulite occurrences of the Taivalkoski area lack garnet-bearing rocks that would allow reliable PT determinations.

Sanukitoid suite granodiorites in the SE part of the Lentua complex locally contain orthopyroxene, but it is not clear whether the mineral assemblages in these rocks were metamorphic or magmatic (Halla & Heilimo 2009). Amphibolites and paragneisses near these charno-enderbites were metamorphosed in upper amphibolite and granulite facies at c. 6.5–7.5 kbar and 670–750 °C. Pressures obtained for amphibolites elsewhere in the southern part of the Lentua complex are slightly lower, 4.7–5.5 kbar (Fig. 26).

Metamorphic pressures obtained for the Nurmes paragneisses and for the amphibolites around are mostly c. 6.5–7.5 kbar, and corresponding temperatures c. 650–740 °C. Many samples give lower temperatures of c. 600 °C, but they probably record post-peak cooling or Proterozoic metamorphism of the Archaean bedrock, because these rocks are normally migmatised, indicating high metamorphic temperatures.

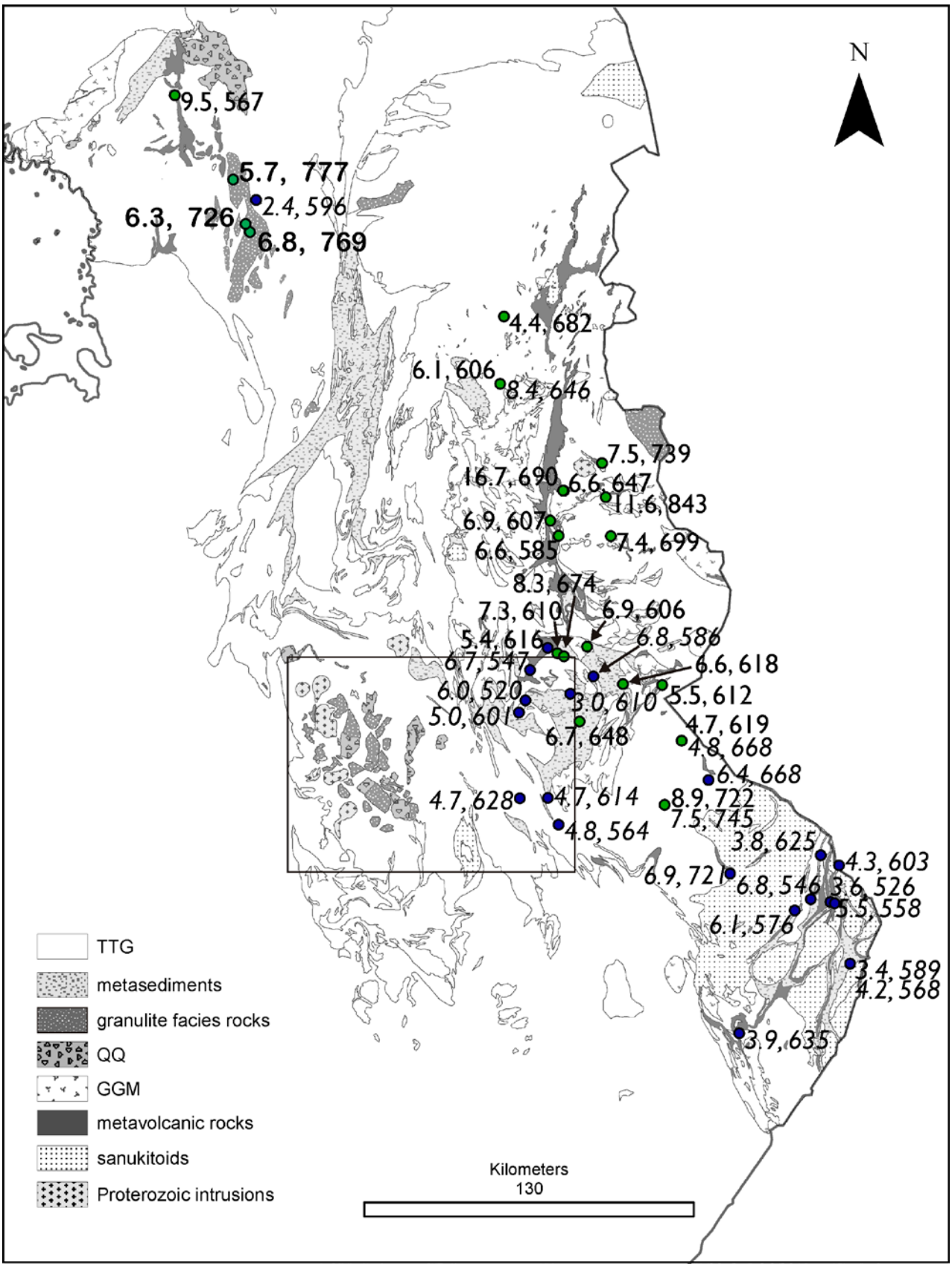

Fig. 26. Metamorphic pressures and temperatures: blue dots = calculated using the garnet-biotite-plagioclase-quartz thermobarometer by Wu et al. (2004); green dots = calculated using the Thermocalc average PT method for garnet-hornblende-plagioclase-quartz assemblage. The inset shows the area of Fig. 26b. The geological base map is from Fig. 2.

Greenstone belts

Garnet bearing samples form supracrustal rocks in the Ilmomantsi belt that typically have the assemblage grt-bt-pl-qtz±ms, occasionally with andalusite and staurolite or more often their muscovite-filled pseudomorphs. Grt-bt thermometry for these samples indicates in most cases crystallization at c. 550–590 °C, similarly to the results of O'Brien et al. (1993) and Männikkö (1988), and these temperatures are in accordance with the observed mineral associations. In the NW part of the Ilomantsi greenstone belt, sillimanite is also present in pelitic rocks, and temperatures from grt-bt thermometry are also higher than in the SE, being c. 600–625 °C. Pressures indicated by the grt-bt-pl-qtz barometer are c. 3.5–5.5 kbar in the central parts of the greenstone belt but >6 kbar in the NW in the sillimanite-bearing metasediments. The lower pressures are of the same order as those obtained by Männikkö (1988) using sphalerite barometry for samples from the Kovero greenstone belt SW of Ilomantsi. Garnets in the Ilomantsi belt samples are often zoned, with cores richer in Mg than rims, indicating a pressure decrease during garnet growth.

Previous studies on the Kuhmo-Suomussalmi greenstone belt have resulted in evidence of a decrease in metamorphic grade from outer to inner parts of the belt. According to Tuisku (1988), geothermometry suggests metamorphic temperatures as low as 500 °C for the inner and up to 660 °C for the outer parts of the belt. Pressures obtained using the sphalerite barometer applied to sphalerite inclusions in pyrite are mostly between 6–7 kbar but range in some cases as high as c. 13 kbar (Tuisku 1988).

An interesting observation was made for a patch of garnet-bearing amphibolites east of the Kuhmo greenstone belt. Noting the standard tholeiite basaltic whole-rock composition of these amphibolites, it is very surprising that they do not comprise any matrix plagioclase, but only minor albite and oligoclase inclusions in garnet (Fig. 28). The observed ranges of the anorthite content in the plagioclase inclusions in two microanalysed samples are An10–An30 and An1–An20, indicating that some of the inclusions are almost pure albite. The garnet hosts are rich in grossular (Xgrs 0.25–0.35, Xgrs = Ca/(Fe+Mn+Mg+Ca)) and spessartine (Xsps 0.10–0.12) but Mg-poor (Xprp 0.05–0.09), which indicates that the meta-

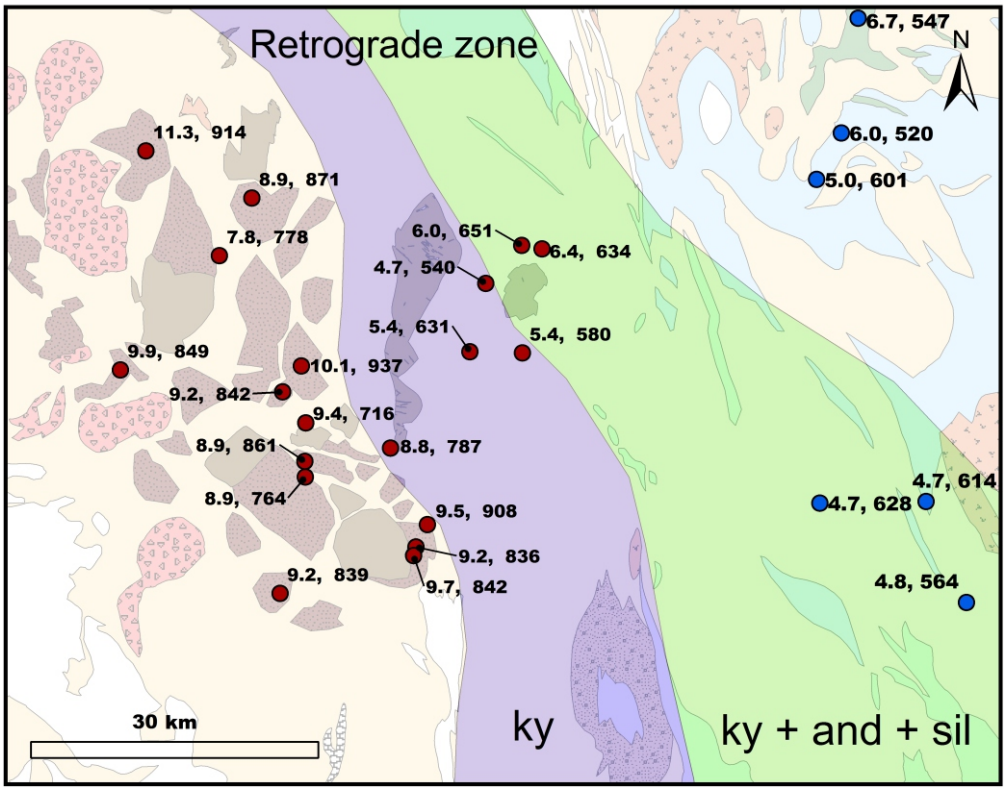

Fig. 27. Metamorphic pressures and temperatures in the Iisalmi and Rautavaara complexes, calculated using the TWQ program, after Hölttä et al. (2000) and Mänttäri and Hölttä (2002) (red dots). Blue dots as in Fig. 26a. Purple and green colours show the zones where the Proterozoic retrogression is pervasive, in purple areas kyanite is the only Al_2SiO_5 polymorph in peraluminous rocks and in green areas all three Al silicates are found, sometimes coexisting.

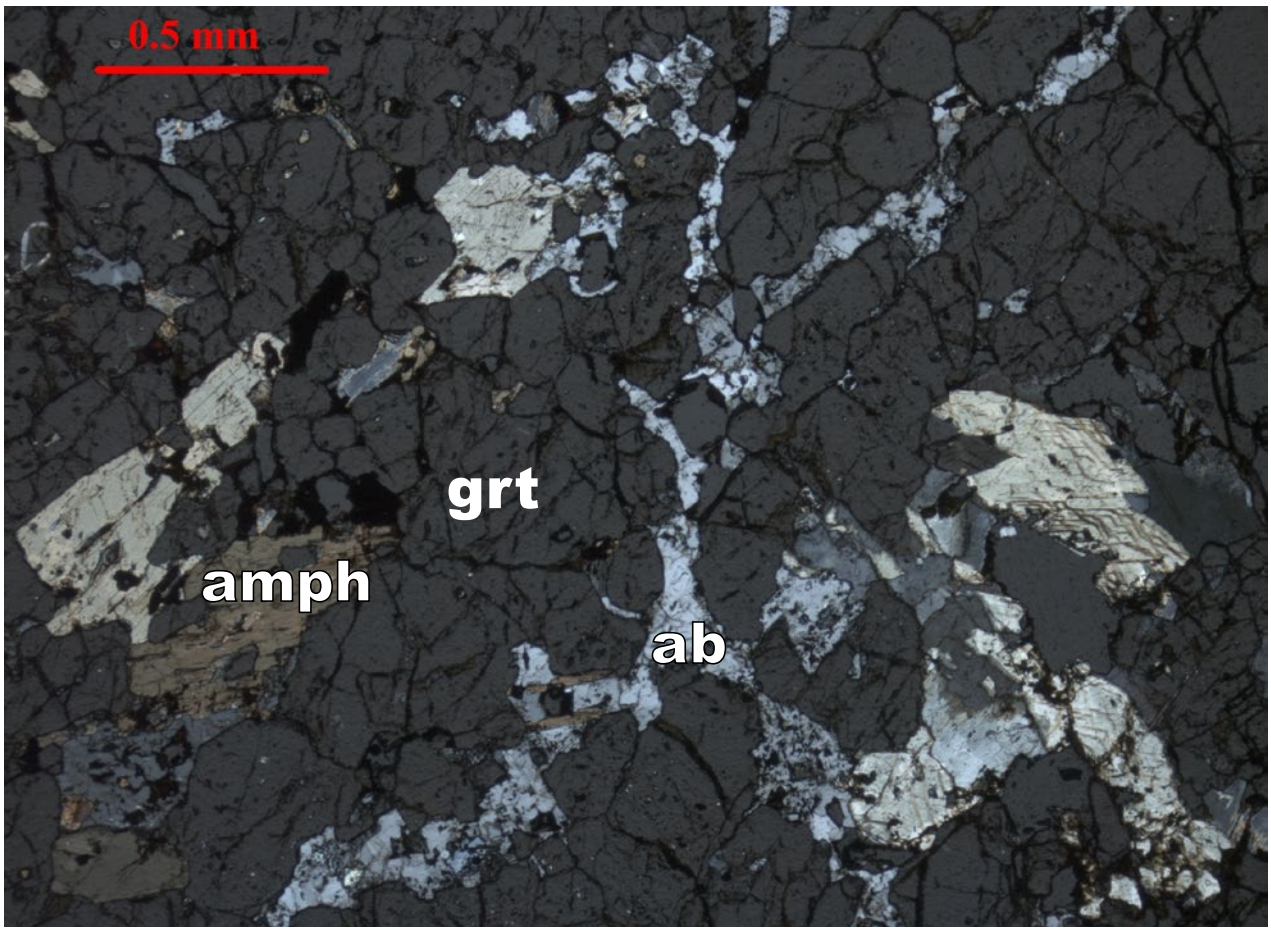

Fig. 28. Albite inclusions in garnet in amphibolite east of the Kuhmo greenstone belt.

morphic temperatures were not very high during garnet crystallization. These rocks often contain epidote, sometimes only as inclusions in garnet but occasionally also in the matrix. The P-T pseudosection in Figure 29, calculated for a typical amphibolite composition in the area, shows the upper stability field of plagioclase in the PT space and compositional isopleths of plagioclase in grt-hbl-ep-pl-qtz and grt-hbl-pl-qtz assemblages (calculations using Thermocalc 3.33 software by Powell et al. (1998); http://www.metamorph.geo.uni-mainz.de/thermocalc/. The pseudosection indicates that plagioclase is not stable at pressures above 13–15 kbar at temperatures of 600–650 °C, and that its composition would change to albitic before decomposition with increasing pressure. If an albitic composition An1 of plagioclase is used in the average P calculation, the Thermocalc gives average pressures of c. 16–17 kbar at 600–700 °C.

In the Oijärvi greenstone belt, garnet amphibolites were found in one locality, and relatively high average pressures of c. 9.5 kbar were also recorded for these rocks using the grt-hbl-pl-qtz barometer.

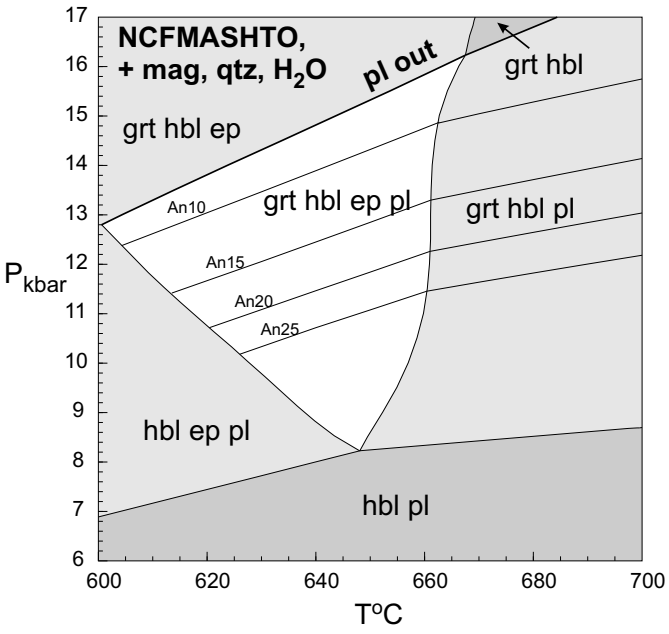

Fig. 29. A pseudosection showing the stability fields of garnet, epidote and plagioclase in a NCFMASHTO system of the composition (mol.%): SiO_2 52.350, Al_2O_3 9.138, CaO 12.598, MgO 11.619, FeO 10.640, Na_2O 2.676, TiO_2 0.653 and O 0.326.

Age of Archaean metamorphism

Because the bulk of TTGs and volcanic rocks in the greenstone belts are from juvenile Neoarchaean additions to the crust, it is not a surprise that signs of Mesoarchaean metamorphic events are difficult to distinguish in the preserved small enclaves of Mesoarchaean rocks. Mänttäri and Hölttä (2002) interpreted a c. 3.1 Ga zircon population to be metamorphic in the 3.2 Ga rocks of the Iisalmi complex. Käpyaho et al. (2007) found an obviously metamorphic zircon population of 2.84–2.81 Ga in a palaeosome of a 2.94 Ga migmatite in the Lentua complex. However, most of the observed high-grade metamorphism and deformation appears Neoarchaean in age.

To more precisely constrain the age of high-grade metamorphism, zircon grains and grain domains from leucosomes of migmatites and from granulites have been dated. The ion probe U-Pb data available on zircon from the leucosomes appear to indicate partial melting over a broad time interval from 2.72–2.67 Ga (Käpyaho et al. 2007). Titanite from amphibolite facies rocks also yields broadly similar U-Pb ages. Zircon grains from leucosomes in the Iisalmi granulites give ages from 2.71–2.65 Ga. Metamorphic monazite and zircon from granulite mesosomes have been dated at 2.64 Ga and 2.68–2.61 Ga, respectively (Hölttä et al. 2000, Mänttäri & Hölttä 2002). In the Siurua complex, a TIMS U-Pb age on metamorphic zircon from a mafic granulite is 2.65 Ga and in the Siurua and Ranua complexes leucosomes of migmatitic amphibolites have been dated at 2.68–2.62 Ga (Mutanen & Huhma 2003, Lauri et al. 2011). These age data indicate that migmatisation was a long-lasting event, and mostly coeval with GGM magmatism. The lower crust, represented by the medium-pressure granulites in the Iisalmi complex, retained higher temperatures for a longer time, which supported relatively late crystallization of zircon. The youngest Sm-Nd garnet-whole rock ages in the Iisalmi complex granulites are <2.5 Ga, which indicates that cooling to the closure temperatures of the Sm-Nd system lasted until the Proterozoic era (Hölttä et al. 2000).

Proterozoic metamorphism

The Archaean bedrock in the western part of the Karelia Province underwent a strong reheating during the Palaeoproterozoic Svecofennian orogeny. Evidence of this includes, for example, that biotite and hornblende sampled from Archaean rocks have K-Ar ages typically in the rage 1.8–1.9 Ga. Archaean K-Ar mineral ages are only present in samples from the Iisalmi and Taivalkoski granulites and the Ilomantsi complex (Kontinen et al. 1992, O'Brien et al. 1993). The heating of the Archaean crust has been explained by its burial under a massive overthrust nappe complex ca. 1.9 Ga ago (Kontinen et al. 1992).

Numerous ductile shear zones were developed in the Archaean bedrock during the Svecofennian orogeny. The widths of these shear zones vary from tens of metres to several kilometres (Kohonen et al. 1991). In many places the Proterozoic shearing was associated with high hydrous fluid flows and related chemical alteration, which is reflected, for instance, in alkali-deficient compositions and kyanite- and cordierite-bearing assemblages in originally TTG rocks (Pajunen & Poutiainen 1999). In the eastern part of the Iisalmi complex (Fig. 27), almost all Archaean rocks were ductilely deformed during the Svecofennian orogeny. This is well demonstrated, for example, by the all-encompassing penetrative deformation of the 2.3–2.1 Ga dolerite dykes common in the Rautavaara area. Many of the dykes show shear folds, schistosity and strong lineations dipping mostly to the SW. The foliations and lineations seen in the dykes are also equally strongly seen in the surrounding Archaean country rocks. In the Rautavaara complex, Archaean granulite facies mineral assemblages were decomposed in the Proterozoic metamorphism that took place at c. 550–650 °C and 5–6 kbar (Mänttäri & Hölttä 2002). Similar temperatures and pressures for the Proterozoic metamorphic overprint have also been reported in the Lentua complex (Pajunen & Poutiainen 1999). Deformation microstructures in the Koitere sanukitoid granodiorites in the Ilomantsi complex indicate temperatures of 400–500 °C during Proterozoic metamorphism (Halla & Heilimo 2009). In the Rautavaara complex, Proterozoic metamorphic zones can even be seen; in retrogressed peraluminous rocks next to the east of the granulites of the Iisalmi complex, kyanite is the only Al_2SiO_5 mineral, whereas farther to the east compositionally similar rocks also contain andalusite and sillimanite (Fig. 27).

Palaeomagnetism

Several palaeomagnetic studies on Archaean rocks have been carried out in the Karelia Province, but only in a few cases has stable Archaean remanent magnetization unaffected by Protero-

zoic overprinting been revealed. The main use of palaeomagnetic data in Archaean geology has been in reconstructing the past positions and movement of the craton at different times and comparing its position with other similar-aged cratons. Continental reconstructions have been made particularly with the Superior Province because of the considerable geological similarity between these two cratonic masses. This section reviews the palaeomagnetic data from Archaean rocks in Finland and NW Russia and present models of the Archaean plate configurations of the Karelia and the Superior Provinces.

The 2913 ± 30 Ma Shilos metabasalts located NW of Lake Onega in NW Russia, with preserved remanent magnetization estimated at 2800 Ma (Arestova et al. 2000 and references therein), are the oldest rocks from the Karelia Province for which palaeomagnetic data are presently available. Another case of old remanence is from the NW of Lake Onega, where the 2890 Ma Semch River gabbro-diorite is interpreted to preserve its primary magnetic remanence (Gooskova & Krasnova 1985). However, in both cases the age of remanence is defined based on comparison to the APWP (Elming et al. 1993). Therefore, due to poor age constraints, the data are not used in either case for continental reconstructions.

The most reliable Neoarchaean palaeomagnetic data from the Karelia Province are obtained from the granulite facies enderbites in the Varpaisjärvi area in the Iisalmi complex (Neuvonen et al. 1981, 1997, Mertanen et al. 2006a) and from the orthopyroxene-bearing sanukitoids of the Koitere area in the Lentua complex (Mertanen & Korhonen 2008, 2011). Younger, well-defined Neoarchaean data come from the Shalskiy gabbronorite dyke and granulite-grade gneisses in the Vodlozero subprovince in NW Russia (Krasnova & Gooskova 1990, Mertanen et al. 2006b). Common to all these cases is that they are generally well-preserved from the 1.9–1.8 Ga Svecofennian overprinting, they show high magnetic anomalies compared to surrounding TTG gneisses and their remanence has high stability, the directions of remanence clearly differing from the known Proterozoic remanences.

The Koitere sanukitoids and the Varpaisjärvi enderbites show a steep characteristic remanence component, but in Lieksa the inclination is negative and in Varpaisjärvi positive (Mertanen et al. 2006a, Mertanen & Korhonen 2011). It is interpreted that the steep remanence directions record the long-lasting Neoarchaean metamorphic event at different times, during which the polarity of the Earth's magnetic field has reversed at least once. The remanence of the Koitere sanukitoids is regarded as ca. 2.7 Ga ($^{207}Pb/^{206}Pb$ monazite age of 2685 Ma, Halla 2002) and the Varpaisjärvi granulites as ca. 2.6 Ga (Sm-Nd garnet-whole rock ages 2590-2480, Hölttä et al. 2000). Based on data from Koitere and Varpaisjärvi, the Karelia Province moved from a high polar palaeolatitude of 83° to the palaeolatitude of c. 68°, respectively. The overall data from Koitere and Varpaisjärvi thus imply that at c. 2.7–2.6 Ga the Karelia Province was located at high palaeolatitudes.

DISCUSSION

Adakitic features of TTGs

The mutual compositional similarity of TTGs and modern adakites has been the basis to suggest petrogenetic kinship between the two rock suites (Martin 1999, Martin et al. 2005). Adakites are spatially related to subduction, and the most likely source of their parental magmas has been the basaltic part of a subducted oceanic slab. They seem to be related to an environment where the subduction zone is abnormally hot, allowing the subducting slab to melt (Moyen 2009). Numerical and petrologic models suggest that partial melting of a subducting slab is possible at 60–80 km depth, but only when the subducting oceanic crust is very young (< 5 Ma) and therefore hot, or as a consequence of heating under abnormally high stresses in the subduction shear zone (Defant & Drummond 1990, 1993, Peacock et al. 1994). However, according to Gutscher et al. (2000), most of the known Pliocene-Quaternary adakite occurrences are related to the subduction of 10–45 Ma lithosphere, which, according to numerical models, should not produce melt under normal subduction zone thermal gradients. Gutscher et al. (2000) addressed this by flat subduction that can produce the temperature and pressure conditions necessary for the fusion of moderately old oceanic crust. Variation in the subduction angle has been proposed as a critical factor also controlling the variation observed in geochemical features of the Archaean TTGs.

Smithies et al. (2003) proposed that Archaean subduction was predominantly flat and that the subduction regimes thus lacked well-developed mantle wedges that would produce melts or interact with possible slab-derived melts, in the latter case increasing the compatible element content and Mg contents of the slab melts.

Recently, the usage of the terms adakite, and especially adakite-like, has been expanded to encompass a wide range of rocks that exhibit the high Sr/Y and La/Yb ratios but not necessarily the other criteria of the original adakite definition. This loose usage has led Moyen (2009) to recommend that separate, more precise terms should be used to describe these "adakitic" rocks, and the term adakite should be reserved only for the high-silica adakites that closely correspond to the rocks originally described as adakites by Defant & Drummond (1990). Halla et al. (2009) argued that the term adakite should only be used for unmistakable slab melts and therefore not for such rocks as the TTGs in the Karelia Province. Smithies (2000) also argued that despite the many compositional similarities, most Archaean TTGs actually differ from Cenozoic adakites, especially in that they have on average lower Mg# and higher SiO_2 contents, suggesting that, unlike adakitic melts, the TTG melts did not interact with mantle peridotite.

High Sr/Y and La/Yb ratios can have several causes, such as high Sr/Y sources, garnet-present melting and interactions with the mantle (Moyen 2009). Melts with an adakitic geochemical signature can also be generated by normal crystal fractionation processes from andesitic parental melts, and slab melting is not mandatory for adakite petrogenesis, but adakites or adakite like rocks can instead originate in various geodynamic settings (Castillo et al. 1999, Castillo 2006, Richards & Kerrich 2007, Petrone & Ferrari 2008).

The thickness of Archaean oceanic crust has been estimated at between c. 15 and 45 km (Bickle 1986, Abbott et al. 1994, Ohta et al. 1996), i.e. significantly thicker than typical modern oceanic crust, which is c. 7 km (e.g. Hoffman & Ranalli 1988). Where it was warm and buoyant, it perhaps did not subduct at all, and probably not at a steep angle (Abbott & Hoffmann 1984, Hoffman & Ranalli 1988, Abbott et al. 1994). Björnerud and Austrheim (2004) argued that one likely consequence of the higher geothermal gradient during the Archaean was that ocean crust became thoroughly dehydrated at shallower depths than occurs today. The residual, dehydrated crust would thus have been very strong and too buoyant to sink into the mantle.

Modelling by van Hunen et al. (2004) suggests that if mantle temperatures were indeed higher during the Archaean than presently, even flat subduction was an unlikely process. If this was the case, the obvious lack of interaction with mantle in many TTGs must be explained in some other way. Halla et al. (2009) attributed the low-HREE TTG group to high-pressure partial melting (>20 kbar) of a garnet-bearing basaltic source with little evidence of subsequent mantle contamination. The high-HREE group was generated by significantly lower pressure melting (c. 10 kbar) of a garnet-poor basaltic crust and shows interaction with the mantle by its higher Mg#, Cr and Ni contents. Halla et al. (2009) proposed that the high-HREE TTGs were produced in an incipient, hot subduction zone underneath a thick oceanic plateau/protocrust. For the low-HREE TTGs, they saw a non-subduction setting as probable, proposing that these rocks were generated by deep melting in the lower parts of thick domains of basaltic oceanic crust.

TTG melts and PTX relations of their protoliths

There is a general agreement that the Archaean TTG suite rocks were formed by partial melting from a compositionally basaltic-gabbroic source. The process was evidently fluid-absent partial melting of amphibolites at temperatures of 900–1100 °C and over a large pressure range from 10 to 25 kbar. The composition of products from partial melting is controlled by pressure and temperature, the composition of the source, water availability during the process and the degree of melting. The composition of the partial melts is further modified, for instance, by magma mixing, fractional crystallization and wall rock contamination on their way from the loci of melting to the crystallization sites (Rapp et al. 1991, Martin 1995, Martin & Moyen 2002, Foley et al. 2002, Rapp et al. 2003, Moyen & Stevens 2006, Moyen 2011).

During the fusion process, pressure and temperature control the assortment and abundance of the residual minerals, such as garnet and plagioclase, and consequently the major and trace element content of the TTG melts. For example, the heavy REE is controlled by residual garnet, which is stable in mafic rocks at pressures above c. 9–12 kbar and increases in abundance with increasing pressure. Sr is controlled by plagioclase, which is stable below c. 15–20 kbar. Nb and Ta depend on the presence of residual rutile, which is stable above c. 16–18 kbar (Foley et al. 2002, Moyen & Stevens 2006, Moyen 2011).

In the low-HREE TTG group with positive Eu anomalies, Sr and Sr/Y ratios are high and Nb low. Positive Eu could be explained by plagioclase accumulation, but as TTGs in this group are no more enriched in Al_2O_3, CaO or Na_2O than the other low-HREE TTGs, it is more probable that they represent melting with residual rutile and garnet. In dacitic and rhyolitic melts, the garnet-melt partition coefficients are higher for Sm (2.66) and Gd (10.5) than for Eu (1.5) (Rollinson 1993). Thus, high pressure melting with abundant garnet in the residue would obviously lead to melts that are HREE poor and show a positive Eu/Eu* ratio, which is also predicted by experimental work (e.g. Springer & Seck 1997).

The melting temperature strongly depends on the starting composition, and the solidus temperatures for arc basalts, tholeiitic basalts and komatiitic basalts are thus very different (Moyen & Stevens 2006). The trace element composition of melts principally depends on their protolith concentrations, but through control of the mineral composition of the restite, the major element content of the protolith also affects the trace element composition of the coexisting melt. According to Nair & Chacko (2008), the increase in residual garnet from 5 to 15 wt% changes the La/Yb ratio in the melt fraction from c. 12 to c. 24. Variation in the La/Yb ratio of the melts may be considerable, even under constant P and T, if there is enough compositional variation in the source. Figure 30 shows simplified pseudosections with melting curves and breakdown curves of amphibole, orthopyroxene, garnet and rutile for two compositionally deviating samples analysed from amphibolite intercalations in TTGs, representing tholeiitic and komatiitic basalts with 1 wt.% H_2O. The pseudosections were constructed using the Perple_X 6.6.6 software (Connolly 1990, 2005, Connolly & Petrini 2002, http://www.perplex.ethz.ch/). The composition has a strong influence on the melting temperature but also on the mineral stability fields. In Na_2O and Al_2O_3-poor komatiitic basalt, plagioclase decomposes at pressures that are c. 7–10 kbar lower than in the case of basaltic composition (Fig. 30). This means that in >800°C temperatures komatiitic basalt can produce melts with elevated Sr at pressures that are far below the c. 19–21 kbar range that is broadly the upper stability limit of plagioclase in tholeiitic basalts in these temperatures. Also in komatiitic basalt rutile is present at several kbar lower pressures than in tholeiitic basalt, and consequently komatiitic basalt can produce Nb and Ta depleted melts at lower pressures than tholeiitic basalt.

According to the model calculations also the abundance of garnet is strongly dependent on the composition so that at above c. 10 kbar the komatiitic basalt produces roughly twice as much garnet as the tholeiitic basalt (Fig. 30). Consequently in TTG melts the La/Yb ratio may significantly differ only on the basis of the composition of the protolith.

Sanukitoids and quartz diorites are partly too Mg-rich to represent melts from crustal sources. The high Sr content and low La_N/Yb_N ratio indicate that the quartz diorites originated from a hot and shallow mantle environment, where the temperature was so high that plagioclase was not stable, and the pressure so low that little garnet was present in the residue. Figure 31 shows the proportion of residual garnet during the dehydration melting of amphibolite, and the corresponding La/Yb ratios in the derived melts, according to the experimental work of Nair and Chacko (2008). The garnet mode in the residue in the case of QQs and high-HREE TTGs would have been 5–15 wt%, and much higher in low-HREE TTGs. This could reflect higher pressures of melting in the case of the low-HREE TTGs, but could also indicate a compositionally different source, which would promote a higher garnet mode in the residue.

In the Archaean Earth, low pressure TTGs could have formed, for example, at the base of thick oceanic plateaus (deWit and Hart 1993, Moyen & Stevens 2006). In the greenstone belts, most sequences of mafic volcanic rocks of plateau basalt signatures are not compositionally homogeneous, but typically comprise a variety of compositionally differing tholeiitic and komatiitic basalts and komatiites. In addition, many greenstone belts also contain calc alkaline basalts and andesites-dacites. Modern oceanic plateaux, such as the Kerguelen Plateau, consist of intermediate, felsic and alkaline volcanic rocks, as well as sediments (Frey et al. 2000). It is evident from the above discussion that melting of such heterogeneous packages would produce melts that would also be compositionally heterogeneous and show variable trace element patterns, even in cases where the melting depth was not very high or highly variable.

Greenstone belts

A picture emerging from previous research suggests that the Karelia Province was a collage of TTG and greenstone complexes that originated in various geodynamic settings related to subduction, collision, continental rifting and mantle plumes (Bibikova et al. 2003, Samsonov et al.

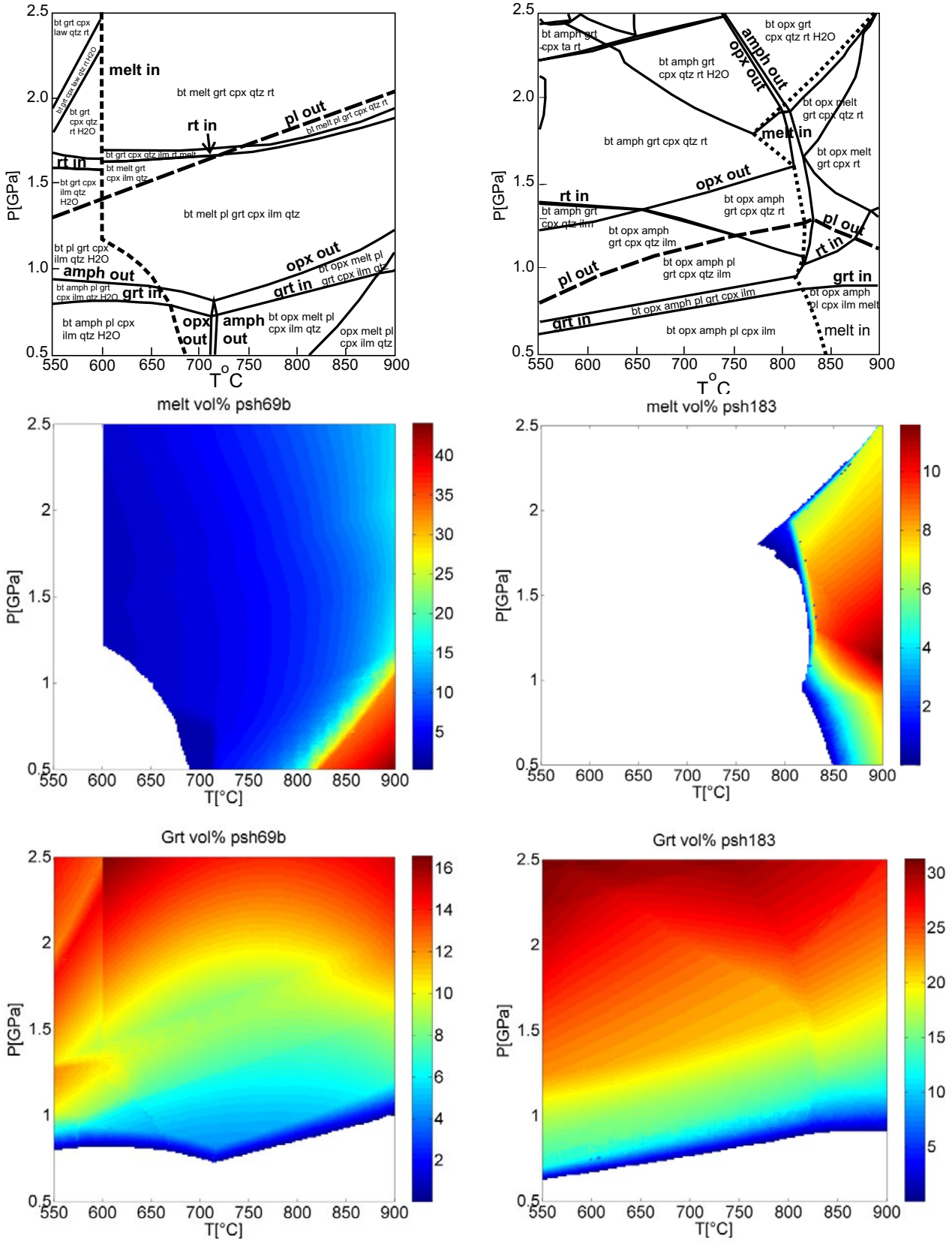

Fig. 30. NCKFMASHTi pseudosections for Fe-rich basaltic granulite (psh69b) and komatiitic basalt (psh183) and lower and upper stability limits of various minerals in these two whole-rock compositions. The solution models used in calculations were: biotite (TCC), amphibole (GlTrTsPg), garnet (HP), orthopyroxene (HP), clinopyroxene (HP), plagioclase (h), ilmenite (WPH), melt (HP). For the original references see http://www.perplex.ethz.ch/PerpleX_solution_model_glossary.html.

Compositions used (in wt.%) are:

	psh69b	psh183		psh69b	psh183
SiO_2	59.63	47.30	CaO	5.49	11.70
TiO_2	1.00	0.35	Na_2O	3.45	1.16
Al_2O_3	13.53	11.50	K_2O	1.97	0.92
FeO	9.68	8.54	H_2O	1.00	1.00
MgO	2.65	14.20			

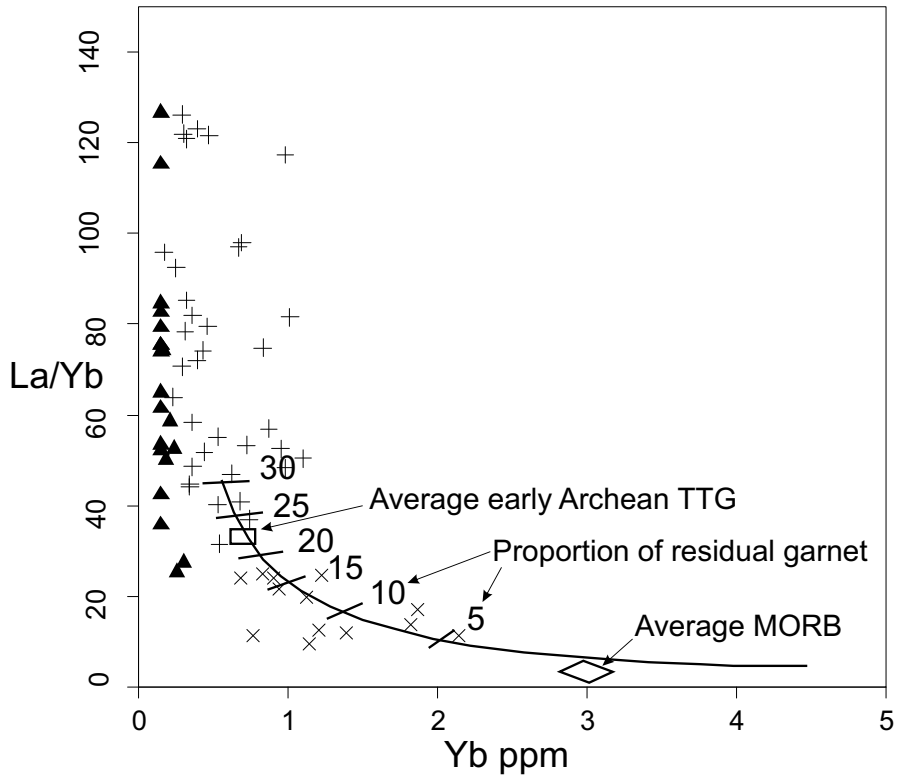

Fig. 31. La/Yb ratios of Karelian TTG plotted on the La/Yb diagram after Nair and Chacko (2008), showing the effect of the abundance of residual garnet on the La/Yb ratio of the melt in 20% melt fraction during dehydration melting of amphibolite. Open triangles = low-HREE TTGs, black triangles = low-HREE, Eu-positive TTGs, crosses = high-HREE TTGs, grey dots = QQs, black dots = orthopyroxene-bearing QQs (enderbites).

2005, Slabunov et al. 2006, Papunen et al. 2009). The greenstone belts have also been interpreted as composite terranes comprising magmatic products from various geodynamic settings involving plumes and arc magmatism (Puchtel et al. 1998, 1999). Archaean greenstone belts can be divided into autochthonous to parautochthonous and allochthonous based on their relationship with the underlying basement rocks (Polat & Kerrich 2000, 2006). According to Thurston (2002), evidence from the Superior Province suggests that many, if not all, greenstone sequences were in autochthonous or parautochthonous units fed from mantle plumes either in continental rift or continental platform settings. Allochthonous models favour the assembly of greenstone belts by horizontal tectonic transport and accretion of various types of oceanic crust in a plate-tectonic geodynamic regime (e.g. Puchtel et al. 1998, 1999, Percival et al. 2004, Percival et al. 2006, Polat & Kerrich 2006). The presence of such features as fold and thrust complexes, orogen-parallel strike-slip faults and tectonically juxtaposed terranes from different tectonic settings, as well as subduction zone geochemical signatures in part of the plutonics and volcanics in the greenstone belts, supports the concept that the accretion of allochthonous terranes was elemental in the growth of many greenstone belts (Polat & Kerrich 2006).

Many komatiite-bearing sequences in Archaean greenstone belts have been interpreted as pieces of dismembered Archaean oceanic plateaux (Kusky & Kidd 1992, Abbott & Mooney 1995, Puchtel et al. 1998). Many greenstone belts are characterized by assemblages that suggest roughly coeval plume-type komatiite-tholeiitic basaltic and arc-type calc alkaline volcanism. This situation has been explained in the Karelia Province in terms of a subduction setting where the arc-type plutonic volcanic rocks formed at the margins of plume-generated thick basalt plateaux that were not able to subduct because of their buoyant nature (Puchtel et al. 1998, 1999). Interlayering of komatiites with subduction-related volcanics has been explained by the interaction of plume and subduction related magmas in such a subduction regime (Grove & Parman 2004).

Grove and Parman (2004) proposed that Archaean komatiites could have been formed by hydrous melting in a subduction environment, which would easily explain the close spatial and temporal association of many komatiites and is-

land arc type volcanic rocks. This idea, which is supported by the experimental work of Barr et al. (2009), is still disputable, however. For example, based on their work on komatiites in Ontario and Barberton, Arndt et al. (2004) and Stiegler et al. (2010) saw little evidence for the hypothesis of hydrous melting.

The Kuhmo greenstone belt – an oceanic plateau?

The basic-ultrabasic volcanics in the Kuhmo greenstone belt consist of komatiites and their evolved counterparts, i.e. komatiitic basalts. The komatiite-basalt sequence is completely devoid of epiclastic and chemical interflow sediments, and it lacks geochemical evidence of contamination by any significantly older continental material. These data suggest an eruptive setting far from continental land masses and hydrothermal vents at oceanic ridges and argues against the origin of the Kuhmo greenstone belt within a continental rift zone, as has been proposed, for instance, by Papunen et al. (2009). Immobile trace element (Zr, Y, Nb, Th) systematics are also inconsistent with the formation in a back-arc setting, but rather suggest an oceanic plateau setting and magma derivation from a mantle plume. The Al-undepleted nature and the trace element characters of the komatiites indicate that they were derived from a source more similar to primitive upper mantle rather than that of depleted MORBs. Furthermore, there is negligible geochemical evidence for the involvement of crust or enriched or recycled mantle sources (EM1, EM2, HIMU). Condie (2005) stressed the clustering of non-arc-related Archaean basalts, in terms of HFSE ratios, close to the primitive mantle values, and suggested on this basis that Archaean mantle plumes had their main source in the "primitive mantle". Our findings support this conclusion, indicating that the late Archaean mantle was less fractionated, or better stirred, than either the early Archaean and post-Archaean mantle.

The U-Pb zircon data (Huhma et al. 2012a) and the Sm-Nd data (Huhma et al. 2012b) on the Kuhmo volcanic rocks provide no evidence for their deposition on a significantly older basement in the Kuhmo region. Felsic volcanic rocks in the central part of the Kuhmo belt formed 2.80 Ga ago, giving the minimum age for the mafic-ultramafic magmatism (Huhma et al. 2012a). We conclude that the Kuhmo komatiites represent fissure-controlled eruptions onto a pre-existing rhyolitic-dacitic-tholeiitic oceanic plateau.

The Ilomantsi greenstone belt – a volcanic arc within an attenuated continental margin?

Komatiites within the Ilomantsi greenstone belt, which is located c. 150 km SSE of the Kuhmo belt, were emplaced within a volcano-sedimentary basin. Magmatism was dominated by felsic volcanism in two major pulses and coeval granitoid plutons. The komatiites were emplaced as thin but extensive sheet flows, and probably also as sills beneath the felsic volcanic edifices. The komatiites and dacites-rhyolites occur intercalated, suggesting that ultrabasic and felsic volcanism was coeval. Both the komatiites and the felsic volcanic rocks have distinctly low Nb/Th, suggesting that the komatiites contain a significant component assimilated from the felsic volcanic rocks. Alternatively, the komatiites could have inherited their arc-signature from a subduction-enriched mantle wedge. However, we consider this model less likely, because the samples enriched in lithophile-incompatible elements are depleted in PGE, which is best explained by the segregation of a sulphide melt from the magma in response to contamination by sulphidic metasediments during emplacement. There is evidence of a significantly older cryptic granitoid basement in the region in the form of inherited c. 3.0 Ga zircon grains in plutonic and subvolcanic felsic rocks and old T_{DM} ages of metasedimentary units in the Ilomantsi belt (Vaasjoki et al. 1993, Huhma et al. 2012a, b). We suggest that the Ilomantsi volcanic rocks represent arc magmatism within an attenuated continental margin where older basement rocks were assimilated by younger arc magmatism.

Supercontinent reconstruction

Several similarities in their geological evolutions can be cited in support of the concept that the Archaean Superior, Hearne and Karelia Provinces were parts of the Neoarchaean-Palaeoproterozoic supercontinent Superia (Bleeker & Ernst 2006).

Comparison of palaeomagnetic data from the Karelia Province with similar-aged poles from the Superior Province (Mertanen & Korhonen 2011, and references therein) shows that Superior was also located at relatively high palaeolatitudes at 2.68–2.60 Ma (Fig. 32a,b). However, the Karelia and Superior Provinces were significantly separated, as there is a c. 30° difference between the latitudes both at 2.68 Ga and 2.60 Ga. Taking into account the maximum errors of the poles from both cratons, the latitudinal distances become

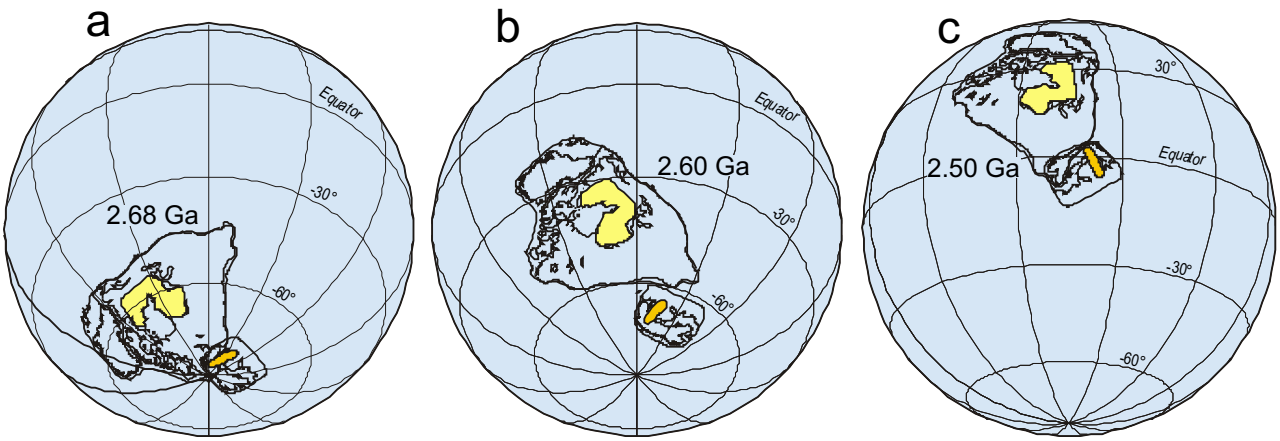

Fig. 32. Continental reconstructions between the Karelia and Superior cratons at 2.68 Ga (a), 2.60 Ga (b) and 2.50 Ga (c).

shorter, and it may be possible that they were even joined at that time. The relative palaeopositions of the two cratons cannot be resolved unequivocally, especially at 2.68 Ga, due to the nearly polar position of the Karelia Province, which allows its rotation in several directions with respect to Superior.

The steeply inclined remanence of the Varpaisjärvi and Lieksa rocks differs distinctly from the 2.50 Ga remanence of the Shalskiy gabbronorite dyke dated at 2510 ± 1.6 Ma in the Vodlozero subprovince (Bleeker et al. 2008). The Shalskiy dyke, as well as the Shalskiy basement gneisses and Vodla River gneisses ca. 50 km east of the Shalskiy dyke, has a shallow southwards pointing remanence direction (Krasnova & Gooskova 1990, Mertanen et al. 2006b) which is interpreted to be 2.50 Ga. This remanence direction positions the Karelia Province at a low equatorial palaeolatitude. The data thus suggest substantial movement of the Karelia Province between the time of cooling at c. 2.60 Ga after the high grade metamorphism and subsequent rifting and minor reworking of the craton at c. 2.50 Ga.

Palaeomagnetic reconstruction between Karelia and Superior Provinces at 2.50 Ga is presented in Figure 32c. Compared with the 2.6 Ga configuration, the palaeopositions between Karelia and Superior are now completely different. The Superior province had drifted across the equator to the latitude of approximately 20° and rotated clockwise by about 45°, so that at 2.50 Ga both provinces were located near the equator, and the Karelia Province along the southern margin of the Superior Province. This reconstruction is in close agreement with the Superia model of Bleeker and Ernst (2006), who suggested that the provinces were together at 2.50 Ga.

Tectonic evolution of the Karelia Province

If the Karelia province was indeed once a part of the supercontinent Superia, then many of the observations and models presented for the evolution of the Superior and Hearne Provinces must also be applicable to the Karelia Province. Several major characteristics in the crustal architecture and composition of the Superior province have long been considered to provide strong support for the operation of modern-style plate tectonics during the Neoarchaean (e.g. Goodwin 1968, Langford & Morin 1976, Card 1990). Tectonic build-up of the province, mostly between 2.72–2.68 Ga, is interpreted in terms of accretionary growth process that involved collisions of many microcontinental blocks and juvenile volcanic arcs (Percival et al. 2006).

Accretionary-type orogeny is often considered one of the main processes behind growth of continental crust with time (Şengör & Natal'in 1996, Cawood et al. 2003, Brown 2009). It may also be applicable to Archaean granite–greenstone terranes, as these are often characterized by linear belt structures in which early accretion of formations from various oceanic tectonic environments and microcontinents is followed by arc-type magmatism (e.g. Kusky & Polat 1999, Bibikova et al. 2003, Samsonov et al. 2005). Neoarchaean accretion of exotic terranes at c. 2.83–2.75 Ga, culminating in a subsequent major collisional event/orogeny at around 2.73–2.67 Ga, may have been the mechanism that generated the basic structure of the Karelia Province, and which was then strongly reworked during the Svecofennian orogeny. The subduction events enriched the lithospheric mantle in LIL elements. At c. 2.76 Ga, a new volcanic arc began to form above a subduction

zone at the margin of the Western Karelia Province, represented now by the Ilomantsi plutonic-volcanic complex. A subsequent slab breakoff or some other subduction-related process at c. 2.72 Ga led to melting of the enriched wedge mantle, producing voluminous sanukitoids and also small amounts of TTGs (Lobach-Zhuchenko et al. 2008, Halla et al. 2009, Heilimo et al. 2010, 2011).

Kontinen et al. (2007) interpreted SHRIMP and TIMS U-Pb age determinations on zircon grains from the paragneiss mesosomes and crosscutting granitoid plutons to constrain the deposition of protolith wackes to c. 2.70 Ga. Some caution should be taken with this interpretation, as the newly obtained precise age of 2715 ± 2 Ma for the Loso sanukitoid intrusion (Huhma et al. 2012a), which crosscuts the local Nurmes type paragneisses, suggests that metamorphic effects may have influenced the youngest ages obtained for detrital zircon grains in the paragneisses. Deposition more likely took place in a short (10 Ma or less) period just before 2715 Ma, and it is possible that deposition of the Nurmes sediments and sanukitoid plutonism were partly overlapping events. Trace element and U–Pb data suggest that the source comprised mainly 2.75–2.70 Ga TTG and/or sanukitoid-type plutonic and mafic volcanic rocks. The close similarity of the paragneiss and sanukitoid compositions is an important clue to the timing and tectonic setting of the deposition. It is clear that TTG-dominated crust, presently characterizing the Western Karelia subprovince, was not the dominant source of the Nurmes sediments. The presence of MORB-type volcanic intercalations in Nurmes wackes suggests that they were deposited in a back arc or intra-arc setting (Kontinen et al. 2007). The exotic nature of the Nurmes sediments as overthrust must be considered as a serious option.

After the intrusion of the last juvenile granitoids, the QQ quartz diorites at 2.70 Ga, the crust was deformed and metamorphosed. The related process could have been collisional stacking after closure of ocean basins, which thickened the crust between 2.71–2.64 Ga. Vibroseismic images of the crust, as well as tectonic observations from the exposed bedrock, indicate ductile thrusting and related crustal stacking with tectonic transportation from southeast to northwest (Kontinen & Paavola 2006, Korja et al. 2006, Sorjonen-Ward 2006). A similar seismic structure characterised by gently dipping, often listric reflections, is also common in other Neoarchaean cratons, and it is interpreted to result from horizontal compression (van der Velden et al. 2006). Fragments of Mesoarchaean (micro)continental fragments, such as the Siurua and Iisalmi complexes, are present as slices in the thickened Neoarchaean crust. Reflecting heat production by radioactive decay in the thickened, predominantly felsic-granitoid crust, a Barrovian-type medium P/T metamorphic framework was developed. The middle and lower parts of the crust were partially melted, producing migmatites and the GGM suite intrusions (Mänttäri & Hölttä 2002, Käpyaho et al. 2007, Lauri et al. 2011).

The thickness of the Neoarchaean crust in the Iisalmi complex was at least c. 40 km on the basis of c. 10–11 kbar pressures from the granulites that represent lower crust and bear evidence of long-term residence at high-temperatures (Mänttäri & Hölttä 2002). The significance of the amphibolite facies high-pressure rocks from the other areas is more problematic to interpret as these rocks record a geothermal gradient that is lower than the normal continental gradient. Apart from Kuhmo garnet-amphibolites, other examples of Archaean high P/T rocks in the Fennoscandian Shield are the eclogites in the Belomorian Province which were metamorphosed at c. 700–800 °C and c. 14–17 kbar, possibly even at pressures exceeding 20 kbar (Volodichev et al. 2004, Mints et al. 20101, Shchipansky et al. 2012), i.e. in an eclogite–high-pressure granulite (E-HPG)-type environment, which is consistent with subduction of crustal rocks into the mantle depths (Brown 2007). In Kuhmo the rocks metamorphosed under high pressure only seem to occur in a restricted area surrounded by amphibolite facies rocks that were metamorphosed at c. 6–7 kbar. Therefore, their exhumation might be explained by similar subduction-related tectonic processes that exhume high-pressure rocks at present convergent margins (Beaumont et al. 1996, 1999, Agard et al. 2009).

The Ilomantsi greenstone belts shows low pressure metamorphism at 3.5–5.5 kbar and 550–600 °C, which indicates a gradient that is warmer than the normal continental geotherm. These rocks are juxtaposed with migmatites that normally show pressures of c. 6–8 kbar, and in the Kuhmo amphibolite even 15–16 kbar, which represents the amphibole-epidote eclogite facies in the classification of Brown (2009). The duality of thermal environments is typical for modern plate tectonics, where the belts representing different gradients are juxtaposed by plate tectonic processes (Brown 2009). Although the metamorphic structure in the Karelia Province is not quite similar to that in modern subduction-related orogenic belts, the significant differences in the metamorphic gradient between adjacent domains is easy to explain by subductional/collisional processes that

assembled rocks representing various geodynamic settings.

One major problem is that we do not currently have a clear conception of the extent to which the present crustal structure is due to Archaean accretion/thickening or to Palaeoproterozoic orogenic events. Nevertheless, at least the western and eastern parts of the Karelia Province were strongly reworked in the Palaeoproterozoic Svecofennian and Lapland–Kola orogenies, when it was compressionally thickened and subjected to medium P/T type amphibolite facies metamorphism at 1.9–1.8 Ga (Kontinen et al. 1992, Daly et al. 2001, 2006, Bibikova et al. 2001). One manifestation of the Palaeoproterozoic reworking is the anomaly patterns on airborne magnetic maps, such as in Fig. 33. The general E–W strike of foliation and magnetic banding in the northern part of the Lentua complex suddenly changes to a roughly N–S direction in the Siurua and Ranua complexes when crossing over the Palaeoproterozoic Kainuu schist belt, which forms the boundary between the eastern and western complexes (Fig. 33). A Palaeoproterozoic rotation component is implied, as the same happens with the strikes of the Palaeoproterozoic dyke swarms contained in the two terranes (Vuollo & Huhma 2005). In the pristine Superior Province, Palaeoproterozoic dolerites tend to occur in radiating swarms where the strikes of individual dykes remain much the same over hundreds of kilometres (Ernst & Buchan 2001). In marked contrast, dolerite dykes in the Western Karelia subprovince often abruptly change their strikes from one domain to another, reflecting block movements after their emplacements mostly between 2.45–1.95 Ga. Tectonic transport to the N–NE during the Svecofennian orogeny at 1.9–1.8 Ga and related ductile to brittle Proterozoic deformation involving uplifts and rotations of rigid blocks largely caused the present framework of linear structures in the Archaean bedrock.

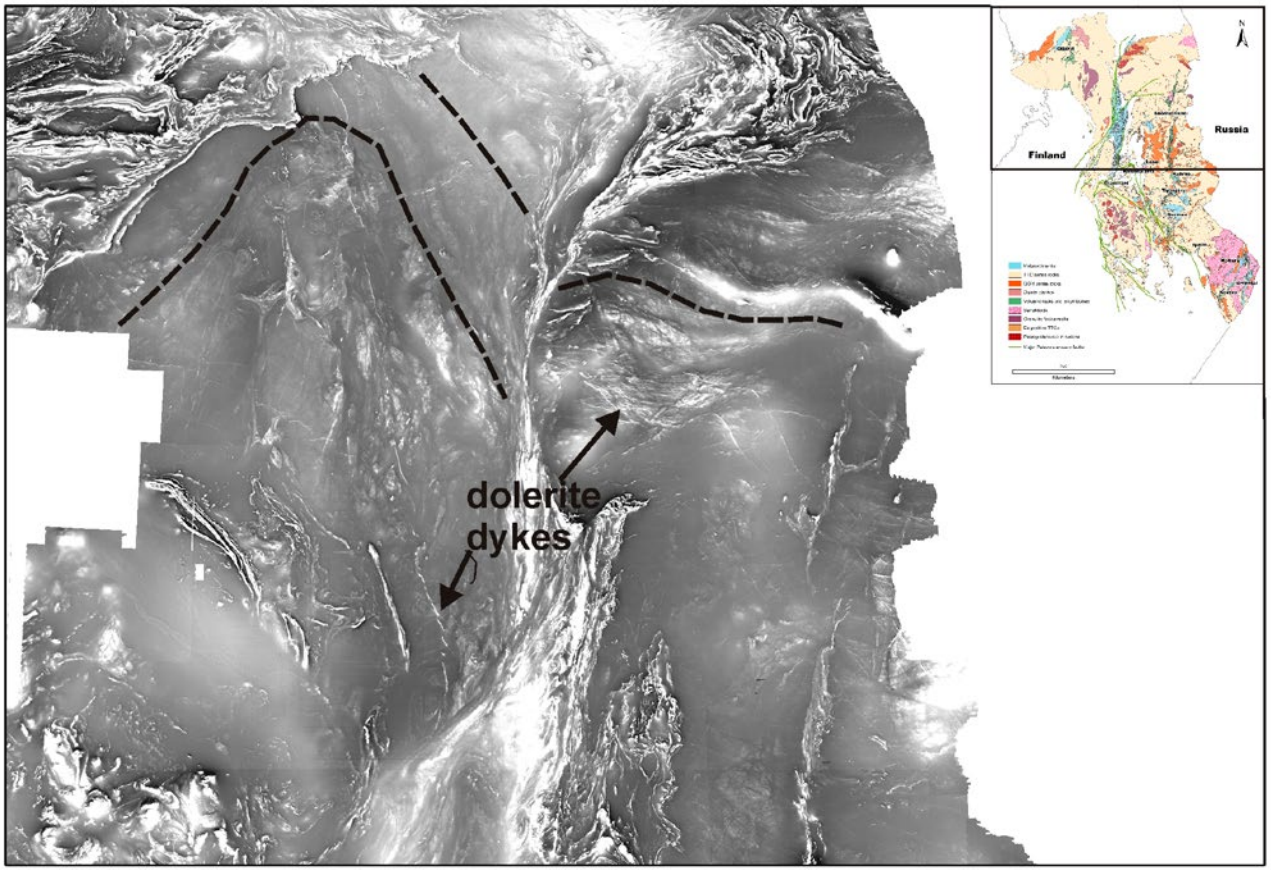

Fig. 33. Airborne magnetic map of the northern part of the Karelia Province in Finland. Dashed lines are for the general strike of foliation.

CONCLUSIONS

1. The Western Karelia Province mostly consists of Neoarchaean gneissic granitoids, while Palaeoarchaean and Mesoarchaean granitoids (>2.9 Ga) are only locally present. The granitoid rocks are classified into four main groups, which are the TTG (tonalite-trondhjemite-granodiorite), sanukitoid, QQ (quartz diorite-quartz monzodiorite) and GGM (granodiorite-granite-monzogranite) groups. Most ages obtained from TTGs are between 2.83–2.72 Ga, and they seem to define two age groups separated by a c. 20 Ma time gap. TTGs are 2.83–2.78 Ga in the older group and 2.76–2.72 Ga in the younger group. Sanukitoids have been dated at 2.74–2.72 Ga, QQs at c. 2.70 Ga and GGMs at 2.73–2.66 Ga. Based on REE, the TTGs fall into two major compositional groups, low-HREE TTGs and high-HREE TTGs, which obviously originated at different crustal depths, but the composition of the protolith has a significant effect on the REE patterns. Sanukitoids are interpreted as products of melting of subcontinental metasomatized mantle. The GGM group represents partial melting of pre-existing TTG crust that also caused high-grade metamorphism and migmatisation.

2. Existing isotope data on volcanic rocks of the Kuhmo greenstone belt do not provide much evidence for their deposition on significantly older basement in intracratonic environment. The composition of the komatiites in Kuhmo indicates that they were derived from primitive upper mantle, representing fissure-controlled eruptions onto a pre-existing oceanic plateau. The volcanic rocks in the Ilomantsi greenstone belt represent arc magmatism within an attenuated continental margin where older basement rocks were assimilated by younger arc magmatism. Metamorphic evolution of the greenstone belts differs from that of the surrounding migmatites, indicating late-tectonic juxtaposition of greenstone belts and TTG migmatites.

3. Neoarchaean accretion of exotic terranes at c. 2.83–2.75 Ga and subsequent crustal stacking at around 2.73–2.68 Ga is a possible mechanism that largely generated the present structure of the Karelia Province, although it was again strongly reworked during the Svecofennian orogeny.

ACKNOWLEDGEMENTS

Jaana Halla is thanked for a critical review that greatly improved the manuscript.

REFERENCES

Abbott, D. H. & Hoffman, S. E. 1984. Archean plate tectonics 529–549. revisited 1: Heat flow, spreading rate, and the age of sub-ducting oceanic lithosphere and their effects on the origin and evolution of continents. Tectonics 3, 429–448.

Abbott, D., Burgess, L., Longhi, J. & Smith, W. H. F. 1994. An empirical thermal history of the Earth's upper mantle. Journal of Geophysical Research 99, 13835–13850.

Abbott, D. H. & Mooney, W. D. 1995. Crustal Structure and Evolution: Support for the Oceanic Plateau Model of Continental Growth. Reviews of Geophysics, Supplement, US National Report to the IUGG, 231–242.

Agard, P., Yamato, P., Jolivet, L. & Burov, E. 2009. Exhumation of oceanic blueschists and eclogites in subduction zones: Timing and mechanisms. Earth-Science Reviews 92, 53–79.

Arestova, N. A., Gooskova, E. G. & Krasnova, A. F. 2000. Palaeomagnetism of the Shilos Structure rocks in the Southern Vygozero greenstone belt, East Karelia. Fizika Zemli (Earth Physics − English translation) 5, 70−75.

Arndt, N. T., Lesher, C. M., Houl, M. G., Lewin, E. & Lacaze, Y. 2004. Intrusion and Crystallization of a Spinifex-Textured Komatiite Sill in Dundonald Township, Ontario. Journal of Petrology 45, 2555–2571.

Barnes, S. J. & Roeder, P. L. 2001. The range of spinel compositions in terrestrial mafic and ultramafic rocks. Journal of Petrology, 42, 2279−2302.

Barr J. A., Grove T. L. & Wilson A. H. 2009. Hydrous komatiites from Commondale, South Africa: An experimental study. Earth and Planetary Science Letters 284, 199–207.

Beaumont, C., Ellis, S., Hamilton, J. & Fullsack P. 1996. Mechanical model for subduction-collision tectonics of Alpine-type compressional orogens. Geology 24, 675–78.

Beaumont, C., Ellis, S. & Pfiffner, A. 1999. Dynamics of sediment subduction-accretion at convergent margins: short-term modes, long-term deformation, and tectonic implications. Journal of Geophysical Research 104, 17573–602.

Benn, K., Mareschal, J.-C. & Condie, K. C. 2006. Introduction: Archean Geodynamics and Environments. In: Benn,

K., Mareschal, J.-C. & Condie, K. C. (eds.) Archean Geodynamics and Environments. Geophysical Monograph 164, 1–5.

Berman, R. G. 1988. Internally-consistent thermodynamic data for stoichiometric minerals in the system Na2O-K2O-CaO-MgO-FeO-Fe2O3-Al2O3-SiO2-TiO2-H2O-CO2. Journal of Petrology 29, 445−522.

Berman, R. G. 1991. Thermobarometry using multiequilibrium calculations: a new technique with petrologic applications. Canadian Mineralogist 29, 833–855.

Bibikova, E., Skiöld, T., Bogdanova, S., Gorbatschev, R. & Slabunov, A. 2001. Titanite-rutile thermochronometry across the boundary between the Archaean Craton in Karelia and the Belomorian Mobile Belt, eastern Baltic Shield. Precambrian Research 105, 315–330.

Bibikova, E. V., Samsonov, A. V., Shchipansky, A. A., Bogina, M. M., Gracheva, T. V. & Makarov, V. A. 2003. The Hisovaara Structure in the Northern Karelian Greenstone Belt as a Late Archean Accreted Island Arc: Isotopic Geochronological and Petrological Evidence. Petrology 11 (3), 261–290.

Bibikova, E. V., Petrova, A. & Claesson, S. 2005. The temporal evolution of sanukitoids in the Karelian Craton, Baltic Shield: an ion microprobe U–Th–Pb isotopic study of zircons. Lithos 79, 129–145.

Bickle, M. J. 1986. Implications of melting for stabilisation of the lithosphere and heat loss in the Archaean. Earth and Planetary Science Letters 80, 314–324.

Björnerud, M. G. & Austrheim, H. 2004. Inhibited eclogite formation: The key to the rapid growth of strong and buoyant Archean continental crust. Geology 32, 765–768.

Blake, T. S., Buick, R., Brown, S. J. A. & Barley, M. E. 2004. Geochronology of a Late Archaean flood basalt province in the Pilbara Craton, Australia: constraints on basin evolution, volcanic and sedimentary accumulation, and continental drift rates. Precambrian Research 133, 143–173.

Bleeker, W. & Ernst, R. 2006. Short-lived mantle generated magmatic events and their dyke swarms: the key unlocking Earth's palaeogeographic record back to 2.6 Ga. In: Hanski, E., Mertanen, S., Rämö, O. T. & Vuollo, J. (eds.), Dyke Swarms − Time Markers of Crustal Evolution. Proceedings of the Fifth International Dyke Conference 2005 Rovaniemi, Finland, 31 July−3 Aug. 2005 & Fourth International Dyke Conference, Kwazulu-Natal, South Africa 26−29 June 2001. London: Taylor & Francis Group, 3−26.

Bleeker, W., Hamilton, M. A. Ernst, R. E. & Kulikov, V. S. 2008. The search for Archean-Paleoproterozoic supercratons; new constraints on Superior-Karelia-Kola correlations within supercraton Superia, including the first ca. 2504 Ma (Mistassini) ages from Karelia. 33rd International Geological Congress, Abstracts.

Blichert-Toft, J. & Albarede, F. 1994. Short-lived chemical heterogeneities in the Archean mantle with implications for mantle convection. Science 263, 1593–1596.

Bornhorst, T. J., Rasilainen, K. & Nurmi, P. A. 1993. Geochemical character of lithologic units in the late Archean Hattu schist belt, Ilomantsi, eastern Finland. In: Nurmi, P. A. & Sorjonen-Ward, P. (eds.) 1993. Geological development, gold mineralization and exploration methods in the late Archean Hattu schist belt, Ilomantsi, eastern Finland. Geological Survey of Finland, Special Paper 17, 133–145.

Brown, M. 2007. Metamorphic conditions in orogenic belts: A record of secular change. International Geology Review 49, 193–234.

Brown, M. 2009. Metamorphic patterns in orogenic systems and the geological record. In: Cawood, P. A. & Kröner, A. (eds.) Earth Accretionary Systems in Space and Time. London: The Geological Society, Special Publications, 318, 37–74.

Card, K. D. 1990. A review of the Superior Province of the canadian shield, a product of Archean accretion. Precambrian Research 48, 99−156.

Castillo, P. R. 2006. An overview of adakite petrogenesis. Chinese Science Bulletin 51, 3, 257—268.

Castillo, P. R., Janney, P. E. & Solidum, R. U. 1999. Petrology and geochemistry of Camiguin Island, southern Philippines: insights to the source of adakites and other lavas in a complex arc setting. Contributions to Mineralogy and Petrology 134, 33–51.

Cawood, P., Kröner, A. & Windley, B. 2003. Accretionary orogens: definition, character, significance. Geophysical Research Abstracts 5.

Condie, K. C. 1998. Episodic continental growth and supercontinents: a mantle avalanche connection? Earth and Planetary Science Letters 163, 97–108.

Condie, K. C. 2000. Episodic continental growth models: afterthoughts and extensions. Tectonophysics 322, 153–162.

Condie, K. C. 2005. High field strength element ratios in Archean basalts: a window to evolving sources of mantle plumes? Lithos 79, 491– 504.

Condie, K. C. & Benn, K. 2006. Archean geodynamics: similar to or different from modern geodynamics. In: Benn, K., Mareschal, J.-C. & Condie, K. C. (eds.) Archean Geodynamics and Environments. Geophysical Monograph 164, 47–60.

Connolly, J. A. D 1990. Multivariable phase-diagrams - an algorithm based on generalized thermodynamics. American Journal of Science 290, 666−718.

Connolly, J. A. D. 2005. Computation of phase equilibria by linear programming: A tool for geodynamic modeling and its application to subduction zone decarbonation. Earth and Planetary Science Letters 236, 524−541.

Connolly, J. A. D. & Petrini, K. 2002. An automated strategy for calculation of phase diagram sections and retrieval of rock properties as a function of physical conditions. Journal of Metamorphic Geology 20, 697−708.

Corcoran, P. L., Mueller, W. U. & Kusky, T. M. 2004. Inferred ophiolites in the Archean Slave Craton. In: Kusky, T. M. (ed.) Precambrian ophiolites and related rocks. Developments in Precambrian Geology 13, 363–404.

Daly, J. S., Balagansky, V. V., Timmerman, M.J., Whitehouse, M.J., de Jong, K., Guise, P., Bogdanova, S., Gorbatschev, R. & Bridgwater, D. 2001. Ion microprobe U-Pb zircon geochronology and isotopic evidence supporting a transcrustal suture in the Lapland Kola Orogen, northern Fennoscandian Shield. Precambrian Research 105, 289–314.

Daly, J. S., Balagansky, V. V., Timmerman, M. J. & Whitehouse, M. J. 2006. The Lapland-Kola Orogen: Palaeoproterozoic collision and accretion of the northern Fennoscandian lithosphere. In: Gee, D. G. & Stephenson, R. A. (eds.) European Lithosphere Dynamics. Geological Society of London, Memoir 32, 579–598.

de la Roche, H., Leterrier, J., Grandclaude, P. & Marchal, M. 1980. A classification of volcanic and plutonic rocks using R1R2-diagram and major element analyses – its relationships with current nomenclature. Chemical Geology 29, 183–210.

Defant, M. J. & Drummond, M. S. 1990. Derivation of some modern arc magmas by melting of young subducted lithosphere. Nature 367, 662−665.

Defant, M. J. & Drummond, M. S. 1993. Mount St. Helens: potential example of the partial melting of the subducted lithosphere in a volcanic arc. Geology 21, 547–550.

deWit, M. J. 1998. On Archean granites, greenstones, cratons and tectonics: does the evidence demand a verdict? Precambrian Research 91, 181–226.

deWit, M. J. & Hart, R. A. 1993. Earth's earliest continental lithosphere, hydrothermal flux and crustal recycling. Lithos 30, 309–335.

Dilek, Y. & Polat, A. 2008. Suprasubduction zone ophiolites and Archean tectonics. Geology 36, 431–432.

Dilek, Y. & Furnes, H. 2011. Ophiolite genesis and global tectonics: Geochemical and tectonic fingerprinting of ancient oceanic lithosphere. Geological Society of America Bulletin 123, 387–411.

Elming, S.-Å., Pesonen, L. J., Leino, M. A. H., Khramov, A. N., Mikhailova, N. P., Krasnova, A. F., Mertanen, S., Bylund, G. & Terho, M. 1993. The drift of the Fennoscandian and Ukrainian Shields during the Precambrian: a Palaeomagnetic analysis. Tectonophysics 223, 177–198.

Ernst, R. E. & Buchan, K. L. 2001. The use of mafic dike swarms in identifying and locating mantle plumes. In: Ernst, R. E. & Buchan. K. L. (eds.) Mantle Plumes: Their Identification Through Time. Geological Society of America Special Paper 352, 247−265.

Foley, S., Tiepolo, M. & Vannucci, R. 2002. Growth of early continental crust controlled by melting of amphibolite in subduction zones. Nature 417, 837−840.

Fowler, M. B., Kocks, H., Darbyshire, D. P. F. & Greenwood, P. B. 2008. Petrogenesis of high Ba-Sr plutons from the Northern Highlands Terrane of the British Caledonian Province. Lithos 105, 129–148.

Frey, F. A., Coffin. M. F., Wallace, P. J., Weis, D., Zhao, X., Wise, S. W. Jr., Wähnert, V., Teagle, D. A. H., Saccocia, P. J., Reusch, D. N. , Pringle, M. S., Nicolaysen, K. E., Neal, C. R., Müller, R. D., Moore, C. L., Mahoney, J. J., Keszthelyi, L., Inokuchi, H., Duncan, R. A., Delius, H., Damuth, J. E., Damasceno, D., Coxall, H. K., Borre, M. K., Boehm F., Barling, J., Arndt N. T. & Antretter, M. 2000. Origin and evolution of a submarine large igneous province: the Kerguelen Plateau and Broken Ridge, southern Indian Ocean. Earth and Planetary Science Letters 176, 73−89.

Frost, B. R., Barnes, C. G., Collins, W. J., Arculus, R. J., Ellis, D. J. & Frost, C. D. 2001. A geochemical classification for granitic rocks. Journal of Petrology 42, 2033−2048.

Glebovitsky V. A. 1997. The Early Precambrian of Russia. Harwood Academic. 261 p.

Goodwin, A. M. 1968. Archean protocontinental growth and early crustal history of the Canadian shield. 23rd International Geological Gongress, Prague 1968. Vol. 1, 69−89.

Gooskova, E. G. & Krasnova, A. N. 1985. Palaeomagnetism of the basic Archean and Proterozoic intrusions of the eastern part of the Baltic Shield. Izvestia Akademii Nauk SSSR, ser Fizika Zemli (Earth Physics − English translation) 21, 366−373.

Grove, T. L. & Parman, S. W. 2004. Thermal evolution of the Earth as recorded by komatiites. Earth and Planetary Science Letters 219, 173–187.

Gutscher, M.-A., Maury, R., Eissen, J.-P. & Bourdon, E. 2000. Can slab melting be caused by flat subduction? Geology 28, 6, 535–538.

Halla, J. 2002. Origin and Paleoproterozoic reactivation of Neoarchean high-K granitoid rocks in eastern Finland. PhD thesis, University of Helsinki, Finland. Annale Academica Scientiarium Fennicae, Geologica−Geographica 163. 105 p.

Halla, J. 2005. Late Archean high-Mg granitoids (sanukitoids) in the southern Karelian domain, eastern Finland: Pb and Nd isotopic constraints on crust-mantle interactions. Lithos 79, 161–178.

Halla, J. & Heilimo, E. 2009. Deformation-induced Pb isotope exchange between Kfeldspar and whole rock in Neoarchean granitoids: implications for assessing Proterozoic imprints. Chemical Geology 265, 303–312.

Halla, J., van Hunen, J., Heilimo, E. & Hölttä, P. 2009. Geochemical and numerical constraints on Neoarchean plate tectonics. Precambrian Research 174, 155–162.

Hamilton, W. B. 1998. Archean magmatism and tectonics were not products of plate tectonics. Precambrian Research 91, 143–179.

Hamilton, W. B. 2011. Plate tectonics began in Neoproterozoic time, and plumes from deep mantle have never operated. Lithos 123, 1–20.

Heilimo, E., Halla, J. & Hölttä, P. 2010. Discrimination and origin of the sanukitoid series: Geochemical constraints from the Neoarchean western Karelian Province (Finland). Lithos 115, 27–39.

Heilimo, E., Halla, J. & Huhma, H. 2011. Single-grain zircon U–Pb age constraints of the western and eastern sanukitoid zones in the Finnish part of the Karelian Province. Lithos 121, 87−99.

Heilimo, E., Halla, J. & Mikkola, P. 2012. Overview of Neoarchaean sanukitoid series in the Karelian Province, eastern Finland. In: Hölttä, P. (ed.) The Archaean of the Karelia Province in Finland. Geological Survey of Finland, Special Paper 54.

Heilimo, E., Halla, J., Andersen, T. & Huhma, H. 2013. Neoarchean crustal recycling and mantle metasomatism: Hf–Nd–Pb–O isotope evidence from sanukitoids of the Fennoscandian shield. Precambrian Research (in press). Available at: http://dx.doi.org/10.1016/j.precamres.2012.01.015

Hirose, K. 2010. The Earth's missing ingredient. Scientific American 302, 6, 58−65.

Hoffman, P. F. & Ranalli, G. 1988. Archean oceanic flack tectonics. Geophysical Research Letters 15 (10), 1077–1080.

Hölttä, P. 1997. Geochemical characteristics of granulite facies rocks in the Varpaisjärvi area, central Fennoscandian Shield. Lithos 40, 31–53.

Hölttä, P. & Paavola, J. 2000. P-T-t development of Archaean granulites in Varpaisjärvi, Central Finland, I: Effects of multiple metamorphism on the reaction history of mafic rocks. Lithos 50, 97–120.

Hölttä, P., Huhma, H., Mänttäri, I. & Paavola, J. 2000. P-T-t development of Archaean granulites in Varpaisjärvi, Central Finland, II: Dating of high-grade metamorphism with the U-Pb and Sm-Nd methods. Lithos 50, 121–136.

Hölttä, P., Balagansky, V., Garde, A. A., Mertanen,S., Peltonen, P., Slabunov, A., Sorjonen-Ward, P. & Whitehouse, M. 2008. Archean of Greenland and Fennoscandia. Episodes 31 (1), 1–7.

Hölttä, P., Heilimo, E., Huhma, H., Juopperi, H., Kontinen, A., Konnunaho, J., Lauri, L,, Mikkola, P., Paavola, J. & Sorjonen-Ward, P. 2012. Archaean complexes of the Karelia Province in Finland. In: Hölttä, P. (ed.) The Archaean of the Karelia Province in Finland. Geological Survey of Finland, Special Paper 54.

Howell, D. G. 1989. Tectonics of Suspect Terranes. New York: Chapman and Hall. 232 p.

Huhma, H., Kontinen, A. & Laajoki, K. 2000. Age of the metavolcanic-sedimentary units of the Central Puolanka Group, Kainuu schist belt, Finland. In: 24. Nordiske Geologiske Vintermøte, Trondheim 6.–9. januar 2000. Geonytt 1, 87–88.

Huhma, H., Mänttäri, I., Peltonen, P., Kontinen, A., Halkoaho, T., Hanski., E., Hokkanen. T., Hölttä, P., Juopperi, H., Konnunaho, J., Lahaye, Y., Luukkonen., E., Pietikäinen, K., Pulkkinen, A., Sorjonen-Ward, P. , Vaasjoki, M. & Winehouse, M. 2012a. The age of Archean greenstone belts in Finland. In: Hölttä, P. (ed.) The Archaean of the Karelia Province in Finland. Geological Survey of Finland, Special Paper 54.

Huhma, H., Kontinen, A., Mikkola, P., Halkoaho, T., Hokkanen, T., Hölttä, P., Juopperi, H., Konnunaho, J., Luukkonen, E., Mutanen, T. Peltonen, P., Pietikäinen, K. & Pulkkinen, A. 2012. Nd isotopic evidence for Archean crustal growth in Finland. In: Hölttä, P. (ed.) The Archaean of the Karelia Province in Finland. Geological Survey of Finland, Special Paper 54.

Hyppönen, V. 1983. Ontojoen, Hiisijärven ja Kuhmon karttaalueiden kallioperä. Summary: Pre-Quaternary Rocks of the Ontojoki, Hiisijärvi and Kuhmo Map-Sheet areas. Geological Map of Finland 1:100 000, Explanation to the Maps of Pre-Quaternary Rocks, Sheets 4411, 4412, 4413. Geological Survey of Finland. 60 p.

Jones, D. L. 1990. Synopsis of late Palaeozoic and Mesozoic terrane accretion within the Cordillera of western North America. In: Dewey, J. F., Gass, I. G., Curry, G. B., Harris, N. B. W. & Sengör, A. M. C. (eds.) Allochthonous Terranes. Cambridge: Cambridge University Press, 23–30.

Jones, D. L., Howell, P. G., Coney, P. J. & Monger, J. W. 1983. Recognition, character and analysis of tectonostratigraphic terranes in western North America. Journal of Geological Education, 31, 295–303.

Käpyaho, A., Mänttäri, I. & Huhma, H. 2006. Growth of Archaean crust in the Kuhmo district, eastern Finland: U-Pb and Sm-Nd isotope constraints on plutonic rocks. Precambrian Research 146, 95–119.

Käpyaho, A. Hölttä, P. & Whitehouse, M. 2007. U-Pb zircon geochronology of selected Neoarchaean migmatites in eastern Finland. Bulletin of the Geological Society of Finland 79 (1), 95–115.

Kontinen, A., Paavola, J. & Lukkarinen, H. 1992. K-Ar ages of hornblende and biotite from Late Archaean rocks of eastern Finland – interpretation and discussion of tectonic implications. Geological Survey of Finland, Bulletin 365. 31 p.

Kontinen, A. & Paavola, J. 2006. A preliminary model of the crustal structure of the eastern Finland Archaean complex between Vartius and Vieremä, based on constraints from surface geology and FIRE 1 seismic survey. In: Kukkonen, I. T. & Lahtinen, R. (eds.) 2006. Finnish Reflection Experiment FIRE 2001–2005. Geological Survey of Finland, Special Paper 43, 223–240.

Kontinen, A., Käpyaho, A., Huhma, H., Karhu, J., Matukov, D. I., Larionov, A. & Sergeev, S. A. 2007. Nurmes paragneisses in eastern Finland, Karelian craton: provenance, tectonic setting and implications for Neoarchaean craton correlation. Precambrian Research 152, 119–148.

Korenaga, J. 2006. Archean geodynamics and the thermal evolution of Earth. In: Benn, K., Mareschal, J.-C. & Condie, K. C. (eds.) Archean Geodynamics and Environments. Geophysical Monograph 164, 7–32.

Korja, A., Lahtinen, R., Heikkinen, P. & Kukkonen, I. T. 2006. A geological interpretation of the upper crust along FIRE 1. In: Kukkonen, I. T. & Lahtinen, R. (eds.) 2006. Finnish Reflection Experiment FIRE 2001–2005. Geological Survey of Finland, Special Paper 43, 45–76.

Kozhevnikov, V. N., Berezhnaya, N. G., Presnyakov, S. L. Lepekhina, E. N. Antonov, A. V. & Sergeev, S. A. 2006. Geochronology (SHRIMP-II) of zircon from Archean lithotectonic associations in the greenstone belts of the Karelian craton: implications for stratigraphic and geodynamic reconstructions. Stratigraphy and Geological Correlation 14(3), 240–259.

Krasnova, A. F. & Gooskova, E. G. 1990. Geodynamic evolution of the Wodlozero block of Karelia according to palaeomagnetic data. Izvestiya. Earth Physics 26, 80–85.

Kröner, A. & Layer, P. W. 1994. Crust formation and plate motion in the early Archean. Science 256, 1405–1411.

Kusky, T. M. & Kidd, W. S. F. 1992. Remnants of an Archean oceanic plateau, Belingwe greenstone belt, Zimbabwe. Geology 20, 43–46.

Kusky, T. M. & Polat, A. 1999. Growth of granite-greenstone terranes at convergent margins, and stabilization of Archean cratons. Tectonophysics 305, 43–73.

Kusky, T. M., Li, J.-H. & Tucker, R. D. 2001. 2.505-Billion-Year-Old Oceanic Crust and Mantle The Archean Dongwanzi Ophiolite Complex, North China Craton. Science 292, 1142–1145.

Kusky, T. M., Li, J. H., Raharimahefa, T. & Carlson, R. W. 2004. Origin and emplacement of Archean ophiolites of the Central Orogenic Belt, North China Craton. In: Kusky, T. M. (ed.) Precambrian ophiolites and related rocks. Developments in Precambrian Geology 13, 223–282.

Laajoki, K. 1991. Stratigraphy of the northern end of the early Proterozoic (Karelian) Kainuu Schist Belt and associated gneiss complexes, Finland. Geological Survey of Finland, Bulletin 358. 105 p.

Laajoki, K. & Luukas, J. 1988. Early Proterozoic stratigraphy of the Salahmi-Pyhäntä area, central Finland, with an emphasis on applying the principles of lithodemic stratigraphy to a complexly deformed and metamorphosed bedrock. Bulletin of the Geological Society of Finland 60 (2), 79–106.

Lalli, K. 2002. Petrography, geochemistry and metamorphic petrology of the Isokumpu area in the Pudasjärvi granulite belt. Unpublished Master's Thesis, University of Oulu. (in Finnish)

Langford, F. F. &Morin, J. A. 1976. The development of the Superior Province of northwestern Ontario by merging island arcs. American Journal of Science 276, 1023–1034.

Lauri, L. S., Rämö, O. T., Huhma, H., Mänttäri, I. & Räsänen, J. 2006. Petrogenesis of silicic magmatism related to the 2. 44 Ga rifting of Archean crust in Koillismaa, eastern Finland. Lithos 86, 137–166.

Lauri, L. S., Andersen, T., Hölttä, P., Huhma, H. & Graham, S. 2011. Evolution of the Archaean Karelian Province in the Fennoscandian Shield in the light of U–Pb zircon ages and Sm–Nd and Lu–Hf isotope systematics. London: Journal of the Geological Society, 167, 1–18.

Lobach-Zhuchenko, S. B., Rollinson, H. R., Chekulaev, V. P., Arestova, N. A., Kovalenko, A. V., Ivanikov V. V., Guseva, N. S., Sergeev, S. A., Matukov, D. I. & Jarvis K. E. 2005. The Archaean sanukitoid series of the Baltic Shield: geological setting, geochemical characteristics and implications for their origin. Lithos 79, 107– 128.

Lobach-Zhuchenko, S. B., Rollinson, H., Chekulaev, V. P.,

SavatenkoV, V. M., Kovalenko, A.V., Martin, H., Guseva, N. S. & Arestova, N. A. 2008. Petrology of a late Archaean, highly potassic, sanukitoid pluton from the Baltic Shield: Insights into late Archaean mantle metasomatism. Journal of Petrology 49 (3), 393–420.

Luukkonen, E. J. 1985. Structural and U-Pb isotopic study of late Archaean migmatitic gneisses of the Presvecokarelides, Lylyvaara, Eastern Finland. Transactions of the Royal Society of Edinburgh, Earth Sciences 76, 401–410.

Luukkonen, E. 1988. Moisiovaaran ja Ala-Vuokin karttaalueiden kallioperä. Summary: Pre-Quaternary Rocks of the Moisiovaara and Ala-Vuokki Map-Sheet areas. Geological Map of Finland 1:100 000, Explanation to the Maps of Pre-Quaternary Rocks, Sheets 4421 and 4423+4441. Geological Survey of Finland. 90 p.

Luukkonen, E. J. 1992. Late Archaean and early Proterozoic structural evolution in the Kuhmo-Suomussalmi terrain, eastern Finland. Publications of the University of Turku, Series A. II. University of Turku, Biologica−Geographica−Geologica 78. 115 p.

Luukkonen, E., Halkoaho, T., Hartikainen, A., Heino, T., Niskanen, M., Pietikäinen, K. & Tenhola, M. 2002. Report of the GTK project 'The Archaean areas of eastern Finland' in the years 1992−2001 in the communities of Suomussalmi, Hyrynsalmi, Kuhmo, Nurmes, Rautavaara, Valtimo, Lieksa, Ilomantsi, Kiihtelysvaara, Eno, Kontiolahti, Tohmajärvi and Tuupovaara. Geological Survey of Finland, archive report M 19/4513/2002/1. 265 p. (in Finnish)

Männikkö, K. H. 1988. Myöhäisarkeeisen Koveron liuskejakson länsiosan deformaatio ja metamorfoosi. Pohjois-Karjalan malmiprojekti. Oulu: Oulun yliopisto, Raportti 15. 108 p.

Mänttäri, I. & Hölttä, P. 2002. U-Pb dating of zircons and monazites from Archean granulites in Varpaisjärvi, central Finland: evidence for multiple metamorphism and Neoarchean terrane accretion. Precambrian Research 118, 101−131.

Martin, H. 1995. The Archean grey gneisses and the genesis of the continental crust. In: Condie, K.C. (ed.) The Archean crustal evolution: Amsterdam: Elsevier, 205–259.

Martin, H. 1999. The adakitic magmas: modern analogues of Archaean granitoids. Lithos 46, 411–429.

Martin, H. & Moyen, J.-F. 2002. Secular changes in tonalite-trondhjemite-granodiorite composition as markers of the progressive cooling of Earth. Geology, 30, 4, 319–322.

Martin, H., Smithies, R. H., Rapp, R., Moyen, J.-F. & Champion, D. 2005. An overview of adakite, tonalite–trondhjemite–granodiorite (TTG), and sanukitoid: relationships and some implications for crustal evolution. Lithos 79, 1–24.

Mertanen, S., Pesonen, L. J., Hölttä, P. & Paavola, J. 2006a. Palaeomagnetism of Palaeo-proterozoic dolerite dykes in central Finland. In: Hanski, E., Mertanen, S., Rämö, O. T. & Vuollo, J. (eds.) Dyke Swarms − Time Markers of Crustal Evolution, Proceedings of the Fifth International Dyke Conference, IDC5, Rovaniemi, Finland, 31 July−3 August 2005. Taylor & Francis Group/ Balkema, 243−256.

Mertanen, S., Vuollo, J. I., Huhma, H., Arestova, N. A. & Kovalenko, A. 2006b. Early Paleoproterozoic-Archean dykes and gneisses in Russian Karelia of the Fennoscandian Shield–new paleomagnetic, isotope age and geochemical investigations. Precambrian Research 144 (3−4), 239−260.

Mertanen, S. & Korhonen, F. 2008. Archean-Paleoproterozoic configuration of Laurentia and Baltica focusing on paleomagnetic data from Baltica. 33rd International Geological Congress, 6−14 August 2008, Oslo, Norway. Abstracts.

Mertanen, S. & Korhonen, F. 2011. Paleomagnetic constraints on an Archean – Paleoproterozoic Superior–Karelia connection: new evidence from Archean Karelia. Precambrian Research 186, 193–204.

Mikkola, P. 2008. Koillis-Kainuun kallioperä. Summary: Pre-Quaternary rocks of Northeast Kainuu. Geological Survey of Finland, Report of Investigation 175. 53 p. + 5 app. (Electronic publication)

Mikkola, P., Huhma, H., Heilimo, E. & Whitehouse, M. 2011a. Archean crustal evolution of the Suomussalmi district as part of the Kianta Complex, Karelia; constraints from geochemistry and isotopes of granitoids. Lithos 125, 287−307.

Mikkola, P., Salminen, P., Torppa, A. & Huhma, H. 2011b. The 2. 74 Ga Likamännikkö complex in Suomussalmi, East Finland : lost between sanukitoids and truly alkaline rocks? Lithos 125, 716−728.

Mikkola, P., Lauri, L. S. & Käpyaho, A. 2012. Neoarchean leucogranitoids of the Kianta Complex, Karelian Province, Finland: Source characteristics and processes responsible for the observed heterogeneity. Precambrian Research 206–207, 72–86.

Mints, M. V., Berzin, R. G., Suleĭmanov, A. K., Zamozhnyaya, N. G., Stupak, V. M., Konilov, A. N., Zlobin, V. L. & Kaulina, T. V. 2004. The deep structure of the early Precambrian crust of the Karelian craton, southeastern Fennoscandian shield: results of investigation along CMP profile 4B. Geotectonics 38 (2), 87–102.

Mints, M. V., Belousova, E. A., Konilov, A. N., Natapov, L. M., Shchipansky, A. A. Griffin, W. L., O'Reilly, S. Y., Dokukina, K. A. & Kaulina, T. V. 2010. Mesoarchean subduction processes: 2.87 Ga eclogites from the Kola Peninsula, Russia. Geology 38, 739–742.

Moyen, J.-F. 2009. High Sr/Y and La/Yb ratios: The meaning of the "adakitic signature". Lithos 112, 556–574.

Moyen, J.-F. 2011. The composite Archaean grey gneisses: Petrological significance, and evidence for a non-unique tectonic setting for Archaean crustal growth. Lithos 123, 21−36.

Moyen, J.-F. & Stevens, G. 2006. Experimental constraints on TTG petrogenesis: implications for Archean geodynamics. In: Benn, K., Mareschal, J.-C. & Condie, K. C. (eds.) Archean Geodynamics and Environments. Geophysical Monograph 164, 149–176.

Mutanen, T. & Huhma, H. 2003. The 3. 5 Ga Siurua trondhjemite gneiss in the Archaean Pudasjärvi Granulite Belt, northern Finland. Bulletin of the Geological Society of Finland 75, 51–68.

Nair, R. & Chacko, T. 2008. Role of oceanic plateaus in the initiation of subduction and origin of continental crust. Geology 36 (7), 583–586.

Nehring, F., Foley, S. F., Hölttä, P. & Kerkhof, A. M. van den 2009. Internal differentiation of the Archean continental crust: fluid-controlled partial melting of granulites and TTG-amphibolite associations in central Finland. Journal of Petrology 50 (1), 3–35.

Neuvonen, K. J., Korsman, K., Kouvo, O. & Paavola, J. 1981. Paleomagnetism and age relationship of the rocks in the Main Sulphide Ore Belt in central Finland. Bulletin of the Geological Society of Finland 53, 109−133.

Neuvonen, K. J., Pesonen, L. J. & Pietarinen, H. 1997. Remanent Magnetization in the Archaean Basement and Cut-

ting Diabase Dykes in Finland, Fennoscandian Shield. Geophysica 33(1), 111−146.

O'Brien, H., Huhma, H. & Sorjonen-Ward, P. 1993. Petrogenesis of the late Archean Hattu schist belt, Ilomantsi, eastern Finland: geochemistry and Sr, Nd isotopic composition. In: Nurmi, P. A. & Sorjonen-Ward, P. (eds.) 1993. Geological development, gold mineralization and exploration methods in the late Archean Hattu schist belt, Ilomantsi, eastern Finland. Geological Survey of Finland, Special Paper 17, 147–184.

Ohta, H., Maruyama, S., Takahashi, E., Watanabe, Y. & Kato, Y. 1996. Field occurrence, geochemistry and petrogenesis of the Archean Mid-Oceanic Ridge Basalts (AMORBs) of the Cleaverville area, Pilbara Craton, Western Australia. Lithos 37, 199–221.

Paavola, J. 1986. A communication on the U-Pb and K-Ar age relations of the Archaean basement in the Lapinlahti-Varpaisjärvi area, central Finland. Geological Survey of Finland, Bulletin 339, 7−15.

Paavola, J. 1999. Rautavaaran kartta-alueen kallioperä. Summary: Pre-Quaternary Rocks of the Rautavaara Map-Sheet area. Geological map of Finland 1:100 000, Explanation to the Map of Pre-Qauternary Rocks, Sheet 3343. Geological Survey of Finland. 53 p.

Paavola, J. 2003. Vieremän kartta-alueen kallioperä. Summary: Pre-Quaternary Rocks of the Vieremä Map-Sheet area. Geological map of Finland 1:100 000, Explanation to the Map of Pre-Qauternary Rocks, Sheet 3342. Geological Survey of Finland. 40 p. + 2 app. maps.

Pajunen, M. & Poutiainen, M. 1999. Palaeoproterozoic prograde metasomatic-metamorphic overprint zones in Archaean tonalitic gneisses, eastern Finland. In: Studies related to the Global Geoscience Transects/SVEKA Project in Finland. Bulletin of the Geological Society of Finland 71 (1), 73−132.

Papunen, H., Halkoaho, T. & Luukkonen, E. 2009. Archaean evolution of the Tipasjärvi-Kuhmo-Suomussalmi Greenstone Complex, Finland. Geological Survey of Finland, Bulletin 403. 68 p. + App. data cd.

Patiño Douce, A. E. 1999. What do experiments tell us about the relative contribution of crust and mantle to the origin of granitic magmas. Geological Society Special Publication 168, 55−76.

Patiño Douce, A. E. 2004. Vapor-absent melting of tonalite at 15–32 kbar. Journal of Petrology 46 (2), 275–290.

Peacock, S. M., Rushmer, T. & Thompson, A. B. 1994. Partial melting of subducting oceanic crust. Earth and Planetary Science Letters 121, 227–244.

Peltonen, P., Mänttäri, I., Huhma, H. & Whitehouse, M. J. 2006. Multi-stage origin of the lower crust of the Karelian craton from 3. 5 to 1. 7 Ga based on isotopic ages of kimberlite-derived mafic granulite xenoliths. Precambrian Research 147, 107−123.

Percival, J. A., McNicoll, V., Brown, J. L. & Whalen, J. B. 2004. Convergent margin tectonics, central Wabigoon subprovince, Superior Province, Canada. Precambrian Research 132, 213−244.

Percival, J., Sanborn-Barrie, M., Skulski, T., Stott, G. M., Helmstaedt, H. & White, D. J. 2006. Tectonic evolution of the western Superior Province from NATMAP and Lithoprobe studies. Canadian Journal of Earth Sciences, 43, 1085−1117.

Petrone, C. M. & Ferrari, L. 2008. Quaternary adakite - Nb-enriched basalt association in the western Trans-Mexican Volcanic Belt: is there any slab melt evidence? Contributions to Mineralogy and Petrology 156, 73–86.

Pietikäinen, K. & Vaasjoki, M. 1999. Structural observations and U-Pb mineral ages from igneous rocks at the Archaean-Palaeoproterozoic boundary in the Salahmi Schist Belt, central Finland: constraints on tectonic evolution. Bulletin of the Geological Society of Finland 71 (1), 133−142.

Polat, A. & Kerrich, R. 2000. Archean greenstone belt magmatism and the continental growth-mantle evolution connection: constraints from Th-U-Nb-LREE systematics of the 2.7 Ga Wawa subprovince, Superior Province, Canada. Earth and Planetary Science Letters 175, 41−54.

Polat, A & Kerrich, R. 2006. Reading the geochemical fingerprints of Archean hot subduction volcanic rocks. In: Benn, K., Mareschal, J.-C. & Condie, K. C. (eds.) Archean Geodynamics and Environments. Geophysical Monograph 164, 198−213.

Powell, R., Holland, T. J. B. & Worley, B. 1998. Calculating phase diagrams involving solid solutions via non-linear equations, with examples using THERMOCALC. Journal of Metamorphic Geology 16, 577–588.

Puchtel, I. 2004. 3.0 Ga Olondo Greenstone Belt in the Aldan Shield, E. Siberia. In: Kusky, T. (ed.) Precambrian Ophiolites and Related Rocks. Developments in Precambrian Geology 13. Amsterdam: Elsevier, 405–423.

Puchtel, I. S., Hofmann, A. W., Mezger, K., Jochum, K. P., Shchipansky, A. A. & Samsonov, A. V. 1998. Oceanic plateau model for continental crustal growth in the Archaean: a case study from the Kostomuksha greenstone belt, NW Baltic shield. Earth and Planetary Science Letters 155, 57–74.

Puchtel, I. S., Hofmann, A. W., Amelin, Yu. V., Garbe-Schönberg, C. D., Samsonov, A. V. & Shchipansky, A. A. 1999. Combined mantle plume–island arc model for the formation of the 2.9 Ga Sumozero-Kenozero greenstone belt, SE Baltic Shield: isotope and trace element constraints. Geochimica et Cosmochimica Acta 63, 3579–3595.

Rapp, R. P., Watson, E. B. & Miller, C. F. 1991. Partial melting of amphibolite/eclogite and the origin of Archaean trondhjemites and tonalites. Precambrian Research 51, 1–25.

Rapp, R. P., Shimizu, N. & Norman, M. D. 2003. Growth of early continental crust by partial melting of eclogite. Nature 425 (9), 605−609.

Rasilainen, K, Lahtinen, R. & Bornhorst, T. 2007. Rock geochemical database of Finland, Manual. Geological Survey of Finland, Report of Investigation 164. 38 p.

Richards, J. P. & Kerrich, R. 2007. Adakite-like rocks: their diverse origins and questionable role in metallogenesis. Economic Geology 102 (4), 537−576.

Samsonov, A. V., Bogina, M. M., Bibikova, E. V., Petrova, A.Y u. & Shchipansky, A. A. 2005. The relationship between adakitic, calc-alkaline volcanic rocks and TTGs: implications for the tectonic setting of the Karelian greenstone belts, Baltic Shield. Lithos 79, 83–106.

Şengör, A. M. C. & Natal'in, B. A. 1996. Turkic-type orogeny and its role in the making of the continental crust, Annual Review of Earth and Planetary Science 24, 263–337.

Şengör, A. M. C. & Natal'in, B. A. 2004. Phanerozoic analogues of Archaean oceanic basement fragments: Altaid ophiolites and ophirags. In: Kusky, T. (ed.) Precambrian Ophiolites and Related Rocks. Developments in Precambrian Geology 13. Amsterdam: Elsevier, 675–726.

Şengör, A. M. C., Sinan, Ö. M., Keskin, M., Sakınç, M., Özbakır, A. D. & Kayan, İ. 2008. Eastern Turkish high plateau as a small Turkic-type orogen: Implications for post-collisional crust-forming processes in Turkic-type

orogens. Earth-Science Reviews 90, 1–48.

Sergeev, S. A., Bibikova, E. V., Matukov, D. I. & Lobach-Zhuchenko, S. B. 2007. Age of the magmatic and metamorphic processes in the Vodlozero Complex, Baltic Shield: an ion microprobe (SHRIMP II) U–Th–Pb isotopic study of zircons. Geochemistry International 45(2), 198–205.

Shchipansky, A. A., Samsonov, A. V., Bibikova, E. V., Babarina, I. I., Konilov, A. N., Krylov, K. A., Slabunov, A. I. & Bogina, M. M. 2004. 2.8 Ga boninite-hosting partial suprasubduction ophiolite sequences from the North Karelian greenstone belt, NE Baltic Shield, Russia. In: Kusky, T. (ed.) Precambrian Ophiolites and Related Rocks. Developments in Precambrian Geology 13, 425–487.

Shchipansky, A. A., Khodorevskaya, L. I., Konilov A. N. & Slabunov A. I. 2012. Eclogites from the Belomorian Mobile Belt (Kola Peninsula): geology and petrology. Russian Geology and Geophysics 53, 1–21.

Skjerlie, K. P., Patiño Douce, A. E. & Johnston A. D. 1993. Fluid absent melting of a layered crustal protolith: implications for the generation of anatectic granites. Contributions to Mineralogy and Petrology 114, 365–378.

Slabunov, A. I., Lobach-Zhuchenko, S. B., Bibikova, E. V., Sorjonen-Ward, P., Balagansky, V. V., Volodichev, O. I., Shchipansky, A. A., Svetov, S. A., Chekulaev, V. P., Arestova, N. A. & Stepanov, V. S. 2006. The Archaean nucleus of the Baltic/Fennoscandian Shield. In: Gee, D. G. & Stephenson, R. A. (eds.) European Lithosphere Dynamics. Geological Society of London, Memoir 32, 627–644.

Smithies, R. H. 2000. The Archaean tonalite-trondhjemite-granodiorite (TTG) series is not an analogue of Cenozoic adakite. Earth and Planetary Science Letters 182, 115–125.

Smithies, R. H., Champion, D. C. & Cassidy, K. F. 2003. Formation of Earth's early Archaean continental crust. Precambrian Research 127, 89–101.

Sorjonen-Ward, P. 1993. An overview of structural evolution and lithic units within and intruding the late Archean Hattu schist belt, Ilomantsi, eastern Finland. In: Nurmi, P. A. & Sorjonen-Ward, P. (eds.) 1993. Geological development, gold mineralization and exploration methods in the late Archean Hattu schist belt, Ilomantsi, eastern Finland. Geological Survey of Finland, Special Paper 17, 9–102.

Sorjonen-Ward, P. 2006. Geological and structural framework and preliminary interpretation of the FIRE 3 and FIRE 3A reflection seismic profiles, central Finland. In: Kukkonen, I. T. & Lahtinen, R. (eds.) 2006. Finnish Reflection Experiment FIRE 2001−2005. Geological Survey of Finland, Special Paper 43, 105–159.

Sorjonen-Ward, P. & Claoué-Long, J. 1993. Preliminary note on ion probe results for zircons from the Silvevaara granodiorite, Ilomantsi, eastern Finland. In: Autio, S. (ed.) 1993. Geological Survey of Finland, Current Research 1991−1992. Geological Survey of Finland, Special Paper 18, 25–29.

Sorjonen-Ward, P. & Luukkonen, E. 2005. Archean rocks. In: Lehtinen, M., Nurmi, P. A. & Rämö, O. T. (eds.) The Precambrian Geology of Finland - Key to the Evolution of the Fennoscandian Shield. Amsterdam: Elsevier, 19−99.

Springer, W. & Seck, H. A. 1997. Partial fusion of basic granulites at 5 to 15 kbar: implications for the origin of TTG magmas. Contributions to Mineralogy and Petrology 127, 30–45.

Stiegler, M. S., Lowe, D. R. & Byerly, G.R. 2010. The Petrogenesis of Volcaniclastic Komatiites in the Barberton Greenstone Belt, South Africa: a Textural and Geochemical Study. Journal of Petrology, 1−26.

Streckeisen, A. & Le Maitre, R. W. 1979. A chemical approximation to the modal QAPF classification of the igneous rocks. Neues Jahrbuch für Mineralogie, Abhandlungen 136, 169–206.

Strik, G., Blake, T. S., Zegers, T. E., White, S. E. & Langereis, C. G. 2003. Palaeomagnetism of flood basalts in the Pilbara Craton, Western Australia: Late Archaean continental drift and the oldest known reversal of the geomagnetic field. Journal of Geophysical Research 108 (B12), 2551, EMP 2-1-2-21.

Svetov, S. A., Kudryashov, N. M., Ronkin, Yu. L., Huhma, H., Svetova, A. I. & Nazarova, T. N. 2006. Mesoarchean island-arc association in the Central Karelian Terrane, Fennoscandian Shield: new geochronological data. Doklady Earth Sciences 406 (1), 103–106.

Tateno, S., Hirose, K., Sata, N. & Ohishi, Y. 2009. Determination of post-perovskite phase transition boundary up to 4400 K and implications for thermal structure in D″ layer. Earth and Planetary Science Letters 277, 130–136.

Thurston, P. 2002. Autochthonous development of Superior Province greenstone belts? Precambrian Research 115, 11−36.

Tuisku, P. 1988. Geothermobarometry in the Archean Kuhmo-Suomussalmi greenstone belt, eastern Finland. In: Marttila, E. (ed.) 1988. Archaean geology of the Fennoscandian Shield: Proceedings of a Finnish-Soviet symposium in Finland on July 28-August 7, 1986. Geological Survey of Finland, Special Paper 4, 171−172.

Tuukki, P. A. 1991. Arkeeinen Koveron liuskejakso ja sen mafisten ja ultramafisten kivien geokemia ja petrogenesis. Pohjois-Karjalan malmiprojekti. Oulu: Oulun yliopisto, Raportti 28. 129 p.

Vaasjoki, M., Sorjonen-Ward, P. & Lavikainen, S. 1993. U-Pb age determinations and sulfide Pb-Pb characteristics from the late Archean Hattu schist belt, Ilomantsi, eastern Finland. In: Nurmi, P. A. & Sorjonen-Ward, P. (eds.) 1993. Geological development, gold mineralization and exploration methods in the late Archean Hattu schist belt, Ilomantsi, eastern Finland. Geological Survey of Finland, Special Paper 17, 103–131.

Vaasjoki, M., Taipale, K. & Tuokko, I. 1999. Radiometric ages and other isotopic data bearing on the evolution of Archaean crust and ores in the Kuhmo-Suomussalmi area, eastern Finland. Bulletin of the Geological Society of Finland 71 (1), 155–176.

Vaasjoki, M., Kärki, A. & Laajoki, K. 2001. Timing of Palaeoproterozoic crustal shearing in the Central Fennoscandian Shield according to U-Pb data from associated granitoids, Finland. Bulletin of the Geological Society of Finland 73 (1−2), 87–101.

van der Velden, A. J., Cook, F. A., Drummond, B .J. & Goleby, B. R. 2006. Reflections of the Neoarchean: a global perspective. In: Benn, K., Mareschal, J.-C. & Condie, K. C. (eds.) Archean Geodynamics and Environments. Geophysical Monograph 164, 255–265.

van Hunen, J., van den Berg, A. & Vlaar, N. J. 2004. Various mechanisms to induce present-day shallow flat subduction and implications for the younger Earth: a numerical parameter study. Physics of the Earth and Planetary Interiors 146, 179–194.

Volodichev, O. I., Slabunov, A. I., Bibikova, E. V., Konilov, A. N. & Kuzenko, T. I. 2004. Archean Eclogites in the Belomorian Mobile Belt, Baltic Shield. Petrology 12 (6), 540–560.

Vuollo, J. & Huhma, H. 2005. Paleoproterozoic mafic dikes in NE Finland. In: Precambrian geology of Finland : key to the evolution of the Fennoscandian Shield. Developments in Precambrian geology 14. Amsterdam: Elsevier, 195−236.

Watkins J. M., Clemens, J. D. & Treloar, P. J. 2007. Archaean TTGs as sources of younger granitic magmas: melting of sodic metatonalites at 0.6–1.2 GPa. Contributions to Mineralogy and Petrology 154, 91–110.

Winter, J. D. 2001. Igneous and metamorphic petrology. PNew Jersey: Rentice Hall. 697 p.

Wu, C.-M., Zhang, J. & Ren, L.-D. 2004. Empirical garnet–biotite–plagioclase–quartz (GBPQ) geobarometry in m edium- to high-grade metapelites. Journal of Petrology 45 (9) , 1907–1921.

Appendix 1. Chemical analyses of granitoids, amphibolites and volcanic rocks of the greenstone belts. Missing or zero values are below detection limits or not analyzed. Analyses NA1-13 are from Paavola (2003), A1602 and A1611 from Mutanen & Huhma (2003) and A1661 from Lauri et al. (2006).

TTGs and QQs.

Sample	Northing (KKJ)	Easting (KKJ)	SiO2	TiO2	Al2O3	FeO	MnO	MgO	CaO	Na2O	K2O	P2O5	Sum of oxides	S	Cl	Cu	Zn	Ga	Sr	Ba	Pb	Ce	Co	Cr	Dy	Er	Eu	Gd	Hf	Ho	La	Lu	Nb	Nd	Ni	Pr	Rb	Sc	Sm	Ta	Tb	Th	Tm	U	V	Y	Yb	Zr
	Map coordinates		wt.%											ppm																																		
			XRF																			ICP-MS																										
low-HREE TTGs, Eu-negative																																																
27-PSH-04	7295076	3409888	65.20	0.60	16.20	3.79	0.05	1.36	3.03	4.54	3.81	0.27	98.84	277	161	0	73	27	1074	2591	34	123	7.41	12.20	1.87	0.88	1.39	4.69	5.10	0.36	67.60	0.12	4.88	46.50	5.52	13.10	73.40	5.07	6.82	0.23	0.53	8.10	0.10	0.47	52.90	9.61	0.69	214.00
47-PSH-04	7288134	3429931	72.00	0.34	14.20	2.30	0.04	0.81	1.87	3.85	4.10	0.09	99.60		140		35	28	272	827	52	85.3	4.39	13.3	1.71	0.75	0.79	3.02	3.98	0.27	61.5	0.11	9.22	31.7	9.16	9.13	172	3.41	4.29	0.83	0.39	31.0	0.15	2.95	26.0	9.27	0.75	126
70.1-PSH-04	7335466	3437280	69.20	0.35	15.80	2.79	0.06	1.04	3.07	5.00	1.92	0.10	99.32				58	26	472	461		17.20	6.63	8.28	0.91	0.52	0.52	1.63	2.74	0.18	6.65	0.00	1.61	7.74	5.76	1.68	130.00	5.30	1.56	0.00	0.20	1.36	0.00	0.00	38.00	4.78	0.40	82.10
33-PSH-04	7251572	3443602	71.00	0.32	15.40	2.65	0.06	1.04	1.74	5.14	1.91	0.09	99.35		70		49	24	345	538		22.20	4.87	5.23	1.22	0.40	0.56	1.76	2.80	0.17	10.30	0.00	2.21	10.30	0.00	2.67	45.90	4.02	1.85	0.00	0.20	1.96	0.00	0.61	29.00	4.64	0.35	94.90
N93001872	7336660	3444840	70.60	0.28	15.50	2.61	0.05	1.02	2.75	4.98	1.83	0.11	99.73				59		414	409		34.7	5.8		1.29	0.67	0.64	2.05	1.69	0.2	18.4	0.1	4.02	17.2		4.49	82	4.92	2.49	0.41	0.28	2.97	0.1	0.81	33.5	7.24	0.58	64.4
99-PSH-04	7332874	3458005	64.50	0.65	16.00	4.24	0.08	2.73	2.02	5.10	3.45	0.30	99.07				95	23	741	1374		203	10.30	7.04	4.05	1.31	3.24	11.20	4.14	0.57	115.00	0.18	5.68	102.00	8.37	26.90	83.80	7.99	14.60	0.32	1.14	8.87	0.17	1.04	67.00	16.10	0.98	169.00
96-PSH-04	7326669	3469776	64.80	0.65	16.30	4.18	0.06	2.02	4.29	4.98	1.57	0.21	99.07		100		68	24	896	988		54.60	12.10	9.02	1.72	0.82	1.38	3.67	3.48	0.32	27.80	0.10	2.86	27.00	7.47	6.15	28.30	7.88	4.62	0.00	0.41	0.65	0.12	0.23	81.70	7.60	0.68	135.00
145-PSH-04	7314783	3474729	68.10	0.41	16.00	3.33	0.06	1.52	2.85	5.56	1.35	0.12	99.29		60		79	24	497	804		45.50	7.72	5.96	1.15	0.50	0.79	2.21	2.08	0.13	25.90	0.00	1.95	19.40	0.00	5.23	27.70	8.03	2.78	0.00	0.25	1.53	0.00	0.00	51.40	4.75	0.15	83.30
102.1-PSH-04	7300662	3477529	71.00	0.26	15.70	1.87	0.03	0.65	2.44	5.20	2.14	0.10	99.39		76		32	27	533	781		45.30	3.92	0.00	0.86	0.29	0.63	1.65	3.09	0.17	27.30	0.00	2.72	16.50	0.00	4.65	63.00	2.68	2.04	0.00	0.19	5.92	0.00	0.34	18.30	4.69	0.32	122.00
101-PSH-04	7304590	3478318	71.00	0.26	15.80	1.85	0.04	0.69	2.55	5.30	1.85	0.10	99.44				45	25	525	676		38.50	3.67	6.02	0.97	0.35	0.42	1.63	2.82	0.15	15.00	0.00	2.85	9.31	5.28	2.97	67.10	2.99	1.74	0.26	0.18	6.32	0.00	0.71	19.10	4.56	0.34	107.00
A1602	7267090	3480520	70.30	0.45	15.60	2.33	0.02	0.92	3.17	4.48	1.83	0.03	99.13		170		52	22	311	503	32	213	5.6		1.9	0.6	1.35	6.77	6.9	0.27	123	0.1	5.2	75.8	8	22.2	57	3.6	10	0.2	0.59	46	0.1	2	32	7.5	0.55	294
113-PSH-04	7270043	3484343	71.00	0.27	15.60	1.97	0.03	0.67	2.62	4.93	2.18	0.10	99.37		120		44	24	483	773	33	41.60	3.98	0.00	0.98	0.50	0.64	1.69	2.88	0.17	22.80	0.00	2.87	14.30	0.00	4.19	53.40	2.93	2.28	0.00	0.23	5.16	0.00	0.37	21.90	4.92	0.44	115.00
119-PSH-04	7273941	3484649	71.20	0.25	15.70	1.85	0.03	0.63	2.55	5.04	2.02	0.09	99.36		77		40	23	490	853	31	32.90	3.37	0.00	0.93	0.49	0.50	1.83	2.94	0.17	17.00	0.00	2.48	12.40	0.00	3.29	51.70	2.95	1.77	0.00	0.21	4.65	0.00	0.43	20.30	6.04	0.54	119.00
135.1-PSH-04	7300169	3487254	68.40	0.38	16.70	2.69	0.05	0.94	3.46	5.24	1.31	0.15	99.31		91		61	22	652	572		64.70	5.71	6.93	1.54	0.66	0.84	2.80	3.49	0.28	27.40	0.11	3.94	20.40	5.98	5.59	57.30	3.57	3.43	0.31	0.33	6.85	0.10	2.29	34.40	8.51	0.74	145.00
103-PSH-04	7286222	3488817	70.30	0.28	16.10	2.07	0.04	0.79	2.92	5.11	1.69	0.08	99.40		69		47	27	584	619		53.00	4.30	5.59	1.17	0.59	0.71	2.17	3.40	0.23	29.20	0.11	2.47	19.10	0.00	5.41	51.30	2.93	2.47	0.00	0.25	8.03	0.00	0.50	23.80	6.59	0.53	123.00
162-PSH-04	7215005	3491679	64.80	0.54	16.70	4.32	0.07	2.55	3.68	4.52	2.20	0.28	99.64		118		70	27	587	700		120	10.6	24.7	2.20	0.83	1.19	4.62	4.22	0.36	65.0	0.11	3.55	43.8	20.1	12.4	68.1	7.97	6.11	0.2	0.54	11.4	0.10	0.31	62.8	9.23	0.67	170
N94002795	7174620	3492960	70.80	0.39	16.20	1.83	0.02	0.63	2.86	5.79	1.11	0.07	99.70		160		34		602	638		85	5.4		0.96	0.31	0.81	3.34	5.35	0.13	42.6	0.1	1.83	34.9		9.35	29.7	1.34	4.89	0.2	0.34	12.4	0.1	0.4	25.1	3.81	0.21	224
170.2-PSH-04	7166515	3495778	70.60	0.34	15.00	2.70	0.05	0.64	2.09	4.29	3.48	0.12	99.31		152		53	29	217	675	41	96.30	4.76	8.87	2.60	1.23	0.68	3.84	6.76	0.47	55.40	0.20	19.00	30.30	6.37	9.06	176.00	5.64	4.39	1.09	0.50	21.60	0.18	4.07	15.00	13.90	1.10	237.00
171.1-PSH-04	7170924	3495952	68.60	0.45	16.00	3.09	0.05	1.18	3.49	4.83	1.50	0.12	99.30		289		62	26	378	511		52.70	7.78	7.97	1.35	0.50	0.72	2.32	4.46	0.24	29.10	0.00	4.02	19.70	11.40	5.20	49.20	5.58	2.62	0.00	0.29	6.16	0.00	0.32	39.60	6.83	0.62	171.00
115-PSH-04	7266784	3496539	72.30	0.24	15.10	1.72	0.03	0.52	2.39	4.71	2.35	0.08	99.42		121		36	23	363	660		34.00	3.12	0.00	1.13	0.34	0.58	1.52	2.85	0.14	20.50	0.00	3.18	13.80	0.00	3.88	68.30	2.79	1.90	0.00	0.27	7.14	0.00	0.38	16.90	4.32	0.29	97.20
90-PSH-04	7331415	3502859	69.70	0.27	16.00	1.92	0.03	0.72	2.60	4.61	3.49	0.09	99.43	165	125		27	27	405	1044		90.50	4.26	0.00	1.33	0.54	0.60	3.02	3.14	0.22	48.00	0.00	2.51	33.90	5.42	9.50	80.70	3.34	4.33	0.00	0.31	19.90	0.00	0.33	24.70	4.93	0.39	113.00
91.1-PSH-04	7327823	3504736	73.40	0.22	14.70	1.48	0.02	0.62	2.86	5.07	1.03	0.10	99.49		84		22	23	417	334		61.40	2.93	6.44	0.78	0.49	0.62	2.02	1.72	0.14	39.40	0.00	1.99	22.00	0.00	6.50	25.20	2.96	2.54	0.00	0.22	4.75	0.00	0.00	12.90	3.74	0.19	59.70
182-PSH-04	7086928	3505776	68.30	0.44	15.50	3.36	0.06	1.87	2.96	4.88	1.77	0.13	99.25	266	145	25	64	25	357	296		52.00	10.10	12.10	1.30	0.51	0.65	2.29	2.91	0.22	28.10	0.00	4.59	19.70	18.90	5.60	72.70	6.91	2.68	0.34	0.28	9.67	0.00	1.26	50.10	5.86	0.39	113.00
155-PSH-04	7197685	3508558	70.30	0.19	17.10	1.15	0.01	0.54	3.52	5.86	0.91	0.07	99.64		71		25	21	1079	456		50.2	3.07	16.4	0.24	0.15	0.46	1.12	1.98	0.1	28.5	0.1	0.55	16.5		4.79	22.3	0.71	1.46	0.2	0.1	2.28	0.1	0.2	14.6	1.25	0.15	91.7
183.1-PSH-04	7086291	3510075	69.40	0.32	16.50	2.33	0.04	0.87	3.51	5.24	1.07	0.11	99.39		61	0	60	25	567	372	0	31.40	4.19	0.00	0.89	0.31	0.57	1.75	3.35	0.14	15.20	0.00	2.16	13.00	0.00	3.44	49.40	2.96	2.01	0.00	0.17	2.11	0.00	0.31	28.10	4.27	0.34	115.00
177-PSH-04	7148157	3510818	65.50	0.62	16.40	4.29	0.06	1.97	3.80	4.45	1.81	0.17	99.07		276	0	87	28	461	477	0	34.40	11.80	13.30	0.78	0.41	0.54	1.67	3.06	0.16	17.50	0.00	3.48	13.70	18.40	3.73	66.80	7.63	2.06	0.00	0.22	1.45	0.00	0.00	73.70	4.60	0.36	108.00
140-PSH-04	7294281	3510825	73.30	0.24	14.60	1.67	0.02	0.66	2.85	4.64	1.37	0.06	99.42		202	0	25	22	365	436	0	105	3.61	6.96	0.71	0.18	0.71	2.05	3.76	0.10	64.90	0.00	2.18	31.30	0.00	10.20	41.90	2.05	3.31	0.00	0.25	15.50	0.00	0.29	17.40	2.77	0.27	141.00